How large is the design space for stratospheric aerosol geoengineering?

Yan Zhang[1], Douglas G. MacMartin[1], Daniele Visioni[1], and Ben Kravitz[2,3]

[1]Sibley School of Mechanical and Aerospace Engineering, Cornell University, Ithaca, NY, USA
[2]Department of Earth and Atmospheric Science, Indiana University, Bloomington, IN, USA
[3]Atmospheric Sciences and Global Change Division, Pacific Northwest National Laboratory, Richland, WA, USA

Correspondence: Yan Zhang (yz2545@cornell.edu)

Abstract. Stratospheric aerosol injection (SAI), as a possible supplement to emission reduction, has the potential to reduce some of the risks associated with climate change. Adding aerosols to the lower stratosphere results in global cooling. However, different choices for the aerosol injection latitude(s) and season(s) have been shown to lead to significant differences in regional surface climate, introducing a design aspect to SAI. Past research has shown that there are at least three independent degrees of freedom (DOF) that can be used to simultaneously manage three different climate goals. Knowing how many more DOFs there are, and thus how many independent climate goals can be simultaneously managed, is essential to understanding fundamental limits of how well SAI might compensate for anthropogenic climate change, and evaluating any underlying trade-offs between different climate goals. Here we quantify the number of meaningfully-independent DOFs of the SAI design space. This number of meaningfully-independent DOFs depends on both the amount of cooling and the climate variables used for quantifying the changes in surface climate. At low levels of global cooling, only a small set of injection choices yield detectably different surface climate responses. For a cooling level of 1-1.5°C, we find that there are likely between 6 and 8 meaningfully-independent DOFs. This narrows down the range of available DOF and also reveals new opportunities for exploring alternate SAI designs with different distributions of climate impacts.

1 Introduction

Reducing emissions of CO_2 and other greenhouse gases (GHG) may not be enough by itself to avoid significant risks associated with climate change. As a supplement to emission reduction, climate interventions such as stratospheric aerosol injection (SAI) may be able to reduce some of these risks. SAI involves adding aerosols or their precursors to the lower stratosphere, which would increase the stratospheric aerosol optical depth (AOD); as a result, more solar radiation would be reflected away before reaching the surface. Most climate model simulations inject SO_2, which results in increased sulfate aerosols. While injecting aerosols (or a precursor gas such as SO_2) into the stratosphere can offset the change in global mean temperature, the resulting climate would not be the same as the climate with the same temperature but without either the excess atmospheric CO_2 or SAI. These residual changes depend on injection choices that could be made. As suggested in previous research, injecting aerosols at different latitudes, altitudes, and seasons would result in different spatiotemporal patterns of AOD, which in turn would lead to different regional surface climate responses (MacMartin et al., 2017; Tilmes et al., 2017, 2018; Dai et al., 2018; Kravitz

et al., 2019; Visioni et al., 2019, 2020c; Lee et al., 2020a, 2021). Understanding the global and spatiotemporal impacts of SAI and even the governance challenges requires that we not treat SAI as one single strategy, but rather understand the range of outcomes across different strategies, the fundamental limits of how well SAI can compensate for GHG-driven climate change, and any underlying trade-offs among SAI strategies.

Choosing where and when to inject aerosols can be thought of as a design problem (Ban-Weiss and Caldeira, 2010; Kravitz et al., 2016; MacMartin and Kravitz, 2019); for a given choice of global cooling, the design space describes the range of all possible such injection strategies. Some strategies produce very different surface climate responses, while others can be relatively similar. These climate responses can be quantified by different metrics, such as surface air temperature, precipitation, and Arctic sea ice. We use the term "degrees of freedom" (DOF) to describe how many independent injection choices there are in the design space. The number of independent injection choices is equivalent to the number of independent climate goals that can be managed by SAI simultaneously. Most studies have only explored a single degree of freedom: injecting SO_2 at one location (often the equator) either at a fixed rate or to meet one climate objective (often global mean temperature (T0)) (e.g., Robock et al., 2008; Rasch et al., 2008; Kravitz et al., 2011, 2015). Kravitz et al. (2016, 2017) demonstrated a strategy in which three DOFs were used to manage three temperature goals: T0, interhemispheric temperature gradient (T1), and equator-to-pole temperature gradient (T2); the same strategy was then used in The Geoengineering Large Ensemble Project (GLENS) (Tilmes et al., 2018). Additional studies have explored variations on these DOFs, such as Visioni et al. (2020c), who injected SO_2 in only one season to meet the same set of climate goals, or Lee et al. (2020a), who used the same set of DOFs as in Tilmes et al. (2018) to meet different sets of climate goals, including T0, the latitude of the Intertropical Convergence Zone (ITCZ), the amount of Arctic September Sea Ice (SSI), and global mean precipitation (P0). Higher-latitude injections in different seasons have been shown to have different efficacies in preserving SSI; e.g., spring-only injection at 60° N restores twice the amount of SSI compared to annually-constant injection at that latitude (Lee et al., 2021). A key open question from these design studies is how many other strategies are unexplored (e.g., MacMartin and Kravitz, 2019); in other words, how many independent degrees of freedom are there?

In this study, we estimate the number of DOF of the design space for SAI. Knowing how many DOFs there are in the design space quantifies the number of independent climate goals that can be managed simultaneously by a SAI strategy. In order to be managed simultaneously, those independent climate goals cannot conflict. (For example, T0 and P0 are conflicting and cannot be managed simultaneously; see e.g., Bala et al., 2008, Tilmes et al., 2013, and Lee et al., 2020a.) Knowing the number of DOF also helps understand the full range of possible climate outcomes and what climate outcomes cannot be achieved by SAI strategies. In this study, we focus only on SO_2 injections, and evaluate the range only in one model. However, the results will depend primarily on the constraints imposed by stratospheric circulation and the lifetime of the aerosols in the stratosphere (Tilmes et al., 2017; MacMartin et al., 2017; Dai et al., 2018); as such, many of the conclusions can be expected to be applicable regardless of aerosol choice.

The aerosols will primarily stay in the same hemisphere where they are injected and be transported mostly poleward by the stratospheric Brewer-Dobson circulation (Tilmes et al., 2017; MacMartin et al., 2017). Thus, injecting in one hemisphere preferentially increases AOD in that hemisphere; injecting further poleward increases the AOD burden further poleward. In-

jecting above the equator produces an AOD peak in the tropics (Kravitz et al., 2019). More generally, different choices of injection latitude, altitude and season lead to different spatiotemporal AOD patterns as a result of the seasonally-varying stratospheric circulation. However, not all choices contribute the same level of "uniqueness" (MacMartin et al., 2017; Visioni et al., 2019, 2020c). For example, injecting at the equator would produce very different patterns of AOD compared to injecting at 30° N, but the patterns of AOD arising from injecting at 31° N should not be expected to be very different from injecting at 30° N. As more choices of injection latitude are considered, there exists a diminishing return on the "uniqueness" contributed by additional choices of injection latitude. That leads to the question of how many meaningfully-independent patterns of AOD are possible given the constraints imposed by stratospheric circulation.

There are two distinct steps in the analysis herein. The first step is to consider how different the spatiotemporal AOD patterns are for different injection choices. And second, to know whether the AOD patterns from two different injection choices are sufficiently similar to treat them as effectively equivalent, or sufficiently distinct to treat them as two separate DOFs, one needs to relate how similar or dissimilar the patterns of AOD are to how similar or dissimilar the resulting climate responses are. Identifying the number of DOF only needs to consider injections that produce meaningfully different climates; herein we define "meaningfully different" based on the ability to detect the difference in climate after 20 years, given natural variability – and this threshold clearly depends on the choice of climate variables to be considered and the amount of cooling desired. For example, injecting aerosols at 30° N only in the summer or only in the fall would yield different patterns of AOD. The difference in resulting climate could be distinguishable against the background climate variability if the desired amount of cooling is high. However, by reducing the level of cooling, the difference would become indistinguishable.

The next section describes the climate model and simulations used. Section 3 assesses the differences in spatiotemporal AOD patterns from 29 different injection choices, sampling different latitudes and seasons of injection, and quantifies the size of design spaces with different numbers of DOF using a metric based on the angle between different patterns of AOD. Section 4 identifies a relationship between how similar or dissimilar AOD patterns are and how similar or dissimilar the corresponding climate responses are, using existing simulations that were conducted with various different choices for climate goals and/or different DOFs. Section 5 then quantifies how large the difference in climates needs to be in order to be meaningfully different at different levels of cooling. Finally, we combine these pieces of analysis in Section 6 to show that for a cooling level of 1-1.5°C, for example, there are between 6 and 8 DOFs.

2 Model and Simulations

All simulations in this study were conducted using the Community Earth System Model version 1 with the Whole Atmosphere Community Climate Model as the atmospheric component, CESM1(WACCM). CESM1(WACCM) is a fully coupled Earth System model which includes atmosphere, ocean, land, and sea ice components (Mills et al., 2017). The model has a horizontal resolution of 0.95° latitude by 1.25° longitude, with 70 vertical levels that extend from the earth surface to 140 km in altitude, and stratospheric aerosols have been shown to reasonably match observations after the Mt. Pinatubo eruption (Mills et al., 2017). With the exception of a few cases noted below, we use existing output from previous simulations for our analysis.

To assess the range of possible spatiotemporal patterns of AOD arising from different injection choices, we sample 29 possible choices in the AOD design space, including injections at low and middle latitudes as described by Visioni et al. (2019), and high latitude injections as described by Lee et al. (2021); the set of 29 possible choices is illustrated in Fig. 1. Visioni et al. (2019) include injections at 5 different latitudes: 30° N, 15° N, equator, 15° S, and 30° S, as in Tilmes et al. (2017). For each latitude, injections are simulated both annually-constant, and restricted to each season: December-January-February (DJF), March-April-May (MAM), June-July-August (JJA), and September-October-November (SON). In each simulation, 6 Tg yr^{-1} of SO_2 are injected into the lower stratosphere, approximately 6-7 km above the tropopause at 180° E (about 25 km for equator and 15° N/S, 23 km for 30° N/S, 16 km for 45° N/S, and 15 km for 60° N/S). Simulations were conducted for 5 years (2040-2044), which is sufficient for estimating the steady-state AOD pattern (Visioni et al., 2019), though of course not for estimating the climate response to this forcing. The high latitude injections included here are not exactly the same as those described in Lee et al. (2021), which have a higher injection rate of 12 Tg yr^{-1} and only consider injection at 60° N and further poleward. To be consistent with simulations performed by Visioni et al. (2019), we conducted additional simulations of spring (MAM or SON) injection at 45° N, 45° S, 60° N, and 60° S for 5 years from 2040 to 2044 with an injection rate of 6 Tg yr^{-1}, to complete the sample set. Following Lee et al. (2021), the other seasons of injection at high latitude are not expected to be particularly effective. Figure 2 shows the spatiotemporal patterns of AOD in each of these four spring injections at high latitudes (see Visioni et al., 2019 for the remaining cases). This gives us a total of 29 different injection cases, and associated spatiotemporal patterns of AOD. In Section 3, we rank the 29 injection cases based on the uniqueness of their AOD patterns, which are then used to identify the number of meaningfully-independent injection choices. In Section 7, we show that the uniqueness of stratospheric AOD patterns does not depend on the altitude of injection, using simulation data from Tilmes et al. (2017) that include SO_2 injection either 1 km above the tropopause or 6-7 km above the tropopause.

In addition to these shorter simulations that we use to assess the range of possible spatiotemporal AOD patterns from different injection choices, five sets of solar geoengineering simulations from existing studies (Tilmes et al., 2018; Kravitz et al., 2019; Visioni et al., 2020c; Lee et al., 2020a) are used to analyze the connection between the patterns of stratospheric AOD and surface climate responses (see Table 1). These 5 sets were all performed in CESM1(WACCM) with RCP8.5 as the background warming scenario, and used a feedback algorithm (Kravitz et al., 2017) to adjust SO_2 injection rates to maintain one or more climate objectives. Each simulation takes the 20-year average of annual mean temperature from 2010-2029 in the Representative Concentration Pathway 8.5 (RCP 8.5) emissions scenario as the target value for T0. Maintaining T0 constant at 2010-2029 average results in 4°C of global mean cooling in each of these simulations by 2070-2089. The equatorial case adjusts the single SO_2 injection rate to meet T0. The other simulations adjust SO_2 injection rates at multiple latitudes to simultaneously meet T0 and additional climate objectives (see Table 1); these additional objectives include T1, T2, ITCZ (using the centroid of precipitation between 20° S and 20° N as a proxy), and SSI. Table 1 lists the injection seasons and latitudes, the number of ensemble members, and the design objectives of the five sets of simulations.

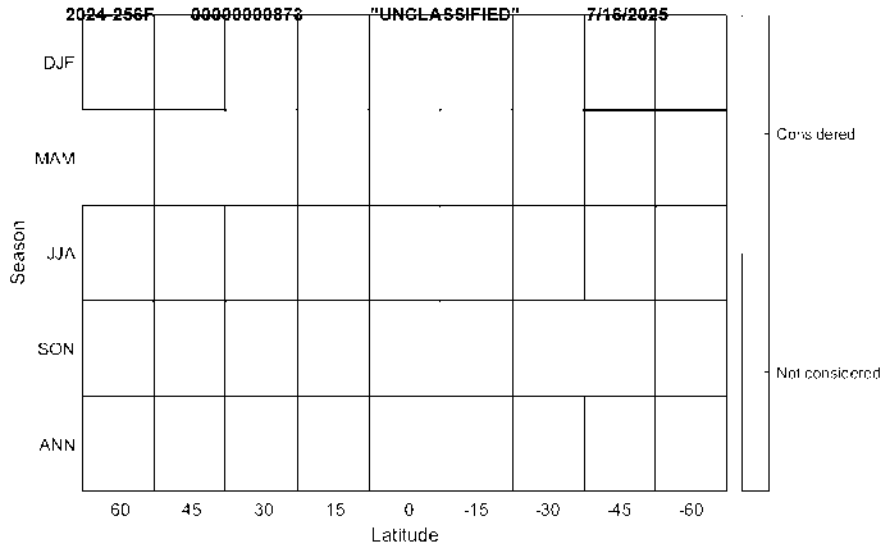

Figure 1. The 29 injection choices that we considered in our analysis for AOD patterns are shown in light green. Vertical axis shows the injection season of each injection choice, either injecting in only one season (DJF, MAM, JJA, or SON) or constantly throughout the year (ANN). Horizontal axis shows the injection latitude, from left to right are 60° N, 45° N, 30° N, 15° N, equator, 15° S, 30° S, 45° S, and 60° S.

Table 1. Injection design and outcomes of the 5 existing SAI simulations analyzed in this study.

Name of simulation	Injection latitude	Injection season	Number of ensemble members	Objectives	Reference
GLENS	30° N, 15° N, 15° S, 30° N	annually-constant	21	T0, T1, T2	Tilmes et al. (2018)
iSpring	30°N, 15° N, 15° S, 30° S	MAM at 30° N and 15° N; SON at 15° S and 30° S	3	T0, T1, T2	Visioni et al. (2020c)
iAutumn	30° N, 15° N, 15° S, 30° S	SON at 30° N and 15° N; MAM at 15° S and 30° S	3	T0, T1, T2	Visioni et al. (2020c)
Equatorial	Equator	annually-constant	3	T0	Kravitz et al. (2019)
PREC (1st simulation in Lee et al., 2020a)	30° N, 15° N, 15° S, 30° N	annually-constant	1	T0, ITCZ, SSI	Lee et al. (2020a)

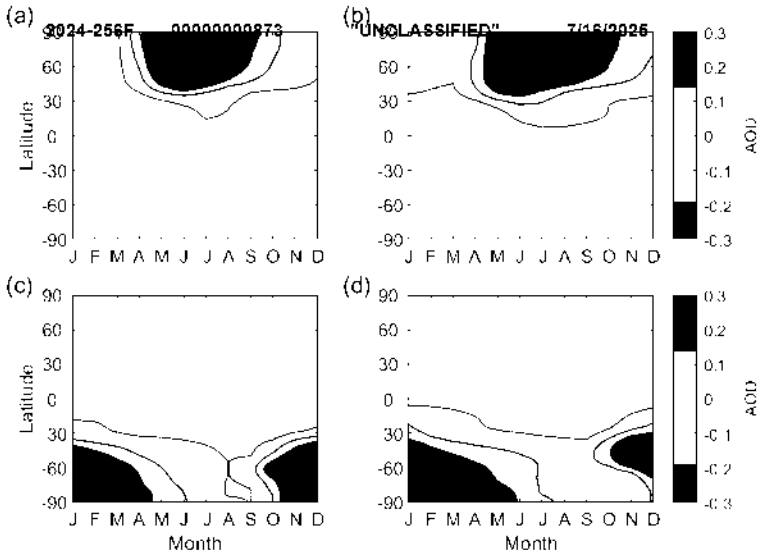

Figure 2. Spatiotemporal AOD patterns of spring injections at (a) 60° N, (b) 45° N, (c) 60° S, and (d) 45° S. The AOD patterns of spring injections in the same hemisphere are similar to each other, while the injections in the opposite hemispheres produce very different AOD patterns.

3 Diminishing Returns on the Number of Degrees of Freedom

In this section, we consider 29 different injection choices, sampling from different latitudes and seasons of injection, as well as 3 additional cases that we use to verify that the set of 29 is sufficiently complete. The AOD pattern from a given injection choice (a given latitude and season of injection) is largely determined by the stratospheric circulation and aerosol lifetime, which constrains what spatiotemporal patterns are achievable (Tilmes et al., 2017; MacMartin et al., 2017). The AOD resulting from any particular choice of latitude and season can be approximated by a linear combination of other choices. Our goal in this paper is to determine how many distinct injection choices are needed to adequately approximate all of the possible AOD patterns. What constitutes "adequacy" is determined in subsequent sections.

To describe any pattern of AOD, we consider the zonal-mean pattern as a function of both latitude and time of year. In order to treat these two dimensions consistently and yield AOD patterns independent of our sampling resolution in each dimension, we weight the monthly-mean zonal mean AOD at each latitude and month by the corresponding incoming solar energy (petajoules) at the top of the atmosphere (TOA). We then represent the weighted spatiotemporal AOD pattern from each injection choice as a vector $\boldsymbol{a}$, the length of which is equal to the number of latitudes times the number of months, $\ell = \ell_{\text{lat}} \times \ell_{\text{month}}$. One way of quantifying how similar or dissimilar two patterns of AOD are is to consider the angle between their vector representations, θ_{AOD}. This implicitly assumes that the patterns of AOD are sufficiently linear for 1-4°C of cooling, although nonlinearities will become increasingly important at higher forcing levels (MacMartin et al., 2017; Visioni et al.,

2020b). Thus, the angle between two vectors $\boldsymbol{a}_i$ and $\boldsymbol{a}_j$ that represent the AOD patterns of the same injection choice with different injection rates is negligible, while only the magnitudes of those vectors are different. Two AOD patterns that are different only in magnitude can thus be matched by adjusting injection rates, and thus are not considered as meaningfully different. Therefore, the angle between two vectors $\boldsymbol{a}_i$ and $\boldsymbol{a}_j$ describes how meaningfully different these two AOD patterns are. We can illustrate this using the AOD patterns shown in Fig. 2. The AOD patterns of injection at 60° N and 60° S are very dissimilar; the angle between the vector representations of these two AOD patterns is 84°. By contrast, the AOD patterns of injection at 60° N and 45° N are similar; the angle between these two AOD patterns is only 12°.

With the vector representation explained above, our goal is to select a subset from the set of 29 injection choices such that any possible AOD pattern can be adequately represented by a linear combination of injection choices from this subset. Determining the dimension of that set necessary to meet this goal is equivalent to determining the number of DOF of SAI.

First, we need to verify that our set of 29 injection choices sufficiently describes all of the possible AOD patterns of other injection choices that we have not simulated. To do so, we choose 3 additional verification cases, which are annual injections at 7.5° N, 22.5° N, and 37.5° N, and quantify how well each of these can be represented by a linear combination of the 29 injection choices.

Mathematically, the linear combination that is most similar to the simulated pattern of AOD is the projection of its vector representation onto the space formed by the 29 injection choices. Solving the best approximation of the pattern of AOD can be formed as a constrained linear least-square problem of finding the projection onto the set of 29 injection choices:

$$\arg\min_{\hat{\boldsymbol{x}}} ||\hat{\boldsymbol{d}}(\hat{\boldsymbol{x}}) - \boldsymbol{d}|| \tag{1}$$

$$\text{sbj} \quad \text{to} \quad \hat{\boldsymbol{d}}(\hat{\boldsymbol{x}}) = Q_{29}\hat{\boldsymbol{x}} \tag{2}$$

$$\hat{x}_i \geq 0, \quad i = 1, ..., 29 \tag{3}$$

where $\boldsymbol{d}$ is the vector representation of the AOD pattern of each verification case, which is obtained from CESM1(WACCM) simulation, $\hat{\boldsymbol{d}}$ is the best approximation of $\boldsymbol{d}$, Q_{29} is the set of vector representations of the 29 injection choices, and $\hat{\boldsymbol{x}}$ is the vector of best approximating linear coefficients. All linear coefficients $\hat{x}_i$ are constrained to be non-negative numbers, as injection rates cannot be negative.

By calculating the angle between the vector representation of the simulated AOD pattern and the vector representation of the approximated AOD pattern, we can assess how similar the simulated and approximated AOD patterns are. For annually-constant injections at 7.5° N, 22.5° N, and 37.5° N, the angles between simulated and approximated AOD patterns are 7.6° , 5.9° , and 6.1° , respectively. The AOD from injection at 7.5° N is roughly a linear combination of injections at the equator and 15° N, with a little over half of SO_2 injected at 15° N. Similarly, the AOD from injection at 22.5° N is roughly a linear combination of injections at 15° N and 30° N, and the AOD from injection at 37.5° N is roughly a linear combination of injections at 30° N and 45° N. The simulated and approximated spatiotemporal AOD patterns of these three verification cases are shown in Fig. 3. Although we do not verify for an injection on the Southern Hemisphere, we expect to see a similar linear combination of injections on the same hemisphere at some latitudes lower and higher than its injecting latitude. Based on this

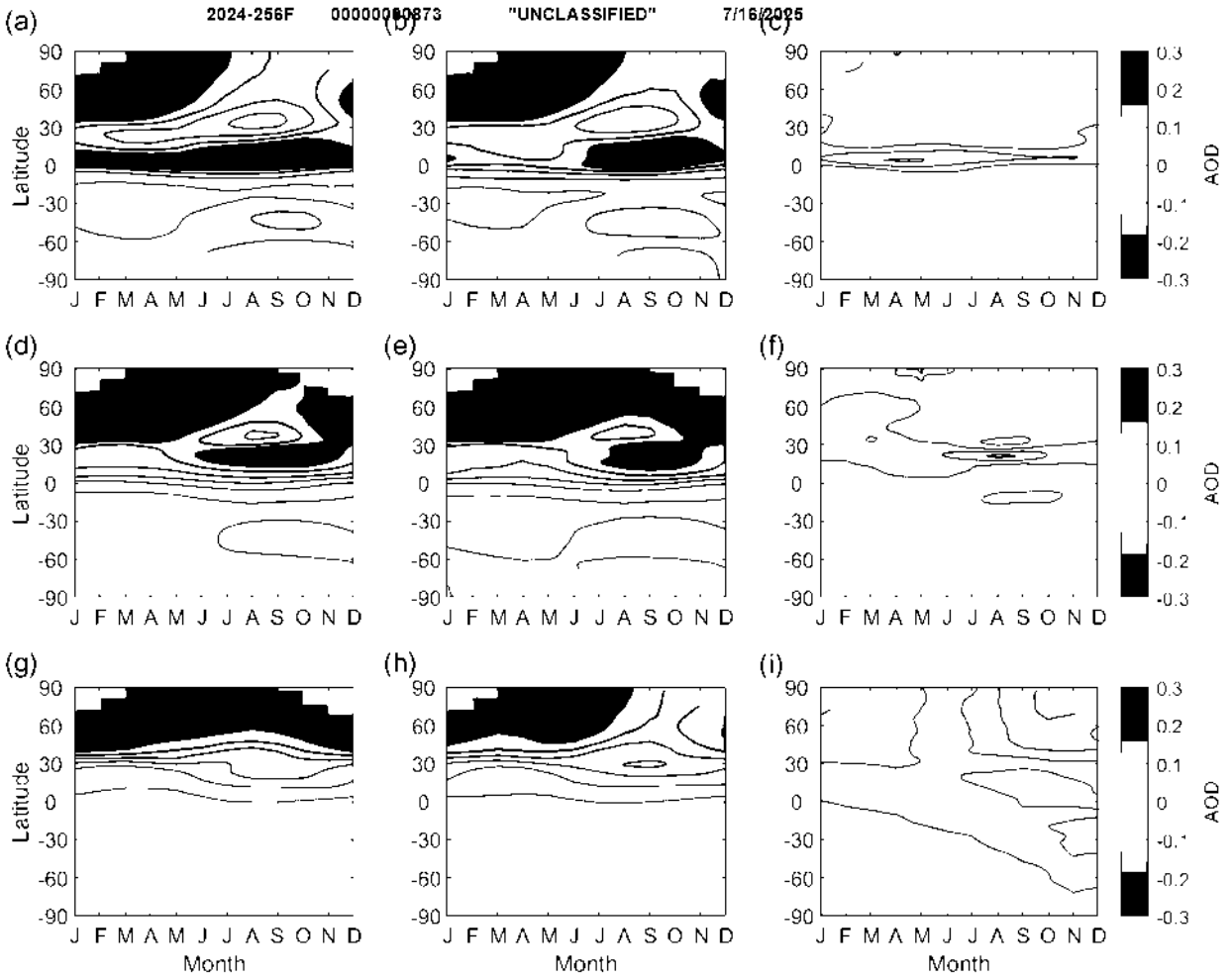

Figure 3. Comparison of simulated AOD patterns and the best approximation to these AOD patterns obtained from a linear combination of other injection choices within the set of 29 cases considered here. From top to bottom are the spatiotemporal AOD patterns for injections at 7.5° N, 22.5° N, and 37.5° N, respectively. In each horizontal panel, plots from left to right are the AOD pattern obtained from CESM1(WACCM) simulations, the AOD pattern approximated using the set of 29 injection cases, and the difference between these. The angles between the simulated AOD pattern and the AOD pattern approximated using the set of 29 cases are 7.6° , 5.9° , and 6.1° , respectively.

comparison, the approximated AOD patterns are adequately similar to the simulated AOD patterns, as long as the threshold for an "adequate" approximation of the AOD is larger than 7.6° (which it will be here, as shown in subsequent sections). Allowing this small difference between the approximated and simulated AOD patterns, the set of 29 injection choices thus adequately describes other possible AOD patterns that we have not simulated.

With the set of 29 choices of injection locations/times, we can evaluate a wide range of possible selections of injection choices. Sets with different numbers of injection choices as well as different selections of the same number of injection choices will do a better or worse job at spanning the space of possible AOD patterns. One way to quantify how well the overall space of possible AOD patterns can be approximated by a particular subset of n injection choices is to compute the maximum angle, θ_{max}, that can be formed between the subset of n choices and any other injection choices that are not selected. That is, how well can the AOD pattern from any other choice be represented by a linear combination of the n elements in the subset? The smaller θ_{max} is, the better the AOD pattern from any other possible injection choice can be equivalently obtained by only choosing injections from the subset of selected injection choices. This provides a way to quantify how well the overall space is approximated by a particular subset of n injection choices. By optimizing over θ_{max}, we can determine both what the "best" subset is of any given dimension (number of DOF or injection choices), and equally important, how much error there would be in trying to capture any achievable AOD pattern with only a relatively few different injection choices.

In choosing subsets, we enforce hemispheric symmetry such that if an injection choice in one hemisphere is included, then the corresponding choice on the opposite hemisphere is also included (e.g., MAM in the Northern Hemisphere and SON in the Southern Hemisphere). While the seasonal circulation patterns are not exactly symmetric between the hemispheres, they are sufficiently similar that this is a reasonable simplification that reduces the number of sets to search over. For injections at the equator, we similarly either include or don't include opposite seasons (e.g., DJF and JJA, or MAM and SON). With hemispheric symmetry, the only way to have a set with an odd number of DOF is to include annually-constant equatorial injection; we revisit this case in the discussion.

Mathematically, the steps above can be described as follows. First, for each subset Q_j of n injection choices, we identify the maximum angle that can be formed between that subset and any other injection choices in the set of 29 that are not selected:

$$\theta_{max}(Q_j) = \max_{1 \le i \le k} \angle(\boldsymbol{a}_i, Q_j), \quad \boldsymbol{a}_i \in [Q_{29} \setminus Q_j] \tag{4}$$

where $k = 29 - n$, the total number of injection choices that are not selected by the set Q_j.

Taking $n = 4$ as an example, we can identify all possible combinations of 4 injection choices from the set of 29. With the enforced constraint of hemispheric symmetry, there are a total of 91 different combinations. For each of these possible combinations, we calculate the angle formed between each of the unselected injection choices and the selected set of 4 and find the maximum angle. For illustration, Fig. 4 shows an example (sub-optimal) set of 4 injection choices: summer injection at 30° N, 15° N, 15° S, and 30° S, and lists the angles formed between each of the unselected injection choices and the example set of 4.

Among all possible subsets of n injection choices ($Q_j \in Q$), we identify which subset has the smallest maximum angle and denote the "best" subset that minimizes θ_{max} as $Q^*(n)$:

$$Q^*(n) = \arg\min_{Q_j \in Q} \theta_{max}(Q_j) \tag{5}$$

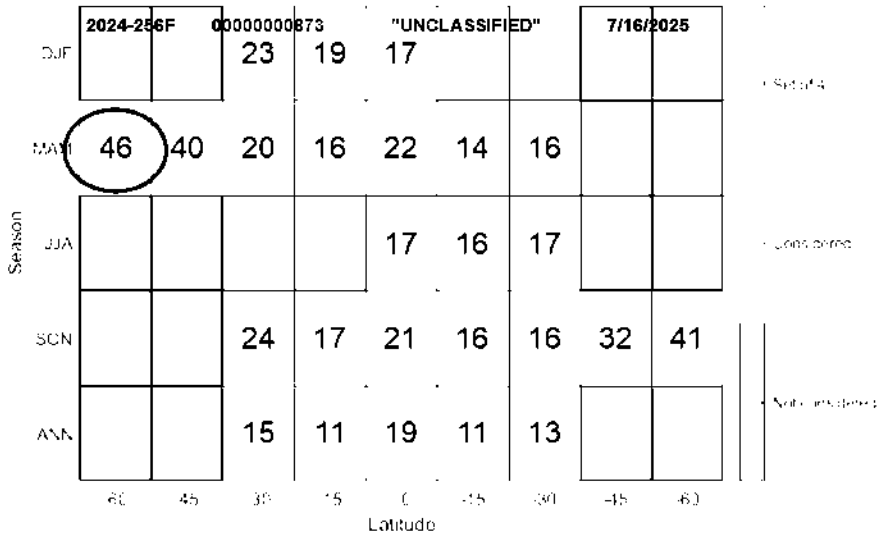

Figure 4. Angles (in degrees) between each unselected injection choice and a set of 4 injection choices (in orange): summer injection at 30° N, 15° N, 15° S, and 30° S. The x-axis is the injection latitude and y-axis is the injection season. The maximum angle is 46° (highlighted by a red circle), formed between spring injection at 60° N and this set of 4.

$Q^*(n)$ is the subset of size n that best approximates any achievable pattern of AOD. The angle θ_{max} of the "best" set of n is denoted as $\theta^*(n)$.

Still using $n = 4$ as an example, we calculate the maximum angle for all possible combinations of 4 injection choices. The set of spring injections at 45° N and 45° S and autumn injections at 15° N and 15° S has the smallest maximum angle, which is 26° (Fig. 5).

For each possible value of n, we find the "best" set and corresponding angle $\theta^*(n)$, plotted in Fig. 6. Strictly speaking, because we only sampled 29 possible injection choices (out of an infinite theoretical space), $\theta^*(n)$ is simply our best estimate for the maximum angle between a subspace of n DOFs and any possible AOD pattern of injection choices that does not fall into this subspace.

4 Comparing AOD and Surface Climate

Figure 6 shows that there are diminishing marginal returns for how many degrees of freedom are included. However, the analysis in Section 3 does not indicate what degree of approximation is sufficient. The next step in our analysis is to evaluate the relationship between how similar or dissimilar two AOD patterns are, and how similar or dissimilar the corresponding surface climate responses are. This relationship is crucial for determining a threshold for whether two patterns of AOD from

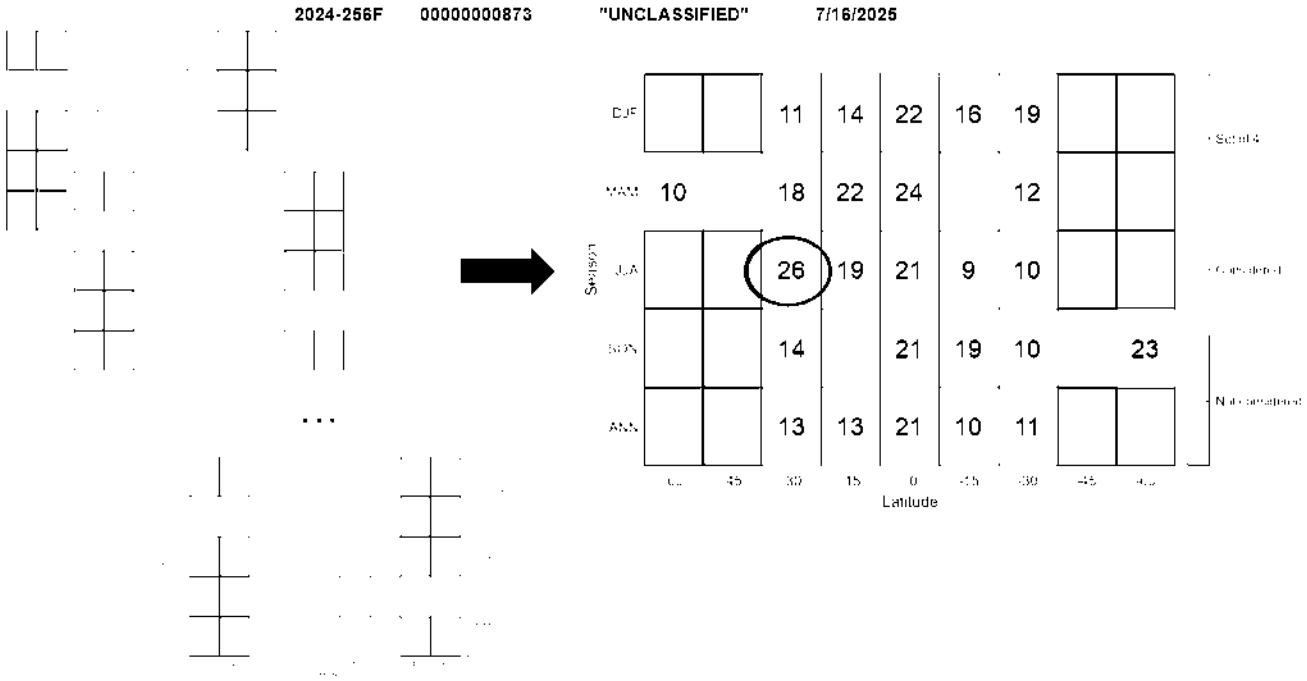

Figure 5. A schematic diagram showing how to find the smallest maximum angle $\theta^*(4)$ for a set of 4 injection choices. We first look through all possible combinations of 4 injection choices and calculate the maximum angle θ_{max}, and then identify which set has the smallest value of θ_{max}. The "best" set of 4 includes spring injections at 45° N and 45° S and autumn injections at 15° N and 15° S. The maximum angle for this "best" set of 4 is 26° (highlighted by a red circle), formed between this set and summer injection at 30° N; this is much smaller than 46° , the maximum angle found in the example in Fig. 4.

different injection choices are sufficiently different to count as two independent degrees of freedom, or sufficiently similar to be effectively the same choice.

To estimate this relationship, we consider the different strategies described in Table 1. Each of these uses either different injection choices or has different climate goals, leading to different patterns of AOD and corresponding different surface climate responses. By comparing the difference in AOD patterns and surface climate responses, we can derive a function that describes how the similarity in surface climate responses relates to the similarity in the AOD patterns that they arise from.

The AOD pattern and corresponding surface climate responses are obtained by averaging over all available ensemble members for each strategy in Table 1, and taking the difference between the 2070-2089 average, and the 2010-2029 average in the RCP8.5 emissions scenario. As explained in Section 3, the monthly-mean zonal-mean AOD is weighted by the TOA incoming solar energy as a function of latitude and time of year. For the climate response, this establishes the changes from a climate with neither SAI nor increased greenhouse gases to a climate with both. To evaluate how the surface climate varies for different strategies, herein we only consider annual-mean surface air temperature and precipitation; this assumes that if these two

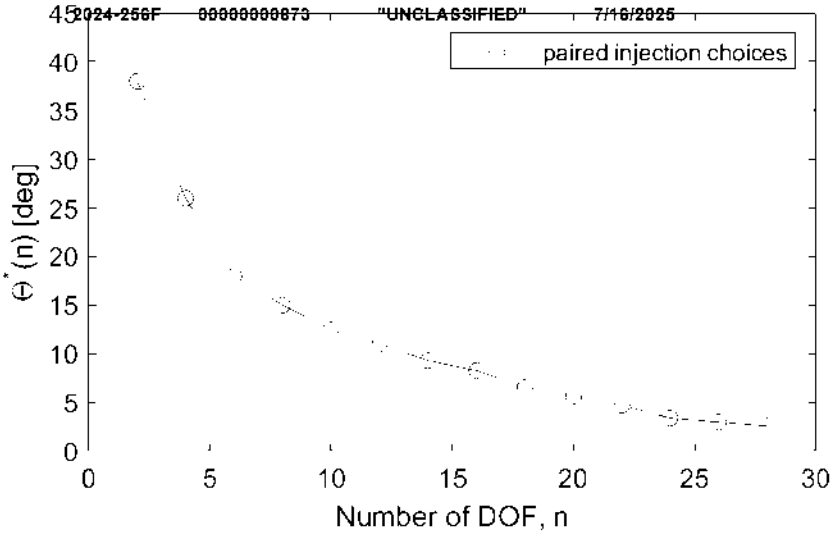

Figure 6. The maximum angle $\theta^*(n)$ formed between a subspace of n DOFs and any other injection choices outside this subspace decreases as the number of DOF n increases.

variables are similar, then changes in other surface climate variables, such as precipitation minus evaporation (P-E), will also be sufficiently similar, and also ignores shifts in the seasonal cycle (Jiang et al., 2019) as these tend to be smaller than the annual-mean changes.

To estimate how large a change in the spatiotemporal pattern of AOD is needed to obtain a detectably different pattern of surface climate response, we consider detectability over a 20-year period. Therefore, we normalize the surface temperature and precipitation changes by the variability in 20-year averages, calculated from the across-ensemble variability from 2010-2029 in RCP8.5 emissions scenario, where 21 ensemble members are available. If the variability were uncorrelated from year to year, this value would simply be a factor of $\sqrt{20}$ smaller than the interannual variability; this would be a reasonable approximation for precipitation but not for temperature. Normalizing by variability also allows temperature and precipitation changes to be compared in consistent units (Ricke et al., 2010).

To analyze the differences in AOD and surface climate for different strategies, we define the AOD space, temperature space and precipitation space. In Section 3, we define the vector representation of AOD patterns as $\boldsymbol{a}$. $\boldsymbol{a}$ represents an achievable spatiotemporal AOD pattern arising from a possible injection choice. The AOD space $\mathcal{A}$ is a ℓ-dimensional space, $\mathcal{A} \subset \mathbb{R}^{\ell}$, that includes all possible values of $\boldsymbol{a}$. Similarly, the temperature space $\mathcal{T}$ and the precipitation space $\mathcal{P}$ are both m-dimensional spaces, $\mathcal{T} \subset \mathbb{R}^{m}$ and $\mathcal{P} \subset \mathbb{R}^{m}$, where m is equal to the number of latitudes times the number of longitudes, $m = m_{\mathrm{lat}} \times m_{\mathrm{lon}}$. Any vector $\boldsymbol{T}$ in $\mathcal{T}$ represents a possible surface air temperature response to a possible injection choice, and any vector $\boldsymbol{P}$ in $\mathcal{P}$ represents a possible precipitation response to a possible injection choice:

$$\boldsymbol{T} = [T_1, T_2, \ldots, T_m]^T, \quad \boldsymbol{T} \in \mathcal{T} \tag{6}$$

$$\boldsymbol{P} = [P_1, P_2, \ldots, P_m]^T, \quad \boldsymbol{P} \in \mathcal{P} \tag{7}$$

where $T_1, \ldots T_m$ are temperature responses, and $P_1 \ldots P_m$ are precipitation responses, both in dimensionless units of standard deviations.

In the AOD space, temperature space and precipitation space defined above, we evaluate the differences between each possible pair of the five SAI strategies described in Table 1, i.e., 10 pairwise comparisons. As in Section 3, the difference between AOD patterns for different pairs of strategies is evaluated by computing the angle between them, θ_{AOD}. For temperature and precipitation, the difference between two strategies is evaluated by computing the temperature distance, d_t, or the precipitation distance, d_p. The temperature distance is defined as the area-weighted L^2-norm (root-mean-square) of the difference between the two vector representations of surface air temperature responses, to count all areas on the Earth equally. Similarly, the precipitation distance is defined as the area-weighted L^2-norm (root-mean-square) of the difference between the two vector representations of precipitation responses. Among the 10 pairwise comparisons, GLENS and EQ have the largest temperature distance, though it's still an order of magnitude smaller than the temperature distance between GLENS and the projected 20-year average (2070-2089) climate response under RCP8.5 (Fig. 7(a) and (b)). The precipitation distance between GLENS and EQ is also smaller than that between GLENS and RCP8.5 (Fig. 7(c) and (d)). Among all 10 pairwise comparisons, the temperature distances are always larger than the corresponding precipitation distance. That is the changes in temperature, compared to variability, are larger than the changes in precipitation. To conclude, a small angle between the vector representations of AOD patterns indicates the two compared SAI strategies yield similar AOD patterns, and a small value of d_t or d_p indicates that the two compared SAI strategies have similar surface air temperature responses or precipitation responses. Likewise, a larger AOD angle, temperature distance, or precipitation distance implies less similar AOD patterns, surface air temperature or precipitation.

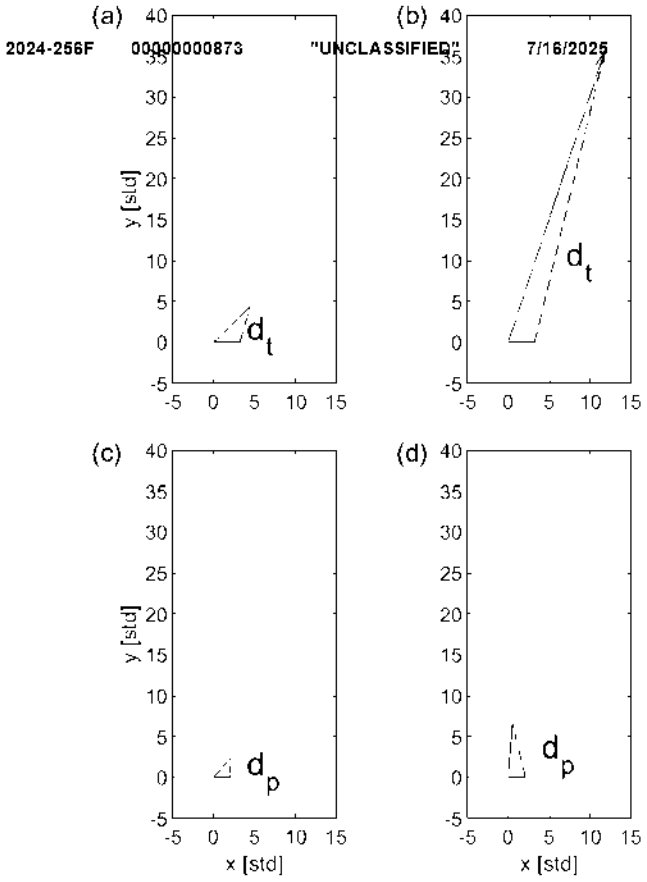

Figure 7. (a) The temperature distance between GLENS (black) and EQ (red), (b) the temperature distance between GLENS (black) and RCP8.5 (blue), (c) the precipitation distance between GLENS (black) and EQ (red), and (d) the precipitation distance between GLENS (black) and RCP8.5 (blue), shown on the 2D plane that contains both area-weighted vectors (while both vectors are m-dimensional, there is a unique plane that contains both). Both temperature and precipitation are expressed in number of standard deviations (and are thus dimensionless). In (a) and (b), std is the standard deviation of 20-year averages of temperature, calculated from the across-ensemble variability from 2010-2029 in RCP8.5 simulations. In (c) and (d), std is the standard deviation of 20-year averages of precipitation.

To estimate the relationships between θ_{AOD} and d_t and between θ_{AOD} and d_p, we perform linear regressions on the data points obtained from the 10 pairwise comparisons among the 5 different SAI strategies in Table 1 (Fig. 8). We constrain the
275 linear regressions to go through zero because an identical AOD pattern should yield an identical temperature and precipitation response. The linear functions are obtained as:

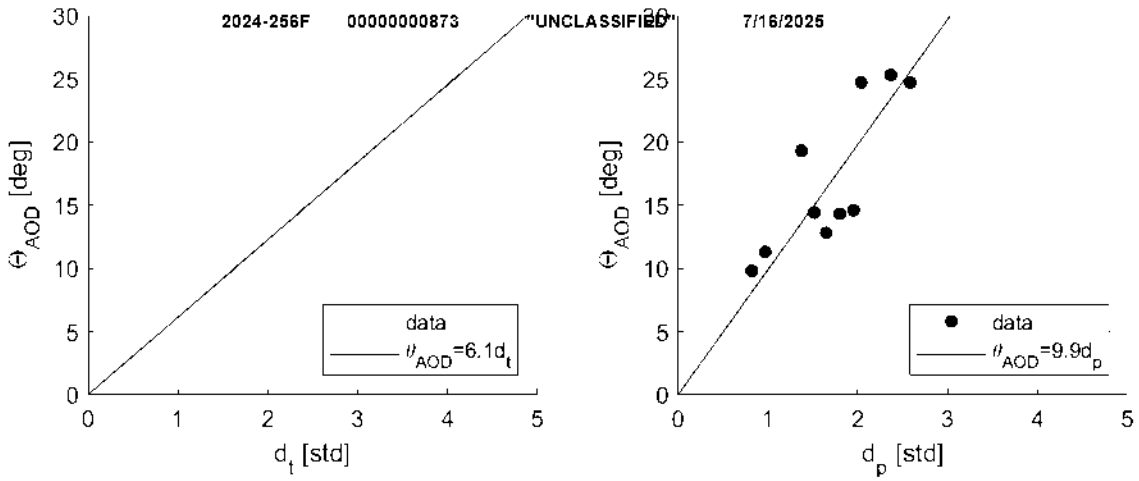

Figure 8. (a) Angle between AOD patterns, θ_{AOD}, and the distance between corresponding temperature responses, d_t, for each pair of strategies in Table 1; (b) angle between AOD patterns, θ_{AOD}, and the distance between corresponding precipitation responses, d_p, for each pair of strategies in Table 1. d_t and d_p are expressed in number of standard deviations (std) of 20-year averages of temperature and precipitation respectively. Orange dots represent the values of θ_{AOD} and corresponding d_t and blue dots represent the values of θ_{AOD} and corresponding d_p of all pairwise comparisons between different strategies. The black lines represent the best-fit linear regression functions, constrained to pass through the origin: θ_{AOD} =6.1 d_t, and θ_{AOD} =9.9 d_p with the coefficient of determination, $R_t^2 = 0.62$ and $R_p^2 = 0.65$, respectively. The error in estimating each point (calculated from across-ensemble variability) is small (less than 0.2° in AOD angle, and less than 0.1 std in both temperature distance and precipitation distance) compared to the fitting error, indicating that a linear approximation to the relationship is only an approximation. Points in the upper-right (most dissimilar AOD and dissimilar surface climate) are the pairwise comparisons between the equatorial injection strategy and the other strategies. In (a), the outlier at approximately (1.6,19), which is the comparison between iSpring and iAutumn, shows that the relationship between θ_{AOD} and d_t isn't exactly linear; similar AOD patterns yield similar climate responses but different AOD patterns do not guarantee different climate responses.

$$\theta_{AOD} = 6.1 d_t \tag{8}$$

$$\theta_{AOD} = 9.9 d_p \tag{9}$$

As shown in Fig. 8, pairs of strategies with relatively similar AOD patterns have relatively similar temperature and precipitation responses, and conversely, pairs of strategies with very different AOD patterns result in very different temperature and precipitation responses.

Data used here are from SA1 designs that were considered in previous studies. Although they are not designed to span either the overall AOD design space or the surface climate design space, these available simulations do provide a useful set of data for analyzing the relationship between how similar or dissimilar the AOD patterns are and how similar or dissimilar the surface climate responses are.

5 Detectability at different levels of cooling

To evaluate how different the surface climate responses are, we first perform Welch's t-test on the five injection strategies, using a single ensemble member of each injection strategy. Welch's t-test assumes that sampled data are independent; we remove the effect of serial autocorrelation from the temperature and precipitation data by estimating the effective sample size assuming both temperature and precipitation follow a first order autoregressive (AR(1)) process (Wilks, 2019). The t-test results for comparing differences in surface air temperature between GLENS and iSpring and between GLENS and EQ are shown in Fig. 9(a)-(b); the t-test results for precipitation comparison are shown in Fig. 10(a)-(b). At a 4°C cooling and a confidence level of 95%, temperature and precipitation responses from GLENS and iSpring are statistically significantly different from each other in 17% and 7% of Earth's area, respectively, as opposed to the comparison between GLENS and EQ, in which 37% and 23% of area on the Earth shows statistically significant difference in temperature and precipitation.

Here, we define that two strategies are considered to be detectably different if the difference in temperature or precipitation responses between them are detectable at a 95% confidence level over a 20-year period on more than 5% of Earth's area. With the temperature and precipitation normalized by the standard deviation of 20-year means, the difference between the temperature or precipitation responses at any grid point will be detectably different if the difference between the normalized data is more than 2. To obtain a global aggregate metric, we note that roughly 5% of the Earth's surface area has a temperature difference more than double the overall temperature distance d_t considered earlier and 5% of the Earth's surface area has a precipitation difference more than double the precipitation distance d_p. (For example, between GLENS and iSpring, only 5.2% of Earth's area have a difference in regional temperature responses that is more than twice the value of d_t, and only 4.7% of Earth's area have a difference in regional precipitation responses that is more than twice the value of d_p.) Thus when the temperature distance d_t between two injection strategies is one standard deviation, then roughly 5% of the Earth's surface area will have detectably different temperature responses at a 95% confidence interval. Similarly, when the precipitation distance d_p between two injection strategies is one standard deviation, then roughly 5% of the Earth's surface area will have detectably different precipitation responses at a 95% confidence interval. Thus, we use one standard deviation of the overall root mean square (RMS) normalized temperature distance or precipitation distance as the threshold for determining whether two strategies result in detectably different temperature or precipitation responses.

We compare the difference in temperature and precipitation responses between GLENS and iSpring and between GLENS and EQ, and show how the difference changes with levels of cooling using detectability plots, as shown in Fig. 9(c)-(d) and Fig. 10(c)-(d). Figure 9(c) and 10(c) show the detectability of difference in temperature and precipitation between GLENS and iSpring at a cooling level of 4°C. Figure 9(d) and 10(d) show the comparison between GLENS and EQ at the same cooling level. In each plot, the length of the vector is equal to the area-weighted L^2-norm of the corresponding temperature or precipitation vector, and the distance between the two vectors is the corresponding temperature distance or precipitation distance. The circle around the tip of each vector represents the temperature or precipitation variability on a 20-year timescale, whose radius is equal to one due to the normalization by the standard deviation of temperature or precipitation variability. In Fig. 9(c), the two temperature variability circles are partially overlapped, while in Fig. 9(d), the two circles are separated from

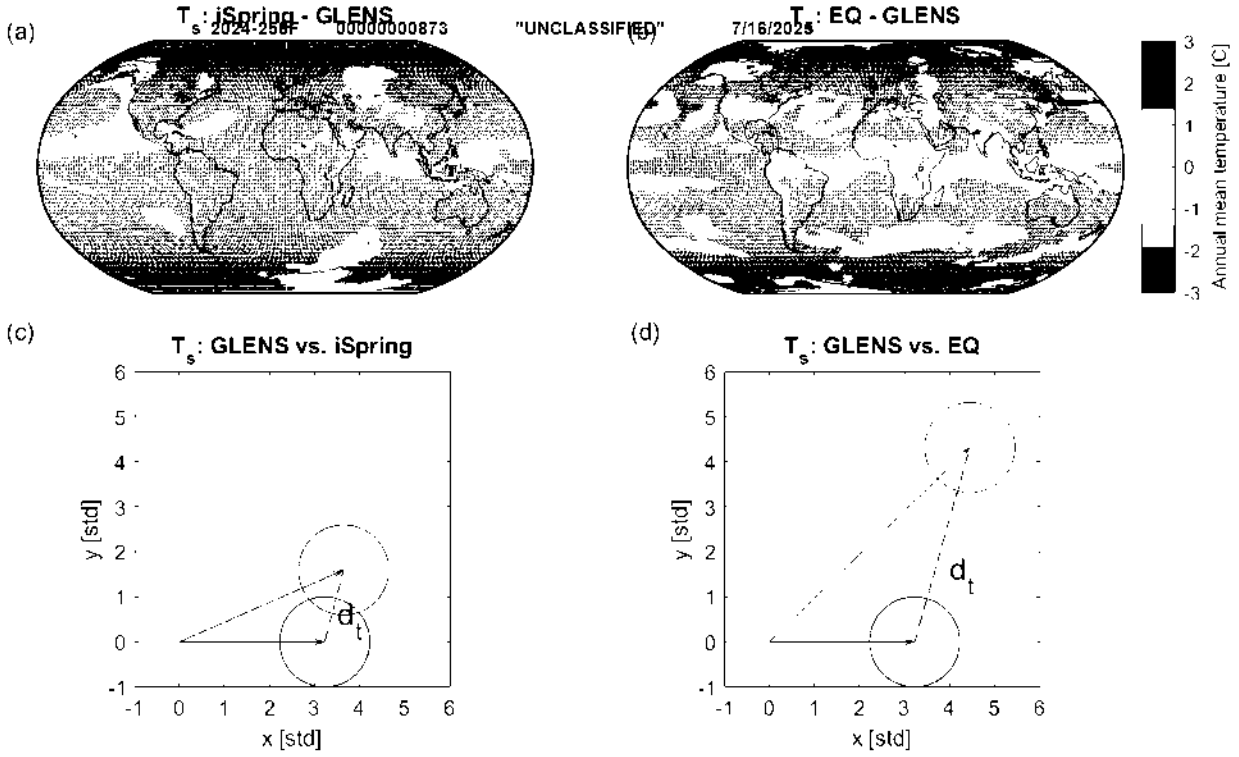

Figure 9. Left column shows the comparison between GLENS and iSpring; the right column shows the comparison between GLENS and EQ. (a) and (b) show the difference in temperature response between GLENS and iSpring and between GLENS and EQ, respectively; shaded areas are where no statistically significant difference is observed, based on a t-test with a confidence level of 95%. (c) and (d) are detectability plots that geometrically show the ability of detecting differences in the temperature responses between GLENS (black) and iSpring (blue) and between GLENS and EQ (red), respectively. The temperature responses are expressed in number of standard deviations (std) of 20-year averages of temperature. The length of each vector represents the area-weighted L^2-norm of surface air temperature response, and the circle represents temperature variability in all possible directions, with a radius of 1 std due to the normalization. The dashed line in (c) and (d) measures the temperature distance, d_t, between GLENS and iSpring and between GLENS and EQ, respectively. GLENS and EQ have a larger distance in the temperature response, which indicates the difference between GLENS and EQ is more detectable at the same level of cooling.

each other. The more overlapped these two circles have, the less area has detectably different temperature responses. When the overlapped area is sufficiently large, it indicates that the difference in the temperature responses is small enough such that it is hard to tell whether the difference could be purely due to natural variability. These implications from the observation of temperature responses also apply to precipitation.

From the detectability plots that compare these different SAI strategies, it is clear that the detectability of different injection strategies depends on both the level of cooling and the choice of climate variables. With the underlying assumption of linearity

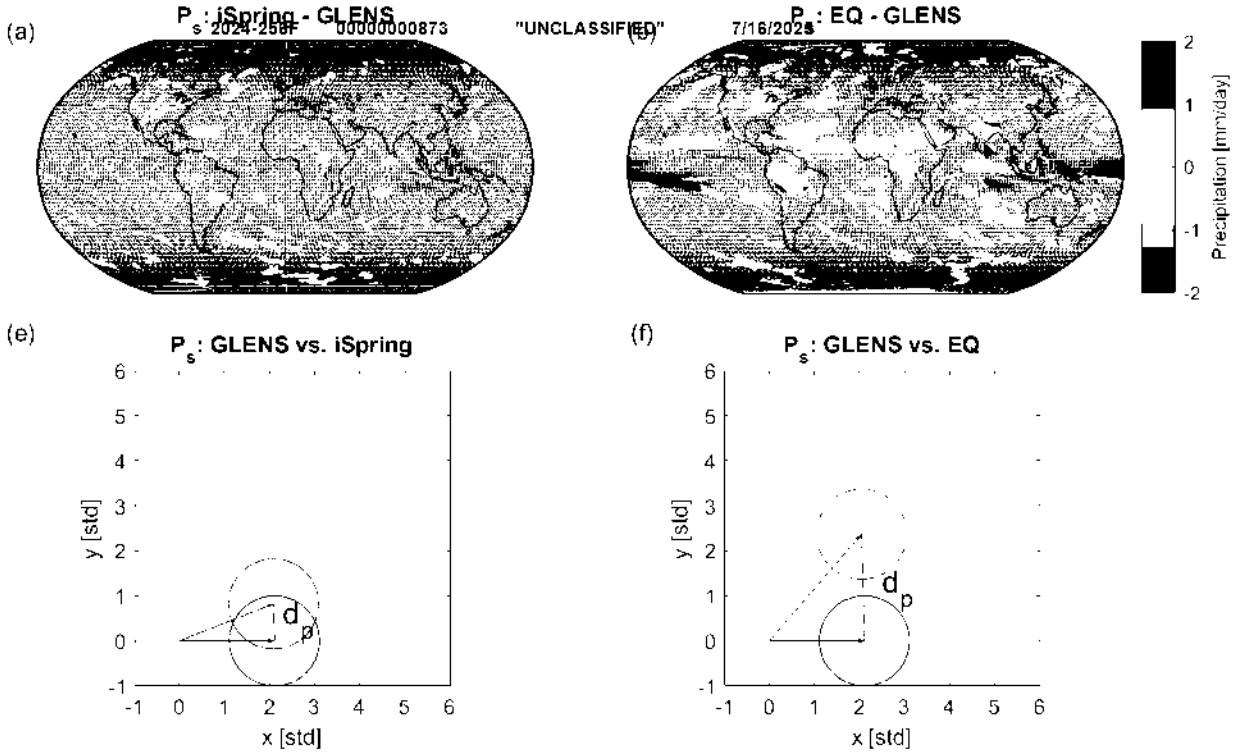

Figure 10. Left column shows the comparison between GLENS and iSpring; the right column shows the comparison between GLENS and EQ. (a) and (b) show the difference in precipitation responses; shaded areas are where no statistically significant difference is observed, based on a t-test with a confidence level of 95%. (c) and (d) are detectability plots that geometrically show the ability of detecting differences in the precipitation responses between GLENS (black) and iSpring (blue) and between GLENS and EQ (red), respectively. The precipitation responses are expressed in number of standard deviations (std) of 20-year averages of precipitation. The length of each vector represents the area-weighted L^2-norm of precipitation response, and the circle represents precipitation variability in all possible directions, with a radius of 1 std due to the normalization. The dashed line in (c) and (d) measures the precipitation distance, d_p, between GLENS and iSpring and between GLENS and EQ, respectively. Similar to temperature response, the difference in precipitation between GLENS and EQ is more detectable than that between GLENS and iSpring at the same level of cooling.

for surface climate responses, we estimate the difference in temperature and precipitation responses between GLENS and EQ at reduced levels of cooling (Fig. 11). For the same pair of strategies, as we reduce the amount of cooling, the temperature distance and the precipitation distance between these two strategies decreases. At 1.8°C cooling, the resulting temperature responses of these two strategies are 2 standard deviations of temperature variability away from each other (Fig. 11(b)); at
330 the same level of cooling, the resulting precipitation responses are 1 standard deviation apart (Fig. 11(e)). At 0.9°C cooling, the resulting temperature responses are exactly 1 standard deviation apart (Fig. 11(c)), and the precipitation responses are 0.5 standard deviation apart (Fig. 11(f)). For any cooling level lower than 0.9°C, temperature responses of GLENS and EQ

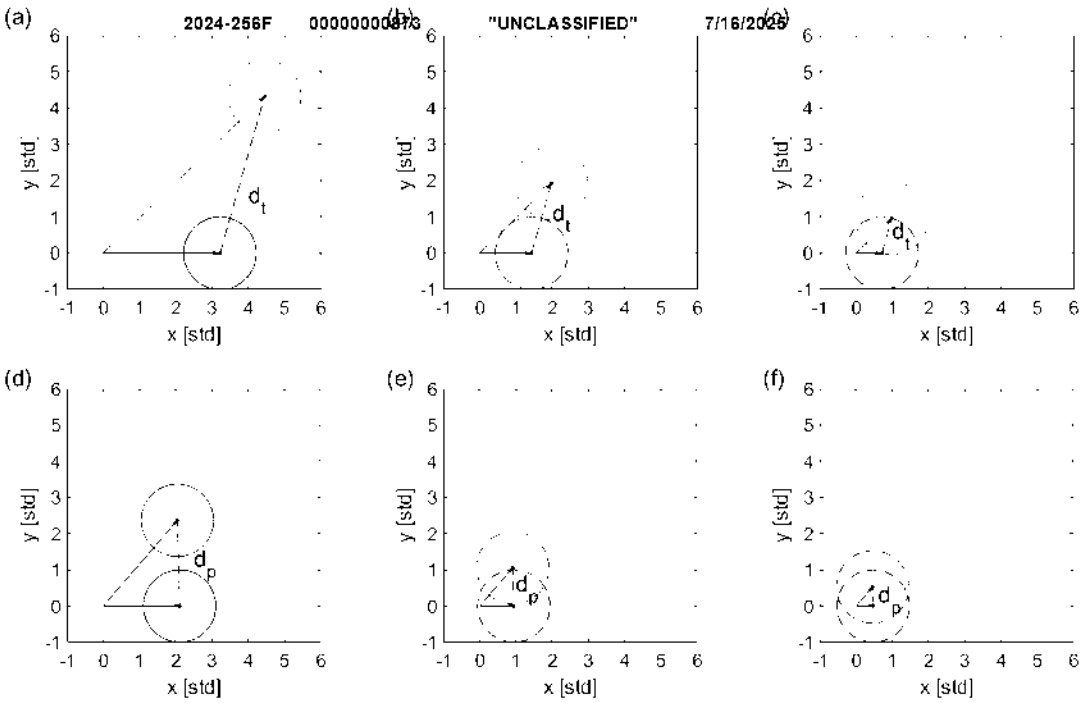

Figure 11. Top panels are detectability plots for the difference in temperature responses between GLENS (black) and EQ (red) at three different levels of cooling: (a) 4°C, (b) 1.8°C, and (c) 0.9°C. Bottom panels are detectability plots for the difference in precipitation responses between GLENS (black) and EQ (red) at those three levels of cooling. Dots represent the estimated mean temperature or precipitation responses for the corresponding levels of cooling. Temperature and precipitation responses are expressed in number of standard deviations (std) of 20-year averages of temperature and precipitation respectively. As the cooling level decreases, less area on the Earth has detectably different climate responses and the ability to detect the difference between GLENS and EQ decreases.

will not be detectably different by our metric; that is to say, less than 5% of area on the Earth is expected to have detectably different temperature responses at a 95% confidence level over a 20-year period. On the other hand, to have detectably different precipitation responses between GLENS and EQ, the cooling level needs to be higher than 1.8°C. The cooling levels of 0.9°C and 1.8°C are defined as the cut-off cooling levels for detectable difference in temperature and precipitation, respectively, between GLENS and EQ. Note that for sufficiently small amounts of cooling, the resulting climate from these strategies will also be undetectably different from the climate with neither increased greenhouse gases nor SAI; from Fig. 7, they will be detectably different from the climate with increased GHG except at very small levels of cooling.

As shown in Fig. 11, the cut-off level of cooling ΔT_t is inversely proportional to d_t and the cut-off level of cooling ΔT_p is inversely proportional to d_p:

$$\Delta T_t = \frac{1}{d_t} \tag{10}$$

$$\Delta T_p = \frac{1}{d_p} \tag{11}$$

By substituting eq. (10) into eq. (8) and substituting eq. (11) into eq. (9), we obtain two functions that can be used to estimate a threshold value of AOD angle, θ_a, which is used to assess the detectability of different injection choices at different levels of cooling:

$$\theta_a^t = 24/\Delta T_t \tag{12}$$

$$\theta_a^p = 40/\Delta T_p \tag{13}$$

Thus, given a particular level of cooling, we can calculate if two injection strategies are expected to result in detectably different temperature or precipitation responses by comparing their AOD patterns. If the angle between the patterns of AOD is smaller than θ_a^t or θ_a^p, these two strategies can be expected to not result in detectably different temperature or precipitation responses. However, if the angle between the patterns of AOD is larger than θ_a^t or θ_a^p, these two strategies can be expected to be meaningfully independent in terms of temperature responses or precipitation responses. In Fig. 12, we compare the cut-off AOD angles predicted by eq. (12) and eq. (13). As shown in Fig. 12, the threshold values of AOD angle predicted using temperature responses are always lower than those predicted using precipitation responses.

6 Estimating the Number of DOF

In the previous sections, we estimate the relationship between the number of DOFs included and the maximum error in approximating AOD, and the relationship between the AOD angles and the level of cooling at which the resulting temperature or precipitation response could be expected to be detectably different. In this section, we combine these two to estimate how many meaningfully-independent DOF there are as a function of the levels of cooling.

As changes in temperature are more detectable than those in precipitation, the extent to which two AOD patterns are sufficiently similar, and thus the number of DOF in the SAI design space, are determined by the temperature response. Using eq. (12), we calculate the cut-off AOD angle θ_a^t (listed in Table 2) for cooling levels of 0.5°C, 1°C, 1.5°C, and 2°C. It is expected that two SAI strategies with AOD differing by any angle smaller than θ_a^t, will not result in detectably different temperature or precipitation responses. Figure 13 shows the four cut-off AOD angles and the corresponding minimum numbers of DOF required for $\theta^*(n)$ not exceeding the cut-off value, θ_a^t (also listed in Table 2).

$$\theta^*(n) \leq \theta_a^t(\Delta T) \tag{14}$$

Any set of injection choices that has a θ_{max} smaller than the cut-off angle $\theta_a^t(\Delta T)$ will form a design space that captures all detectably different climate responses. That is, for any possible injection strategy not included in the design space, you can find

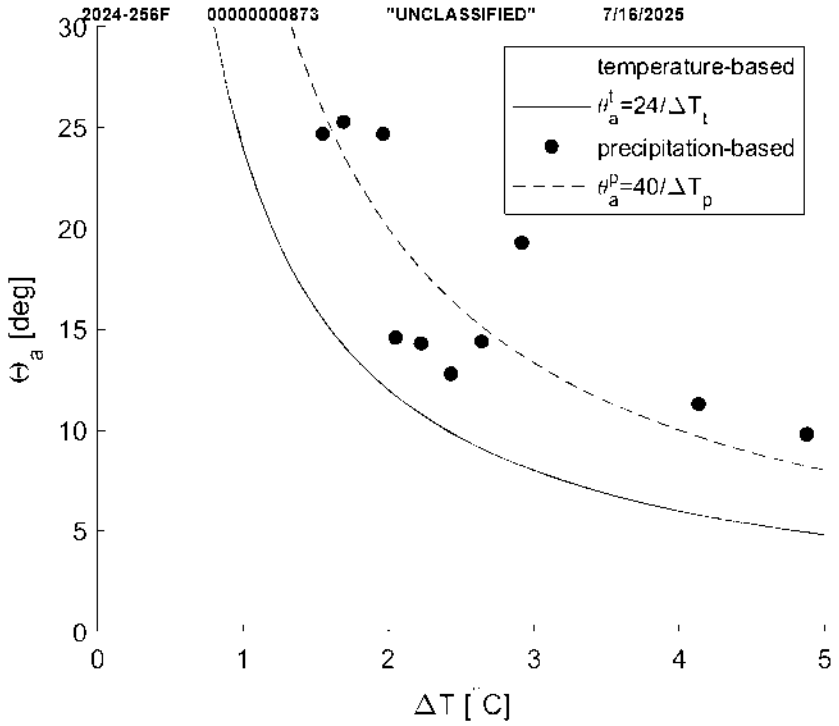

Figure 12. The cut-off AOD angle θ_a at different levels of cooling ΔT estimated using temperature responses and precipitation responses.

Table 2. The minimum number of DOF, n, of the SAI design space for four targeted levels of cooling. At each level of cooling, θ_a^t is the maximum angle that can be formed between two AOD patterns that yield undetectably different temperature responses. $\theta^*(n)$ is the maximum angle that can be formed between any AOD pattern and the design space of n DOF, and must be smaller than θ_a^t.

Targeted level of cooling [°C]	Cut-off angle θ_a^t	Minimum number of DOF, n	$\theta^*(n)$
0.5	48°	2	38°
1	24°	6	18°
1.5	16°	8	15°
2	12°	12	11°

an injection strategy in the design space such that the angle between their AOD patterns is smaller than θ_a^t and the difference in the corresponding climate responses is sufficiently small such that they are not meaningfully different.

As shown in Table 2, as the targeted level of cooling increases, the cut-off value of θ_a^t decreases and the minimum number of DOF increases. For a targeted cooling level of 1°C, we likely need 6 DOFs. For any possible AOD pattern, the angle between it and the AOD pattern approximated by a design space of 6 DOFs is likely to be smaller than 24° , and the resulting difference in climate response will be largely undetectable. For a targeted cooling level of 1.5°C, we likely need 8 DOFs. This finding

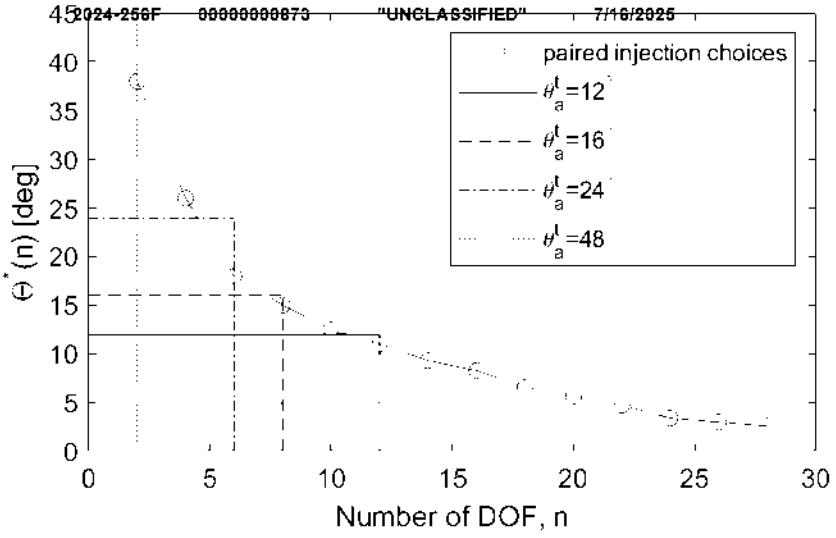

Figure 13. The minimum number of DOF corresponding to the worst-case error in approximating AOD, θ_a^t.

significantly reduces the dimension of the design space needed for evaluating the possible climate impacts of different SAI strategies and associated trade-offs.

For a cooling level of 1°C, the best set of 6 among the set of 29 sample injection choices are: (i) spring injections at 60° N/60° S, (ii) annual injections at 30° N/30° S and (iii) winter and summer injections at the equator. Figure 14 shows the AOD spatiotemporal patterns of the six injections in the best set. A set of 6 that instead includes annually-constant injection at 30° N, 15° N, 15° S, and 30° S (the four cases considered in MacMartin et al. (2017), Kravitz et al. (2017), and Tilmes et al. (2018)) as well as spring injection at 60° N (as in Lee et al. (2021)) and 60° S is only slightly worse than this optimal set, within a range of 0.1° , still sufficient to span the design space for 1°C cooling.

For a cooling level of 1.5°C, the best set of 8 is similar to the best set of 6 but with equatorial injections at the other two seasons instead and the addition of summer injections at 15° N and 15° S. Note that in the optimization earlier, we constrained our search to hemispherically symmetric pairs of injection choices. Including only annually-constant injection at the equator rather than two seasons yields a set of 7 injection choices that performs almost as well as the optimal set of 8 and is still sufficient for 1.5°C cooling.

7 Analysis of injections at different altitudes

The SAI simulations analyzed in the previous sections are all high-altitude injections (6-7 km above the tropopause). Tilmes et al. (2017) also conducted low-altitude (5 km lower) simulations at 50° N, 30° N, 15° N, 0°, 15° S, 30° S and 50° S with an annual injection rate of 6 Tg yr^{-1}, all simulated in CESM1(WACCM). The AOD patterns of low-altitude and high-altitude injections are shown in Fig. 15. For each injection case, the spatiotemporal AOD responses are weighted by TOA incoming

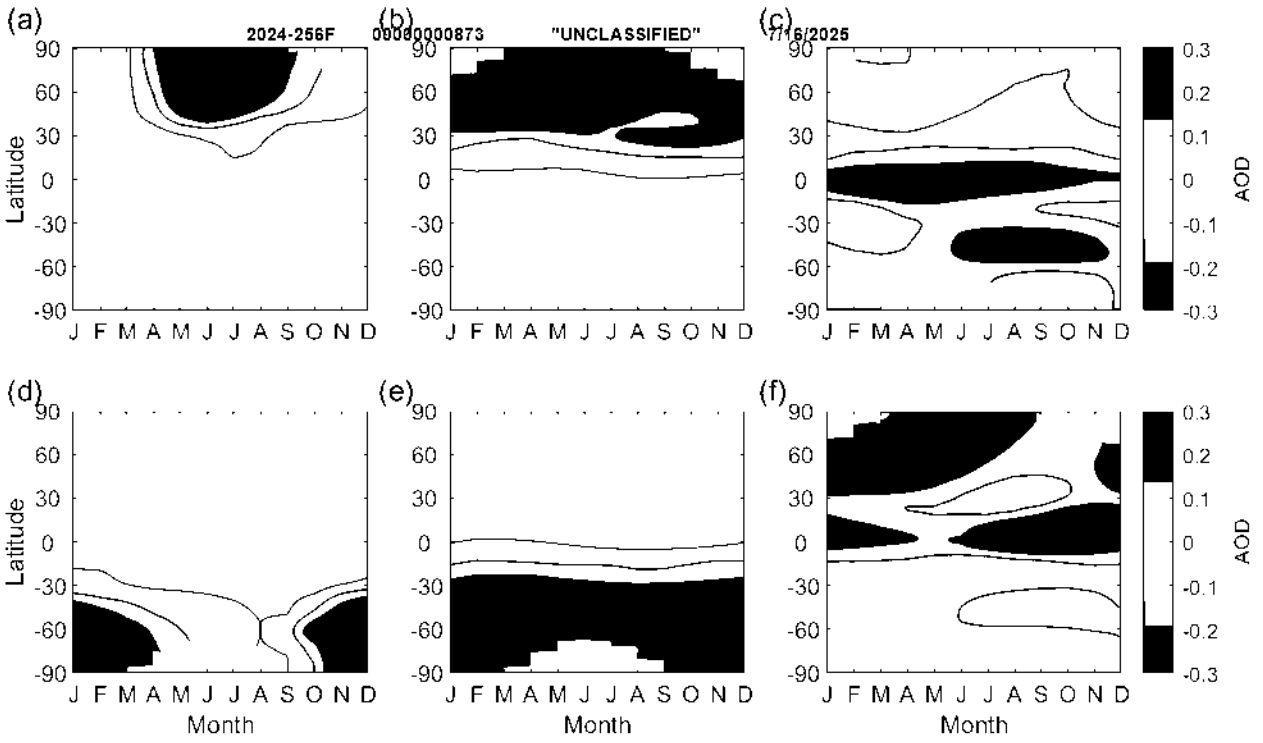

Figure 14. AOD patterns from the best set of 6 injections: (a) spring injection at 60° N, (b) annual injection at 30° N, (c) winter injection at 0° (d) spring injection at 60° S, (e) annual injection at 30° S, and (f) summer injection at 0°.

Table 3. Angle between the AOD vector of each high-altitude injection and the set of all low-altitude injections.

Injection latitude	50° N	30° N	15° N	0°	15° S	30° S	50° S
θ_{AOD}	5.3°	11.6°	6.2°	7.0°	4.5°	6.3°	4.9°

solar energy. The angle of the AOD pattern of each high-altitude injection with respect to the set of all low-altitude injections is listed in Table 3; these high-altitude injections are all within a small angle with respect to the set of low-altitude injections. For a level of cooling under 2°C, the difference of AOD responses due to injecting at these different altitudes is small compared to the differences achievable through injecting at different latitudes and seasons. If a much higher level of cooling is desired, injecting at different altitudes may result in meaningfully different surface climates and injection choices of different altitudes may need to be considered when choosing the design space and evaluating trade-offs. Injection at or below the tropopause, while inefficient, would likely result in more significant differences in AOD patterns (Bernstein et al., 2013).

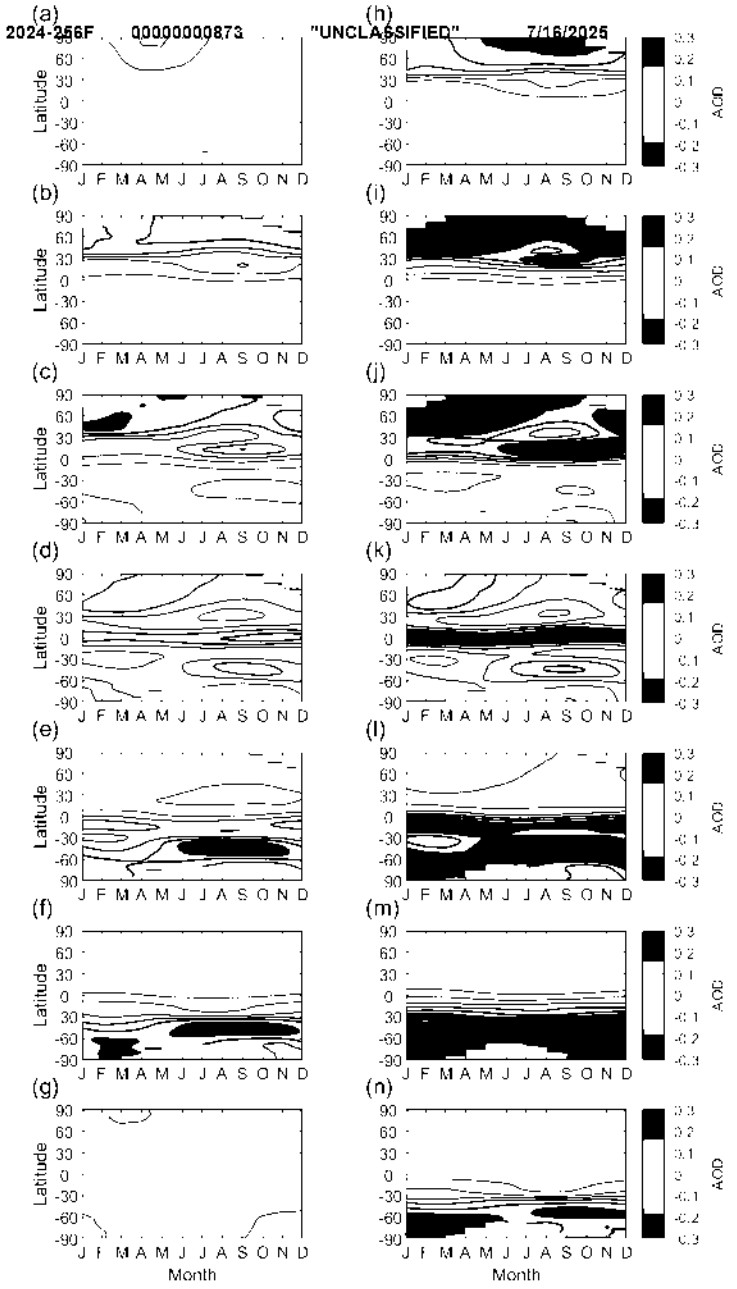

Figure 15. AOD patterns produced by low-altitude annually-constant injection of 6 Tg yr^{-1} at (a) 50° N, (b) 30° N, (c) 15° N, (d) 0°, (e) 15° S, (f) 30° S, (g) 50° S and high-altitude annually-constant injection of 6 Tg yr^{-1} at (h) 50° N, (i) 30° N, (j) 15° N, (k) 0°, (l) 15° S, (m) 30° S, (n) 50° S.

8 Conclusions

Previous studies have shown that different choices of stratospheric aerosol injection latitudes and seasons lead to different surface climate responses. Choosing where and when to inject aerosols to the stratosphere to meet different climate goals can be considered as a design problem. Previous studies have concluded that there are at least 3 degrees of freedom (DOF), that is, at least three independent climate goals can be simultaneously met. These three – basically the global mean aerosol burden, the interhemispheric difference, and the equator-to-pole difference – were motivated by physical intuition regarding stratospheric transport, which will ultimately constrain how many independent DOFs are achievable through different injection choices. A key observation is that the number of DOF effectively depends on the amount of global cooling provided by SAI, because for a small amount of cooling, the difference in the climate response for different strategies may not be detectable. As the amount of cooling increases, the number of meaningfully-independent DOF increases. For a cooling level of 1-1.5°C, there are likely between 6 and 8 meaningfully-independent DOFs. If only precipitation changes mattered, and not temperature changes, then there would be fewer meaningfully-independent DOFs.

Our estimation of the number of DOF provides useful guidance to bound the number of injection choices that need to be considered when evaluating the range of possible different SAI strategies and the trade-offs among them. If only a small amount of cooling is needed from implementing stratospheric aerosol injections, a small set of selected injection choices would be sufficient to capture the range of possible resulting climate responses and evaluate how different those climate responses could be. As all possible injection choices form an extremely high dimensional design space, only considering the meaningfully-independent injection choices significantly reduces the dimension of the design space.

The number of meaningfully-independent DOF determines the number of independent climate metrics that SAI can manage simultaneously. Thus, for a cooling level of 1-1.5°C, for example, SAI can manage 6-8 independent climate metrics at the same time. This expands the manageable number of climate metrics relative to what has been considered in previous studies, opening up new opportunities for exploring alternate designs that will have different distributions of impacts.

It is important to note that all of these results are obtained from a single climate model. Other climate models may produce different numerical results. Nonetheless, the number of independent DOF needed to span the range of possible different stratospheric AOD patterns can be reasonably expected to remain consistent as the transport of aerosols are constrained by stratospheric circulation. We make several simplifying approximations in order to make analysis tractable, particularly to estimate the relationship between how similar or dissimilar two patterns of AOD are and how similar or dissimilar the corresponding surface climate is; future research could explore the impact of these approximations. First, we only consider changes in temperature and precipitation, and we only consider changes in annual mean rather than shifts in seasonality, which could matter at high latitudes in particular (Jiang et al., 2019). Second, we only consider whether the difference in climate response would be detectable over a 20-year period. Third, the globally-aggregated metric we use for determining whether two different climate responses are "detectable" is based on whether they are detectably-different at a 95% confidence level over 5% of the surface area. However, changes that are less-confidently detected may still matter, and since social, agricultural and other economic activities are strongly affected by regional climate changes, just because they only happen in a small percentage

of area, does not necessarily mean that they are not important – the details of where and what the differences are potentially matter.

A key outcome of this study is that further research should be conducted to explore alternate SAI designs that can manage more than 3 and up to 8 independent climate metrics simultaneously, and to compare the resulting climate responses and associated trade-offs. Research into more than 8 is less policy-relevant, simply because any hypothetical deployment scenario would not reach more than 1.5 °C cooling for many decades, if ever. Ultimately, to evaluate the impacts of stratospheric aerosol geoengineering, regional surface climate needs to be considered, as social and economic activities are significantly affected by regional climate change. Alternate SAI designs may enable a better compensation of the impacts from climate change; alternate designs might also lead to the potential to create more novel climates that optimize some metrics at the expense of others – both of these possibilities are important to understand in order to inform not only future scientific research in SAI but also governance challenges.

Data availability. Data for the new simulations presented in this study (specifically, monthly aerosol optical depth (AOD) for spring injections at 60°N, 45°N, 45°S, and 60°S and annually-constant injections at 7.5°N, 22.5°N, and 37.5°N) are available through the Cornell e-Commons Library at https://doi.org/10.7298/f1e4-sq40 (Zhang et al., 2021). Data for GLENS and equatorial (from Tilmes et al., 2018 and Kravitz et al., 2019 respectively) are available at https://doi.org/10.5065/D6JH3JXX, data for iSpring and iAutumn (from Visioni et al., 2020c) are available at https://doi.org/10.7298/c92j-2p46 (Visioni et al., 2020a), and data for PREC (from Lee et al., 2020a) are available at https://doi.org/10.7298/d2qm-1568 (Lee et al., 2020b).

Author contributions. YZ conducted all analyses and wrote the paper with editing from DM, BK and DV; YZ and DM conceived the study with input from all authors and DV assisted with conducting simulations.

Competing interests. The authors declare that they have no conflict of interest.

Acknowledgements. The authors would like to acknowledge high-performance computing support from Cheyenne (https://doi.org/10.5065/D6RX99HX) provided by NCAR's Computational and Information Systems Laboratory, sponsored by the National Science Foundation. Support for Y. Zhang and D. G. MacMartin was provided by the National Science Foundation through agreement CBET-1818759 and CBET-2038246. Support for D. Visioni was provided by the Atkinson Center for a Sustainable Future at Cornell University. Support for BK was provided in part by the National Science Foundation through agreement CBET-1931641, the Indiana University Environmental Resilience Institute, and the Prepared for Environmental Change Grand Challenge initiative. The Pacific Northwest National Laboratory is operated for the U.S. Department of Energy by Battelle Memorial Institute under contract DEAC05-76RL01830. The CESM project is supported primarily by the National Science Foundation.

References

Bala, G., Duffy, P. B., and Taylor, K. E.: Impact of geoengineering schemes on the global hydrological cycle, PNAS, 105, 7664–7669, 2008.

Ban-Weiss, G. A. and Caldeira, K.: Geoengineering as an optimization problem, Environ. Res. Lett., 5, 034 009, doi:10.1088/1748-9326/5/3/034009, 2010.

Bernstein, D. N., Neelin, J. D., Li, Q. B., and Chen, D.: Could aerosol emissions be used for regional heat wave mitigation?, Atmospheric Chemistry and Physics, 13, 6373–6390, https://doi.org/10.5194/acp-13-6373-2013, 2013.

Dai, Z., Weisenstein, D., and Keith, D. W.: Tailoring meridional and seasonal radiative forcing by sulfate aerosol solar geoengineering, Geophys. Res. Lett., dOI: 10.1002/2017GL076472, 2018.

Jiang, J., Cao, L., MacMartin, D. G., Simpson, I. R., Kravitz, B., Cheng, W., Visioni, D., Tilmes, S., Richter, J. H., and Mills, M. J.: Stratospheric Sulfate Aerosol Geoengineering Could Alter the High-Latitude Seasonal Cycle, Geophysical Research Letters, 46, 14 153–14 163, https://doi.org/https://doi.org/10.1029/2019GL085758, 2019.

Kravitz, B., Robock, A., Boucher, O., Schmidt, H., Taylor, K. E., Stenchikov, G., and Schulz, M.: The Geoengineering Model Intercomparison Project (GeoMIP), Atm. Sci. Lett., 12, 162–167, doi:10.1002/asl.316, 2011.

Kravitz, B., MacMartin, D. G., Wang, H., and Rasch, P. J.: Geoengineering as a Design Problem, Earth Systems Dynamics, 7, 469–497, doi:10.5194/esd-7-469-2016, 2016.

Kravitz, B., MacMartin, D. G., Mills, M. J., Richter, J. H., Tilmes, S., Lamarque, J.-F., Tribbia, J. J., and Vitt, F.: First simulations of designing stratospheric sulfate aerosol geoengineering to meet multiple simultaneous climate objectives, J. Geophys. Res. A, 122, 12,616–12,634, doi:10.1002/2017JD026874, 2017.

Kravitz, B. et al.: The Geoengineering Model Intercomparison Project Phase 6 (GeoMIP6): Simulation design and preliminary results, Geoscientific Model Development, 8, 3379–3392, doi: 10.5194/gmd-8-3379-2015, 2015.

Kravitz, B. et al.: Comparing surface and stratospheric impacts of geoengineering with different SO_2 injection strategies, J. Geophys. Res. A, 124, 2019.

Lee, W., MacMartin, D., Visioni, D., and Kravitz, B.: Expanding the design space of stratospheric aerosol geoengineering to include precipitation-based objectives and explore trade-offs, Earth System Dynamics, 11, 1051–1072, https://doi.org/10.5194/esd-11-1051-2020, 2020a.

Lee, W., MacMartin, D., Visioni, D., and Kravitz, B.: Data from: Expanding the design space of stratospheric aerosol geoengineering to include precipitation-based objectives and explore trade-offs [Dataset], Cornell University eCommons Repository, https://doi.org/10.7298/d2qm-1568, 2020b.

Lee, W., MacMartin, D., Visioni, D., and Kravitz, B.: High-Latitude stratospheric aerosol geoengineering can be more effective if injection is limited to spring, Geophysical Research Letters, 48, https://doi.org/10.1029/2021GL092696, 2021.

MacMartin, D. G. and Kravitz, B.: The engineering of climate engineering, Annual Reviews of Control, Robotics, and Autonomous Systems, 2, 445–467, doi:10.1146/annurev-control-053018-023725, 2019.

MacMartin, D. G., Kravitz, B., Tilmes, S., Richter, J. H., Mills, M. J., Lamarque, J.-F., Tribbia, J. J., and Vitt, F.: The climate response to stratospheric aerosol geoengineering can be tailored using multiple injection locations, J. Geophys. Res. A, 122, 12,574–12,590, doi:10.1002/2017JD026868, 2017.

Mills, M., Richter, J. H., Tilmes, S., Kravitz, B., MacMartin, D. G., Glanville, A. A., Tribbia, J. J., Lamarque, J.-F., Vitt, F., Schmidt, A., Gettelman, A., Hannay, C., Bacmeister, J. T., and Kinnison, D. E.: Radiative and chemical response to interactive stratospheric aerosols in fully coupled CESM1(WACCM), J. Geophys. Res. A., 122, 13,061–13,078, doi:10.1002/2017JD027006, 2017.

Rasch, P. J., Crutzen, P. J., and Coleman, D. B.: Exploring the geoengineering of climate using stratospheric sulfate aerosols: The role of particle size, Geophys. Res. Lett., 35, L02 809, doi:10.1029/ 2007GL032179, 2008.

Ricke, K. L., Granger Morgan, M., and Allen, M. R.: Regional climate response to solar-radiation management, Nature Geoscience, 3, 537–541, https://doi.org/10.1038/NGEO915, 2010.

Robock, A., Oman, L., and Stenchikov, G.: Regional climate responses to geoengineering with tropical and Arctic SO_2 injections, J. Geophys. Res., 113, d16101, 2008.

Tilmes, S., Richter, J. H., Mills, M. J., Kravitz, B., MacMartin, D. G., Vitt, F., Tribbia, J. J., and Lamarque, J.-F.: Sensitivity of aerosol distribution and climate response to stratospheric SO_2 injection locations, J. Geophys. Res. A., 122, 12,591–12,615, doi:10.1002/2017JD026888, 2017.

Tilmes, S., Richter, J. H., Kravitz, B., MacMartin, D. G., Mills, M. J., Simpson, I., Glanville, A. S., Fasullo, J. T., Phillips, A. S., Lamarque, J.-F., Tribbia, J., Edwards, J., Mickelson, S., and Gosh, S.: CESM1(WACCM) stratospheric aerosol geoengineering large ensemble (GLENS) project, Bull. Am. Met. Soc., doi:10.1175/BAMS-D-17-0267.1, 2018.

Tilmes, S. et al.: The hydrological impact of geoengineering in the Geoengineering Model Intercomparison Project (GeoMIP), J. Geophys. Res., 118, 11 036–11 058, doi:10.1002/jgrd.50868, 2013.

Visioni, D., MacMartin, D. G., Kravitz, B., Tilmes, S., Mills, M. J., Richter, J. H., and Boudreau, M. P.: Seasonal Injection Strategies for Stratospheric Aerosol Geoengineering, Geophysical Research Letters, 46, 7790–7799, https://doi.org/10.1029/2019GL083680, 2019.

Visioni, D., MacMartin, D., Kravitz, B., Richter, Y., Tilmes, S., and Mills, M.: Data from: Seasonally Modulated Stratospheric Aerosol Geoengineering Alters the Climate Outcomes [Dataset], Cornell University eCommons Repository, https://doi.org/10.1029/2020GL088337, 2020a.

Visioni, D., MacMartin, D. G., Kravitz, B., Lee, W., Simpson, I. R., and Richter, J. H.: Reduced Poleward Transport Due to Stratospheric Heating Under Stratospheric Aerosols Geoengineering, Geophysical Research Letters, 47, e2020GL089 470, https://doi.org/https://doi.org/10.1029/2020GL089470, 2020b.

Visioni, D., MacMartin, D. G., Kravitz, B., Richter, J. H., Tilmes, S., and Mills, M. J.: Seasonally Modulated Stratospheric Aerosol Geoengineering Alters the Climate Outcomes, Geophysical Research Letters, 47, e2020GL088 337, https://doi.org/10.1029/2020GL088337, 2020c.

Wilks, D. S.: Statistical methods in the atmospheric sciences, Elsevier, 2019.

Zhang, Y., MacMartin, D., Visioni, D., and Kravitz, B.: Data from: How large is the design space for stratospheric aerosol geoengineering? [Dataset], Cornell University eCommons Repository, https://doi.org/10.7298/f1e4-sq40, 2021.

High-latitude stratospheric aerosol injection to preserve the Arctic

Walker Raymond Lee[1], Douglas G. MacMartin[1], Daniele Visioni[1], Ben Kravitz[2,3], Yating Chen[4], John C. Moore[4,5,6], Gunter Leguy[7], David M. Lawrence[7], David A. Bailey[7]

[1]Sibley School for Mechanical and Aerospace Engineering, Cornell University, Ithaca, NY, USA
[2]Department of Earth and Atmospheric Science, Indiana University, Bloomington, IN, USA
[3]Atmospheric Sciences and Global Change Division, Pacific Northwest National Laboratory, Richland, WA, USA
[4]College of Global Change and Earth System Science, Beijing Normal University, Beijing, 100875, China
[5]CAS Center for Excellence in Tibetan Plateau Earth Sciences, Beijing, 100101, China
[6]Arctic Centre, University of Lapland, Rovaniemi, Finland
[7]Climate and Global Dynamics Laboratory, National Center for Atmospheric Research, Boulder, CO, USA

Key Points:

- Stratospheric aerosol injection at high latitudes could preferentially reduce the impacts of global warming in the Arctic
- Simulations of such injection increase sea ice and permafrost extents and preserve Greenland ice sheet mass
- High latitude injection preserves the Arctic more efficiently than tropical injection but also substantially affects tropical precipitation

Corresponding author: Walker Raymond Lee, wl644@cornell.edu

Abstract 2024-256F 00000000872 "UNCLASSIFIED" 7/16/2025

Stratospheric aerosol injection (SAI) has been shown in climate models to reduce some impacts of global warming in the Arctic, including the loss of sea ice, permafrost thaw, and reduction of Greenland Ice Sheet (GrIS) mass: SAI at high latitudes could preferentially target these impacts. In this study, we use the Community Earth System Model to simulate two Arctic-focused SAI strategies, which inject at 60°N latitude each spring with injection rates adjusted to either maintain September Arctic sea ice at 2030 levels ("Arctic Low") or restore it to 2010 levels ("Arctic High"). Both simulations maintain or restore September sea ice to within 10% of their respective targets, reduce permafrost thaw, and increase GrIS surface mass balance by reducing runoff. Arctic High reduces these impacts more effectively than a globally-focused SAI strategy that injects similar quantities of SO_2 at lower latitudes. However, Arctic-focused SAI is not merely a "reset button" for the Arctic climate, but brings about a novel climate state, including changes to the seasonal cycles of Northern Hemisphere temperature and sea ice and less high-latitude carbon uptake relative to SSP2-4.5. Additionally, while Arctic-focused SAI produces the most cooling near the pole, its effects are not confined to the Arctic, including detectable cooling throughout most of the northern hemisphere for both simulations, increased mid-latitude sulfur deposition, and a southward shift of the location of the Intertropical Convergence Zone (ITCZ). For these reasons, it would be incorrect to consider Arctic-focused SAI as "local" geoengineering, even when compared to a globally-focused strategy.

Plain Language Summary

The injection of reflective particles called sulfate aerosols into the atmosphere to reflect sunlight, commonly called "stratospheric aerosol injection" (SAI) or simply "geoengineering", could be used alongside emission cuts and CO_2 removal to cool the planet and reduce global warming. Concentrating this particle injection at high latitudes could be used to preserve the Arctic. We simulate such "Arctic-focused" geoengineering and find that it does indeed preserve sea ice, permafrost, and the Greenland Ice Sheet. However, focusing on the Arctic also introduces complications: large quantities of carbon are stored by plants at mid-to-high latitudes, and cooling the Arctic may reduce their ability to take up carbon from the atmosphere. Additionally, cooling the Arctic more than the tropics could affect the way heat is transported around the planet, changing important precipitation patterns near the equator. Finally, most of the injected sulfur would come back down in the highly-populated middle latitudes and the relatively pristine high latitudes, likely affecting ecosystems in both regions. For these reasons, we find that even though such an "Arctic-focused" geoengineering would predominantly cool the Arctic, it would be incorrect to think of it as a "local" intervention, as it would affect the rest of the planet too.

1 Introduction

The Arctic is especially vulnerable to global warming: the northern high latitudes respond more strongly to external forcing than the rest of the planet by a factor of two to four, a phenomenon referred to as Arctic amplification (Previdi et al., 2021; England et al., 2021; Pithan & Mauritsen, 2014), and this faster warming in the Arctic is predicted to have consequences for the rest of the world. The extent of sea ice, which insulates the ocean from sunlight and plays crucial dynamic and thermodynamic roles in the Arctic climate and ecosystems, has decreased in all months of the year over the 1980-2018 period (Stroeve & Notz, 2018), and there is a very high likelihood that the Arctic Ocean will become ice-free in summertime before mid-century (Notz & Stroeve, 2018). The melting of ice and snow at high latitudes will cause more radiation to be absorbed by the darker ground and ocean, and models estimate this ice-albedo feedback could contribute an ad-

ditional 2-4 K of warming in the Arctic by the end of the century in a high-emissions scenario (Pithan & Mauritsen, 2014; Cai et al., 2021). Permafrost - perennially-frozen soil at high latitudes - contains an estimated 1300 Pg (Hugelius et al., 2014) to 1600 Pg (Tarnocai et al., 2009) of carbon, with approximately 500 Pg of this reservoir contained in the topmost meter of soil (1 Pg = 1 Gt = 10^{15} g). Globally, permafrost temperatures have increased by an average of 0.29°C over the last two decades (Biskaborn et al., 2019), and as permafrost thaws under strong warming scenarios, an estimated 5-15% or more of the carbon contained in the permafrost zone may decompose and be released into the atmosphere as CO_2 or CH_4 (Schuur et al., 2015; Plaza et al., 2019). This permafrost-carbon-climate feedback is estimated in models to contribute an additional 0.1°C-0.3°C of global warming by 2100, depending on the emissions scenario, but these estimates are very poorly constrained (Schuur et al., 2015; Stocker et al., 2013; Schaefer et al., 2014; McGuire et al., 2018). Lastly, the mass balance of the Greenland Ice Sheet (GrIS) has transitioned from approximately neutral in the 1990s to increasingly negative over the past 20 years (Bamber et al., 2018). The observed annual contribution of the GrIS to global mean sea level rise has increased since the 1990s (Mouginot et al., 2019), and the IPCC's 6th Assessment Report estimates that the GrIS will likely contribute a total of 1-10 cm of sea level rise by 2100 under a low-emissions scenario and 9-18 cm under a high-emissions scenario (Fox-Kemper et al., 2021).

The artificial reflection of sunlight to cool the earth's surface, referred to henceforth as solar radiation modification (SRM) but also varyingly called solar geoengineering, climate engineering, solar radiation management, or solar climate intervention, has been proposed as a possible additional response to global warming alongside emission mitigation and carbon dioxide removal. Of the proposed methods of SRM, the best understood is stratospheric aerosol injection (SAI), which aims to mimic the global cooling that follows large volcanic eruptions. The effects of SAI on the surface climate depend on the latitude(s) of injection; therefore, the question of SAI is not just whether or not to deploy, but also how. The majority of SAI simulations thus far use low-latitude injections (e.g., 30° and 15°N and S) to cool the planet relatively evenly (Kravitz et al., 2017; Tilmes et al., 2018, 2020; MacMartin & Kravitz, 2019; MacMartin et al., 2022; Richter et al., 2022); such "globally-focused" strategies have been found to preserve sea ice, and they can even be designed with sea ice preservation as a primary goal (W. Lee et al., 2020). Low-latitude SAI could also slow the degradation of permafrost and mitigate carbon loss (Chen et al., 2020; H. Lee et al., 2019) and preserve Greenland ice sheet mass (Moore et al., 2019). However, an "Arctic-focused" strategy (for example, injecting at 60°N in the springtime), could more efficiently cool the high latitudes with less cooling at lower latitudes, thus preferentially targeting impacts in or near the Arctic (Robock et al., 2008; W. Lee et al., 2021). However, Arctic-focused SAI could also introduce complications; for example, hemispherically asymmetric cooling could push the ITCZ towards the opposite hemisphere, impacting tropical precipitation (Haywood et al., 2013; Krishnamohan & Bala, 2022), and both Robock et al. (2008) and Jackson et al. (2015) observed such a disruption in the summer monsoons for high-latitude injection. Additionally, local impacts such as sulfur deposition would impact ecosystems and the people who live in them. Other physical mechanisms could also impact the effectiveness of high-latitude SAI relative to tropical SAI: lower insolation, a higher underlying albedo due to snow and ice cover, and lower aerosol lifetime due to stratospheric dynamics. Lastly, sea ice extent (for example) is not strictly a function of temperature and sunlight, but has complex relationships with atmospheric and oceanic circulation (Moore et al., 2014). Timely research of the physical impacts of SAI is crucial to inform future decision-making (National Academies of Sciences, Engineering, and Medicine, 2021); however, Arctic-focused SAI has received comparatively less research attention relative to globally-focused strategies. Robock et al. (2008) compared tropical and high-latitude injections to observe the effects on surface temperature, precipitation, and sea ice, but the injection amounts were relatively small and the study only considered 10-year averages for many of its results, making the signal-to-noise ratio quite low. That study also injected year-round for both

strategies, whereas springtime has been found to be more efficient for high-latitude injection (W. Lee et al., 2021) Additionally, climate models have evolved substantially over the past 15 years; for example, Robock et al. (2008) used a bulk aerosol treatment, whereas many present-day models use more complex modal treatments. Jackson et al. (2015) found that Arctic sea ice could be recovered with springtime high-latitude injection, but the primary focus of that study was to assess the controllability of Arctic sea ice rather than to diagnose the effects of SAI; those simulations introduced additional noise to the model output, added several explosive volcanic eruptions, and made random changes to the timing of injection to challenge the control algorithms. Beyond surface temperature, precipitation, and sea ice, the other possible impacts of Arctic-focused SAI (such as permafrost and GrIS surface mass balance) remain largely unanalyzed.

While large, hemispherically-asymmetric injections may ultimately prove untenable due to the possible effects on tropical precipitation, it is plausible that an SAI strategy could include some amount of injection at 60°N, possibly alongside Antarctic or tropical southern hemisphere injection. Simulating Arctic-focused SAI is important to begin i) understanding the effects of SAI on the Arctic, and ii) quantifying possible side-effects, such as changes to tropical precipitation. In this study, we aim to provide a comprehensive analysis of Arctic-focused SAI by simulating two high-latitude injection strategies and comparing them to three globally-focused strategies. Section 2 describes our methodology, including the climate model and experimental design process. In Section 3, we investigate how our strategies affect the climate system: we begin by diagnosing changes to shortwave (SW) and longwave (LW) energy budgets, and we then analyze the effects of our strategies on the Arctic and global surface environments, including sea ice extent, permafrost carbon flux, GrIS mass, surface temperature, and precipitation. In Section 4, we present our conclusions and discuss the implications of our research for future work. Additional results (including effects on ozone and the Atlantic Meridional Overturning Circulation) and information about statistical methods and feedback algorithm design are documented in the Supporting Information (SI).

2 Methods

2.1 Climate Model

Our simulations are conducted using version 2 of the Community Earth System Model (CESM2, described by Danabasoglu et al. (2020)) with version 6 of the Whole Atmosphere Community Climate Model (WACCM6, described by Gettelman et al. (2019)) as the atmospheric component, run using the "middle atmosphere" (MA) chemistry mechanism to improve computational efficiency by greatly reducing the tropospheric chemistry scheme. We denote this configuration as CESM2(WACCM-MA). The configuration is the same as that used by the globally-focused strategies of MacMartin et al. (2022), to which we will compare our Arctic-focused simulations. CESM2 is a state-of-the-art Earth System Model with fully-coupled atmosphere, ocean, land, sea ice, land ice, river, and wave components, and WACCM6 has a horizontal resolution of 0.95° latitude x 1.25° longitude and 70 vertical model levels extending up to ~140 km, or 4.5×10^{-6} hPa. CESM2(WACCM6) performs well in modeling sea ice behavior relative to observations; it matches observed seasonal cycles and decreasing trends of sea ice extent and volume (DuVivier et al., 2020) and matches historical sea ice extent and volume observations as well as or better than any other model in Phase 6 of the Coupled Model Intercomparison Project (Notz & SIMIP, 2020). The middle atmosphere variant of CESM2(WACCM6) used here is similar to configurations of CESM1(WACCM) (Mills et al., 2017) used in the Geoengineering Large Ensemble (GLENS) project (Kravitz et al., 2017; Tilmes et al., 2018).

WACCM6 uses version 4 of the Modal Aerosol Model (MAM4), which uses a three-bin aerosol distribution system and has been validated against in-situ observations (Liu et al., 2016; Mills et al., 2017). The oceanic component is version 2 of the Parallel Ocean

Table 1. Simulation Parameters

Name	Inj. Latitude	Inj. Months	Target[a]	Ref. Period[b]
Arctic Low	60°N	MAM[c]	1.98 million km^2	2020-2039
Arctic High	60°N	MAM	4.45 million km^2	2000-2019
Global—1.5	30°N/15°N/15°S/30°S	All	1.5°C above PI[d] (288.5 K)	2020-2039
Global—1.0	30°N/15°N/15°S/30°S	All	1.0°C above PI (288.0 K)	2007-2028
Global · 0.5	30°N/15°N/15°S/30°S	All	0.5°C above PI (287.5 K)	1993-2012

[a]September sea ice extent (if millions km^2) or global mean temperature (if K)
[b]20-year period of Historical/SSP2-4.5 when the average of the target metric equals the target value
[c]March, April, May
[d]Pre-industrial

Program (POP2, Smith et al. (2010); Danabasoglu et al. (2012)); the land component is version 5 of the Community Land Model (CLM5, Lawrence et al. (2019)); and the sea ice component is version 5.1.2 of the Los Alamos Sea Ice Model (CICE5, Hunke et al. (2015)). The land ice component is version 2.1 of the Community Ice Sheet Model (CISM2, Lipscomb et al. (2019)), which is run over Greenland at a 4-km resolution. Surface temperature and surface mass balance for glaciated cells are computed in CLM5, downscaled to the finer resolution through linear (vertical) and bilinear (horizontal) interpolation, and passed to CISM2 through the coupler. CISM2 is run with one-way coupling, meaning the GrIS does not evolve, and the mass changes therefore exclude ice dynamics.

2.2 Simulation Design

Our Arctic Low and Arctic High simulations each begin in the year 2035, branching from the SSP2-4.5 scenario, and end at the beginning of 2070. SSP2-4.5 has three ensemble members; Arctic Low and Arctic High both branch from the first member, but all three ensemble members are used for analysis in subsequent sections except for plots of cloud optical depth and sulfur deposition, for which only the data from the first member was saved. Each SSP2-4.5 ensemble member begins in 2015, branching from three respective ensemble members of a Historical simulation. The SSP2-4.5 background, simulation length, and start date are chosen to allow comparison with the globally-focused strategies of MacMartin et al. (2022), which also use CESM2(WACCM-MA) and have the same background, duration, and start date. 35 years of model output is sufficiently long to account for a transient period (15 years) at the beginning of the simulation after SAI is first introduced while still providing 20 years for analysis.

Both Arctic High and Arctic Low use SAI to regulate the extent of Northern Hemisphere September sea ice (SSI) by injecting at 60°N in springtime, approximately 5 km above the tropopause, as in W. Lee et al. (2021). W. Lee et al. (2021) found that concentrating the injection in the springtime approximately doubles the effect of SAI on SSI recovery relative to year-round injection. We implement our injection strategy by placing SO_2 into the 60.6°N, 180°E grid box bounded by the 110 and 130 hPa pressure interfaces (corresponding to an altitude of approximately 14.7-14.9 km) during March, April, and May (MAM) in each year of simulation. For Arctic Low, the target September sea ice extent is the 2020-2039 SSP2-4.5 average (first ensemble member only) in the CESM2(WACCM6-MA) configuration, equal to 1.98 million km^2; this "reference period" is the same as those of MacMartin et al. (2022). For Arctic High, we choose a higher target, which is the 2000-2019 Historical and SSP2-4.5 average (4.45 million km^2, also using only the first ensemble member). Simulation details are summarized in Table 1.

The quantity of SO_2 injected each year by a feedback algorithm (MacMartin et al., 2014; Kravitz et al., 2017): each year of simulation, the algorithm calculates the amount of SO_2 needed in order to restore sea ice to the target extent. The algorithm consists of a feedforward and a feedback component: the feedforward component prescribes a linearly increasing injection rate chosen based on the best guess of the injection required to maintain the target sea ice extent, and the feedback component corrects for uncertainty by adjusting the injection rate each year based on the performance of the controller. The feedforward and feedback gains are derived from the changes in sea ice extent in the MAM-60 simulation of W. Lee et al. (2021) relative to the background simulation (RCP8.5); while those simulations use an earlier version of the climate model as well as a different forcing scenario, the feedback term in our algorithm corrects for any uncertainty, and our results demonstrate that this is sufficient to control for sea ice despite the difference in model versions. The feedforward gains used for our simulations are 0.272 Tg/yr for Arctic Low and 6.109 Tg + 0.272 Tg/yr for Arctic High (with the offset in the Arctic High case to account for the sea ice difference between the reference time period of 2000-2020 and the first year of the simulation); the feedback gain used for both simulations is 0.491 Tg per year per million km^2 (i.e., the injection quantity each year is adjusted up or down by 0.491 Tg for each million km^2 of the total time-integrated difference between model output and the target). The algorithm design process is described in more detail in Text S1.

In Figure 1, we present SO_2 injection rate and stratospheric aerosol optical depth (AOD) data for our simulations of Arctic-focused SAI, alongside globally-focused simulations from MacMartin et al (2022). Shading and error bars in Fig. 1 and subsequent figures denote standard error as defined in Text S2 of the Supporting Information. The globally-focused simulations considered here all inject year-round at 30°N, 15°N, 15°N, and 30°S to control global mean temperature (T0), the interhemispheric temperature gradient (T1), and the equator-to-pole temperature gradient (T2). The three simulations have global mean temperature targets of 1.5°C, 1.0°C, and 0.5°C above preindustrial conditions, respectively; we refer to them here as "Global + 1.5," "Global + 1.0," and "Global + 0.5," respectively. Each has three ensemble members. Averaged over the last 20 years of simulation (2050-2069), Arctic Low injects 5.57 ± 0.09 Tg/yr, Arctic High injects 10.66 ± 0.10 Tg/yr, and Global+1.5 injects 8.58 ± 0.04 Tg/yr (± denotes standard error as in Text S2 of the Supporting Information). Compared to the Global+1.5 ensemble average, Arctic High and Arctic Low produce less than half and less than a quarter, respectively, of the globally- and annually-averaged AOD (0.06 and 0.03 compared to 0.14). However, for latitudes above 60°N, Arctic High and Arctic Low AODs are twice as large as Global+1.5 and comparable to Global+1.5, respectively (0.24 and 0.14 compared to 0.12). Averaged only over June, July, and August, the high-latitude AOD for Arctic High and Arctic Low approximately doubles relative to year-round, whereas Global+1.5 is unchanged (0.44 and 0.25 compared to 0.12).

3 Results

3.1 Changes to Radiative Fluxes

3.1.1 Shortwave Fluxes

A starting point for understanding how the increased AOD in Fig. 1c affects the climate system is to evaluate the net changes in shortwave (SW) radiative fluxes. These are determined not only by the addition of the aerosols, but also by resulting changes in surface albedo (primarily increases in snow and ice extent at high latitudes) that amplify the initial forcing, and changes in cloud cover that both reduce the net forcing and change the spatial distribution. In Figure 2, we present changes to shortwave (SW) radiative fluxes for Arctic High relative to SSP2-4.5, averaged over the 2050-2069 period; the figure also plots changes to atmospheric sulfur burden, surface albedo, and cloud op-

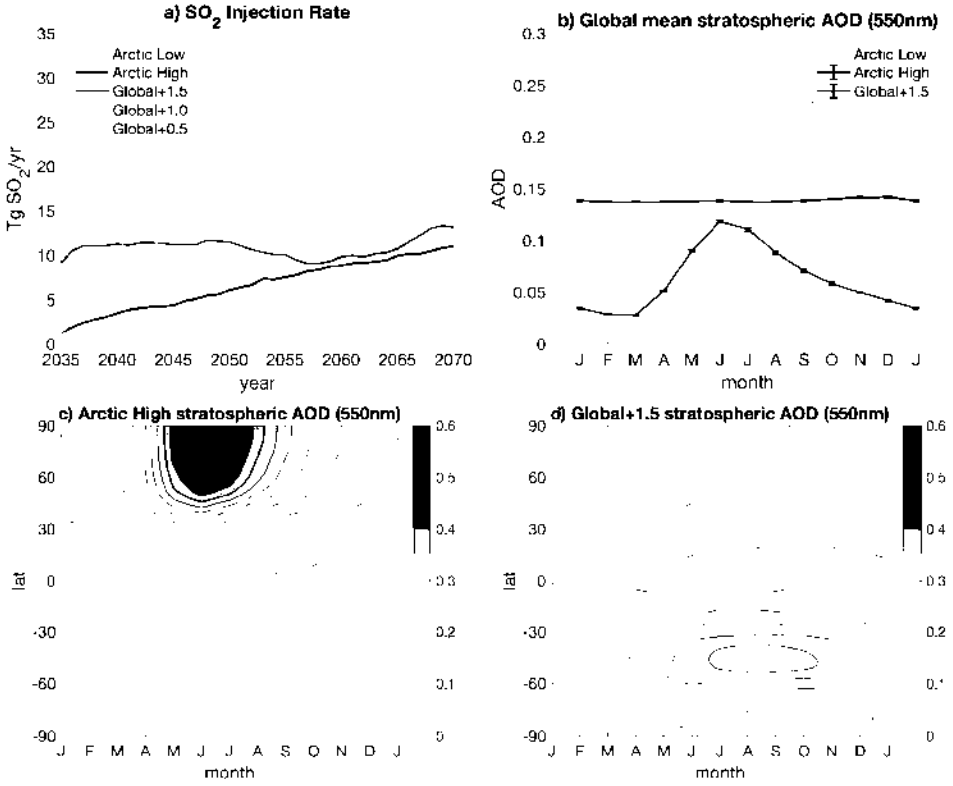

Figure 1. SO_2 injection rates and stratospheric aerosol optical depth (AOD) at the 550nm wavelength for the Arctic Low and Arctic High simulations, with comparison to global strategies described in MacMartin et al. (2022). Panel (a) plots injection rate as a function of time: shading denotes ensemble spread. Panel (b) plots seasonal cycles of global mean 550nm stratospheric AOD, averaged over the 2050-2069 period: error bars denote standard error as described in Text S2. Panels (c) and (d) plot seasonal cycles of zonal mean 550nm stratospheric AOD for Arctic High and Global+1.5, respectively, averaged over the 2050-2069 period.

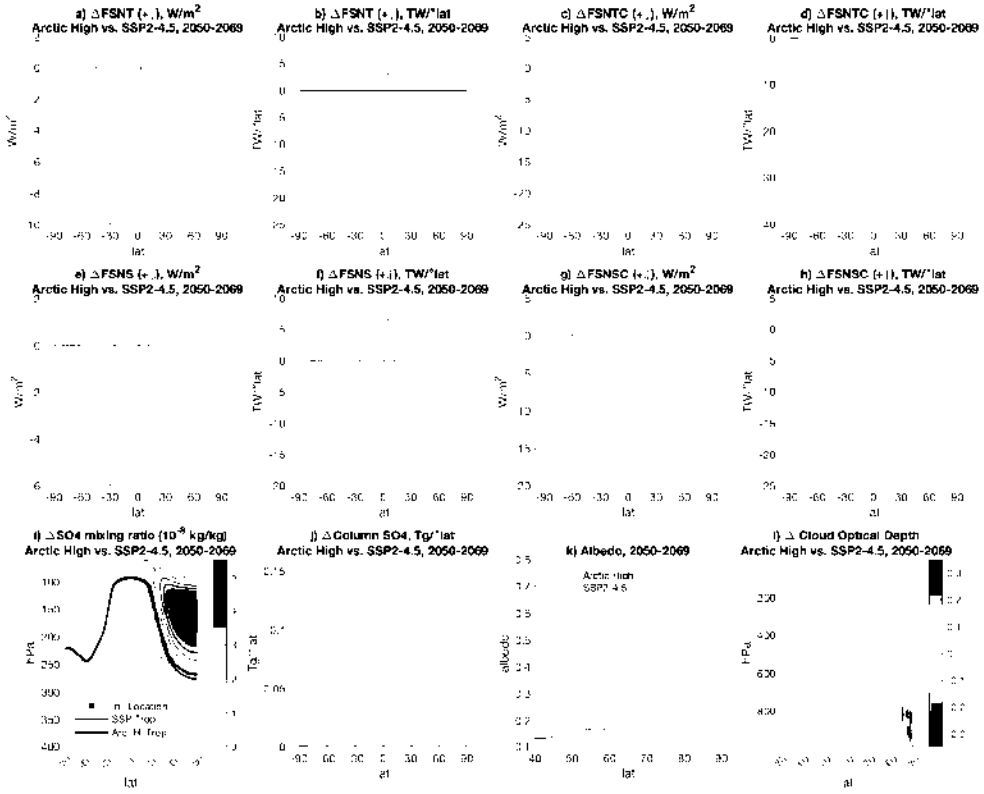

Figure 2. Changes to shortwave (SW) fluxes, SO_4 column burden and mixing ratio, surface albedo, and cloud optical depth for Arctic High relative to SSP-2.45, averaged over 2050-2069. The top row shows changes to top-of-atmosphere (TOA) net SW fluxes, and the middle row shows changes to surface net SW fluxes (positive downward for all); the left two columns show "full-sky" fluxes (considering clouds), and the right two columns show "clear-sky" fluxes (without clouds). Changes to each of these fluxes are shown both as a zonal mean in W/m^2 (columns 1 and 3) and as a zonal integral in TW per degree latitude (columns 2 and 4). The bottom left panels show the distribution of changes to atmospheric SO_4 burden: panel (i) shows zonal mean changes to mixing ratio across latitude and altitude (injection location and tropopause locations for Arctic High and SSP2-4.5 are included for reference), and panel (j) shows changes to altitude-integrated, zonally integrated column SO_4. Panel (k) shows changes to zonal mean surface albedo across 40°N-90°N. Panel (l) shows changes to gridbox cloud SW optical depth (only one ensemble member for SSP2-4.5). All shading for 20-year averages denotes standard error as described in Text S2. "FSNT" and "FSNTC" (top row) denote "flux, SW, net, TOA" full-sky and clear-sky, respectively; "FSNS" and "FSNSC" (middle row) denote "flux, SW, net, surface" full-sky and clear-sky, respectively.

tical depth, which affect SW fluxes. The "UNCLASSIFIED" concentration is found closest to the pole (Fig. 2i); this correlates to the AOD distribution in Figure 1c, as well as to changes in clear-sky (i.e., in the absence of clouds) net surface SW flux, which is highest at high latitudes (2g) (this is also affected by changes in atmospheric water vapor and ozone). The net change in top-of-atmosphere (TOA) SW fluxes is also affected by surface albedo changes that also peak at high latitudes (2k); considering clear-sky fluxes only, the net TOA SW change at high latitudes is slightly higher than the change in net surface SW forcing (compare 2c and 2g). However, the pole has very little surface area: both the zonally-integrated sulfur content (2j) and the total changes in surface and TOA clear-sky SW energy per degree of latitude (2h and 2d) are largest south of the injection location rather than over the Arctic.

These changes are then further modified by changes in cloud cover. Changes to full-sky TOA forcing (2a, 2b) are either identical to or smaller than changes to clear-sky TOA forcing (2c, 2d) in magnitude everywhere in the northern hemisphere, showing that as a whole, changes in cloud cover dampen changes to forcing. Full-sky SW changes in the tropics form a "zig-zag" that is absent in clear-sky SW changes; these changes are predominantly due to changes in cloud cover associated with a southward shift in the ITCZ (discussed in Section 3.3; see Fig. 9). Lastly, at high latitudes, after accounting for cloud changes, downwelling SW at the surface (not shown) actually increases at high latitudes despite the increased sulfur burden and AOD; this change is absent in the clear-sky flux, indicating that reduced clouds under SAI (2l) allow more SW to reach the surface. Therefore, the slight positive change in forcing at very high latitudes due to changes in cloud cover under SAI means that changes in surface net SW are comparable everywhere north of about 30°N (2e).

3.1.2 Longwave Fluxes

Changing the energy coming into the climate system will also affect the energy going out; surface temperature affects the LW energy emitted at the surface, and changes to clouds and humidity affect how that energy is transmitted through the atmosphere. In Fig. 3, we plot changes to surface and TOA LW fluxes, near-surface temperature, and humidity. Surface temperature changes (3c) are largest at high latitudes, corresponding to reduced LW emitted at the surface (3a); however, as with SW fluxes, zonally-integrated changes to emitted LW peak in the mid-latitudes (3b). Increases in sea ice extent under SAI (see Fig. 4 and accompanying discussion) also play a role in this process by covering the warmer ocean water and decreasing LW emitted at the surface. Arctic High also reduces near-surface humidity in the northern hemisphere (3d), which has implications for GrIS SMB (see Fig. 7 and accompanying discussion). Humidity reduction is largest near the tropics; comparing 3a-b with 3g-h, Arctic High actually increases upwelling surface LW in the tropics despite reduced emitted LW, indicating a reduction in trapped LW that correlates with the region of reduced near-surface humidity. Comparing full-sky (3e-f) and clear-sky (3g-h) net upwelling surface LW, the addition of clouds moves the change in forcing at high latitudes from negative to positive, indicating a strong reduction in LW trapped near the surface by clouds in the Arctic. The net effect of Arctic High on TOA outgoing LW radiation (OLR) is a reduction in OLR in the Arctic, the northern hemisphere mid-latitudes, and the southern hemisphere tropics and extratropics, and an increase in outgoing OLR in the northern hemisphere tropics (3i-j). The effect of the southward ITCZ shift on cloud cover is also visible, as the addition of clouds increases OLR in the northern hemisphere tropics and decreases OLR in the southern hemisphere tropics (compare 3i-j with 3k-l).

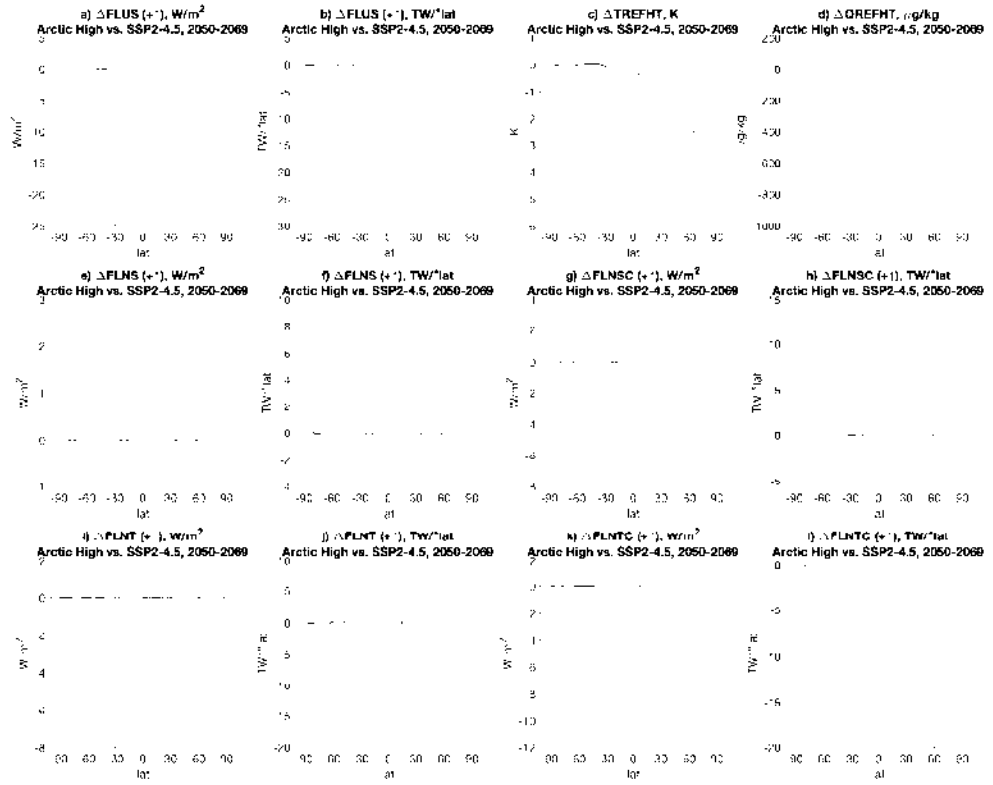

Figure 3. Changes to LW fluxes and near-surface temperature and humidity for Arctic High relative to SSP2-4.5, averaged over 2050-2069. The top row plots changes to upwelling LW at the surface (a, b) and near-surface temperature (c) and humidity (d); the middle row plots changes in net LW flux at the surface, and the bottom row plots changes in top-of-atmosphere (TOA) net LW fluxes. All LW fluxes (positive up for all) are plotted in both W/m^2 (1st and 3rd columns) and in TW per degree latitude (2nd and 4th columns); the two left columns show "full-sky" fluxes with clouds, and the two right right columns show "clear-sky" fluxes without clouds. All shading shows standard error as described in Text S2. "FLUS" (top row) denotes "flux, LW, upwelling, surface"; "FLNS" and "FLNSC" (middle row) denote "flux, LW, net, surface" full-sky and clear-sky, respectively; and "FLNT" and "FLNTC" (bottom row) denote "flux, LW, net, TOA" full-sky and clear-sky, respectively.

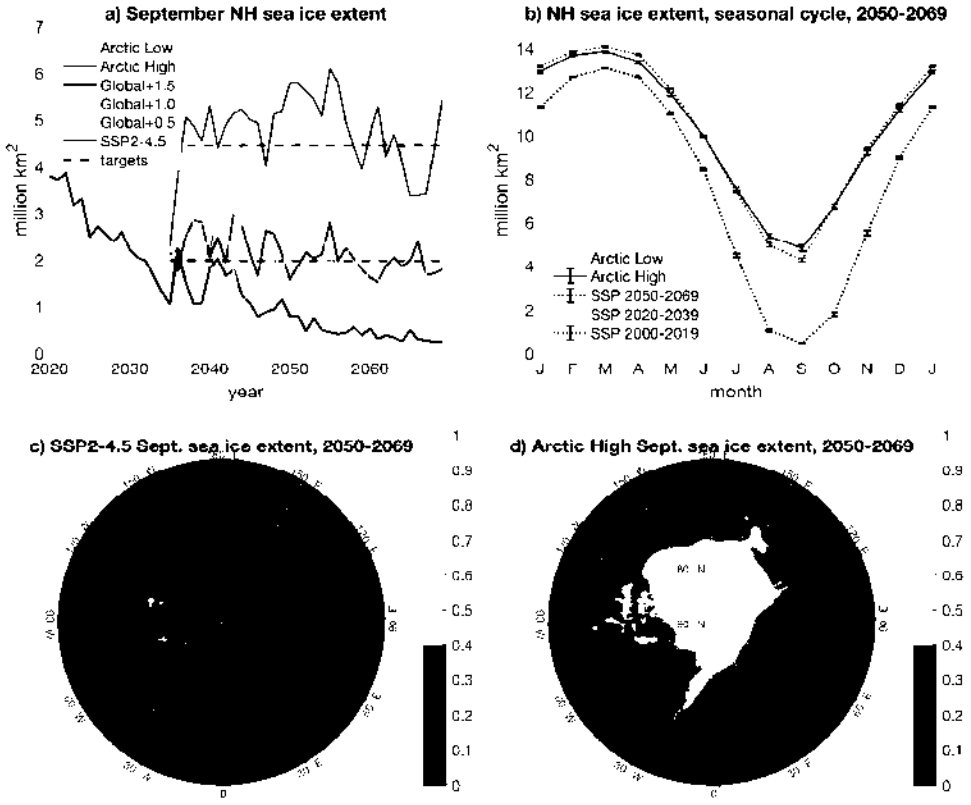

Figure 4. Northern Hemisphere (NH) sea ice extent, computed as fraction of grid cell covered in sea ice multiplied by grid cell area. Panel (a) plots NH September sea ice (SSI) extent as a function of time. Global and SSP2-4.5 data are ensemble means: shading denotes ensemble spread. Panel (b) compares seasonal cycles of NH sea ice extent for Arctic High and Arctic Low (averaged over 2050-2069) to their respective reference periods from Historical/SSP2-4.5 (see Table 1 for reference periods). Errorbars denote standard error as in Text S2. Dashed lines in panels (a) and (b) denote SSI targets for Arctic High and Arctic Low strategies. Panels (c) and (d) plot maps of SSI extent for SSP2-4.5 ensemble average and Arctic High, respectively, averaged over 2050-2069. The color scale denotes the fraction of each grid cell covered in sea ice.

3.2 Arctic Impacts

3.2.1 Sea Ice

The loss of Arctic sea ice has been shown to be reversible in climate models (Armour et al., 2011; Ridley et al., 2012; Boucher et al., 2012; Samanta et al., 2010); both globally-focused SAI (Jiang et al., 2019; W. Lee et al., 2020) and high-latitude SAI (Robock et al., 2008; Jackson et al., 2015; W. Lee et al., 2021) have been shown to increase sea ice extent. In Fig. 4, we present sea ice model output for the Arctic-focused SAI strategies against the globally-focused SAI strategies and Historical/SSP2-4.5. In 2035, at the start of the SAI simulations, NH September sea ice (SSI) under SSP2-4.5 has an extent of 1.0 $\pm$ 0.1 million km^2, and this decreases to 0.39 $\pm$ 0.03 million km^2 by the 2050-2069 period. Arctic High restores SSI extent to 4.8 + 0.1 million km^2 during this period, slightly above the target for that simulation (4.45 million km^2; recall that the SSI targets for Arctic High and Arctic Low are defined by the sea ice extents during their respective reference periods as shown in Table 1). The Arctic High SSI extent is also statistically identical to the Global | 0.5 average during the 2050-2069 experimental period (4.85 $\pm$ 0.06). Arctic Low restores SSI extent to 2.1 $\pm$ 0.1 million km^2, also slightly above the target value (1.98) and indistinguishable from Global+1.5 (1.95 $\pm$ 0.06). Comparing annual mean surface temperatures in the 60°N-90°N region, Arctic High during the 2050-2069 experimental period (264.9 $\pm$ 0.1 K) is identical to its reference period (265.04 $\pm$ 0.05 K), but Arctic Low 2050-2069 (266.5 $\pm$ 0.1 K) is slightly warmer than its reference period (266.21 $\pm$ 0.06 K), so the novel Arctic climate generated by SAI is not necessarily promotive of sea ice at a given temperature. Changes to the seasonal cycle of sea ice (Fig. 4) relative to the reference period (see Table 1 for reference periods) can also be observed: both Arctic High and Arctic Low have lower sea ice extent than their respective reference periods in the winter months, meaning that while the Arctic-focused SAI strategies restore September sea ice to or above their targets, they restore a smaller fraction of the lost winter sea ice. This may be due at least in part to the seasonality of the injection strategy, in which AOD (see Fig. 1c) and temperature changes (see Fig. 8b) are dominant in the summer and autumn; in contrast, all three global strategies, which inject year-round and primarily in the southern hemisphere, overcompensate winter sea ice extent relative to the reference period (this is a change from global strategies in CESM1(WACCM); Jiang et al. (2019) found that GLENS, which also used a global strategy but injected primarily in the northern hemisphere, overcompensated summer sea ice extent and undercompensated winter sea ice extent, the same pattern seen in Arctic High). However, the extent of sea ice is not only affected by SW radiation and temperature, but also other factors such as atmospheric and oceanic circulation (Moore et al., 2014), including dynamic effects of SAI-induced stratospheric heating (Jiang et al., 2019) and further study would be needed to investigate these influences. As discussed in Jiang et al. (2019), changes to the seasonal cycle have environmental and ecological implications: Dai et al. (2019) found that Arctic Amplification (AA) in response to sea ice loss mainly occurs in the cold season because winter surface waters are much warmer than sea ice and therefore emit more longwave (LW) radiation, and therefore undercompensating winter sea ice extent may affect the ability of Arctic-focused SAI to limit AA. Additionally, sea ice extent may influence the strength of the Atlantic Meridional Overturning Circulation (AMOC) via freshwater flux changes (Xie et al., 2022), and therefore changes to the seasonal cycle of sea ice may affect the seasonal cycle of the oceanic circulation.

35 years is too short to diagnose long-term variability in the sea ice response, but we would expect our feedback algorithm suppresses variability at long time scales and increases variability at time scales commensurate with the controller time constant (in our study, our intent had to been to set this at 5 years, implying content at frequencies of $2\pi\tau \approx 31$ years, but the actual time-constant was likely shorter). However, there is no reason to think that feedback would change the mean (i.e., there are no local minima in the function of injection rate $\rightarrow$ SSI to which the algorithm would converge). For

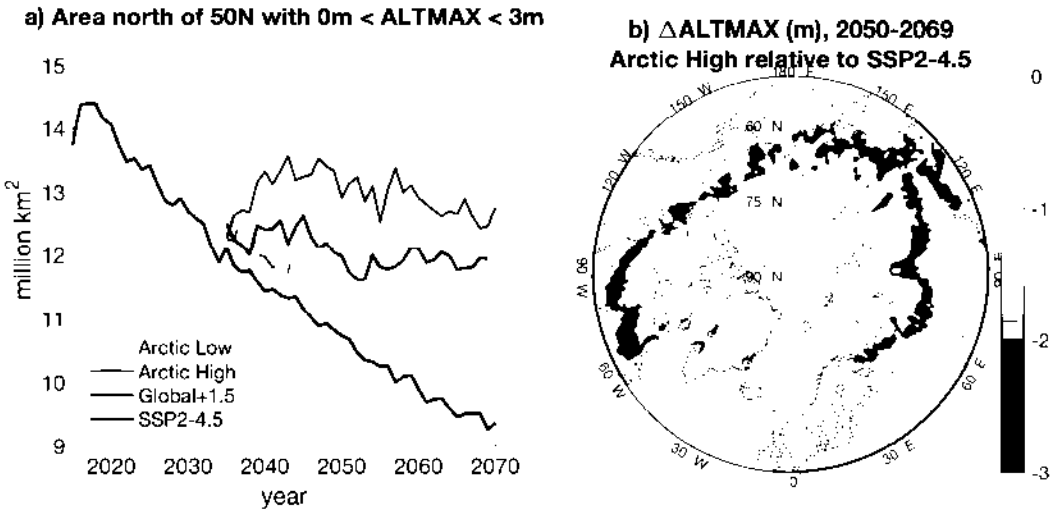

Figure 5. Annual maximum active layer thickness (ALTMAX). Panel (a) plots a timeseries of the area north of 50°N with ALTMAX between 0 and 3 meters; for Global+1.5 and SSP2-4.5, shading denotes ensemble spread. Panel (b) shows changes in ALTMAX for Arctic High relative to SSP2-4.5, averaged over the 2050-2069 period for both simulations. Hatching represents areas with no statistically detectable difference at the 95% confidence level according to the two-sample t-test. Light blue (ΔALTMAX < 3m) indicates a decrease in active layer thickness in permafrost and near-permafrost regions, whereas dark blue (ΔALTMAX $\geq$ 3m) indicates increased permafrost area relative to SSP2-4.5.

a 20-year average (as used in analyses throughout the paper), we find that our algorithm appears to slightly increase variability: during the 2050-2069 experimental period, the detrended 20-year SSI for Arctic High has a standard deviation of 0.62 million km^2, compared to 0.50, 0.58, and 0.59 for the three Historical/SSP2-4.5 ensemble members during the 2000-2019 reference period. Arctic Low has a bigger increase in variability relative to the 2020-2039 reference period (0.75 vs. 0.44, 0.50, and 0.56, respectively). Both the suppression of longer-term variability by our feedback algorithm and amplification of variability at intermediate time-scales would of course affect the choice of injection rates (which would in turn affect the impacts of SAI), but this is accounted for in our uncertainty estimates, which use an AR(1) approximation; the AR(1) model captures all of the statistically significant autocorrelation in the SSI timeseries (i.e., all of the lags greater than 1 are not statistically significant), and is thus a reasonable approximation for estimating degrees of freedom.

In regions containing permafrost, the upper portion of the ground that thaws in the summer and re-freezes in the autumn is called the active layer. The maximum annual depth of the active layer is commonly used to diagnose permafrost extent (e.g., Lawrence et al. (2015)); a small annual maximum active layer thickness (i.e., ≤ 3m) is indicative that only the near-surface soil has become unfrozen during the past year, and there is permafrost underneath. In Fig. 5, we present permafrost diagnostics for our Arctic-focused strategies against Global | 1.5 and SSP2-4.5. Panel (a) shows timeseries of near-surface permafrost extent. When SAI begins in 2035, the permafrost extent under SSP2-4.5 is 12.1 million km^2, and the extent decreases to 9.96 ± 0.03 million km^2 by the 2050-2069 period. Arctic Low, Arctic High, and Global+1.5 all increase permafrost area relative to SSP2-4.5, but none of them restore permafrost to the extent of their respective reference periods: 11.46 ± 0.03 for Arctic Low and 11.88 ± 0.03 for Global−1.5 (compared to 12.70 ± 0.03 for SSP2-4.5 2020-2039), and 12.86 ± 0.06 for Arctic High (compared to 14.26 ± 0.03 for Historical/SSP2-4.5 2000-2019). A map of the changes for Arctic High is shown in panel (b); Arctic High both decreases ALTMAX in permafrost regions (light blue), which means a deeper column of soil remains frozen year-round, and increases permafrost area (dark blue). This expanded permafrost area reaches furthest to the south in northeastern Asia, but also spans the entire width of Russia and most of the width of North America. In contrast with sea ice, Global · 1.5 increases permafrost area more than Arctic Low; this may be because Global+1.5 cools the mid-latitudes more effectively than Arctic Low (see Fig. 8c below), whereas September sea ice is mainly found north of 75°N, where these strategies provide comparable amounts of cooling.

In Fig. 6, we present land model carbon output for our Arctic-focused simulations and SSP2-4.5. Under SSP2-4.5, the Arctic ecosystem as a whole continues to take up carbon during the simulation period due to enhanced vegetation growth associated with CO_2 fertilization and due to a warmer and more hospitable climate for plants. Soil carbon also increases in response to the enhanced litter and root carbon inputs near the surface, even though the permafrost thawing is leading to soil carbon losses due to enhanced decomposition at depth. In the Arctic SAI scenarios, the high-latitudes continue to be a sink of carbon as the plants respond positively to the increasing CO_2. In Arctic High, the stronger cooling slows the rate of vegetation carbon gains, and also decreases permafrost soil carbon losses. The reduction in vegetation carbon gains is more impactful, which leads to the high-latitudes being a weaker carbon sink in Arctic High compared to Arctic Low and SSP2-4.5. For Arctic Low and Global+1.5, the changes to soil and vegetation carbon storage are the same signs as those of Arctic High, but the opposing effects are comparable in magnitude, and the overall effect is no significant difference in the total ecosystem carbon relative to SSP2-4.5 during the 2050-2069 period. This difference may be in part because Arctic High cools the mid-latitudes more efficiently than Arctic Low and Global+1.5 (Fig. 8c-d), but changes between 50°N-60°N do not completely account for this nonlinearity.

For Arctic High, the total reduced carbon uptake by 2050-2069 relative to SSP2-4.5 is 7.31 ± 0.04 Pg, or about 26.8 Gt of CO_2-equivalent. However, inclusion of permafrost and other high-latitude climate-carbon feedbacks within ESMs like CESM is relatively new and remains highly uncertain; a recent intercomparison project of permafrost-enabled land models found a very large spread in response of both high-latitude soil and vegetation carbon stocks to projected climate change (McGuire et al., 2018). Therefore, the high-latitude carbon stock results presented here should be viewed with caution and treated as indicative only as representative of possible carbon budget consequences from SAI. Additionally, plants take up carbon in the form of CO_2, whereas soil carbon can be released as both CO_2 and CH_4, and so directly comparing carbon stocks does not fully quantify the effects of SAI on greenhouse gases in the atmosphere. Further development and validation of permafrost and carbon flux representation in Earth System models are

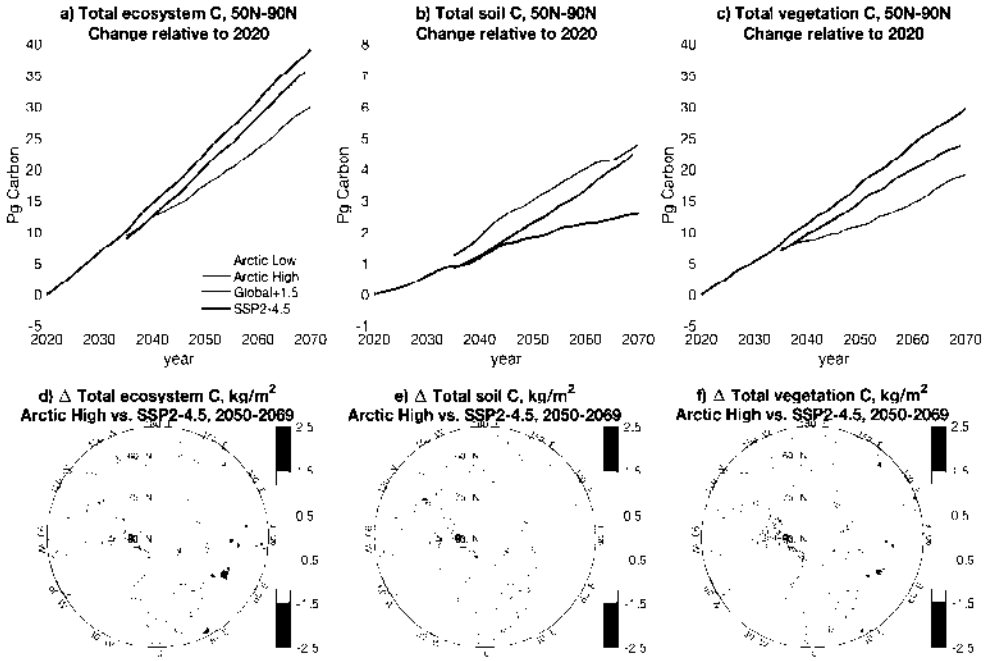

Figure 6. Carbon and carbon density. The top row plots timeseries of ecosystem (a), soil (b), and vegetation (c) carbon content relative to 2020 (note the different y-axis scaling for panel b); for SSP2-4.5, shading denotes ensemble standard error as described in Text S2 of the Supporting Information. The bottom row plots maps of changes in ecosystem (d), soil (e), and vegetation (f) carbon density in the 50°N-90°N region for Arctic High relative to SSP2-4.5, averaged over 2050-2069 for both simulations. Hatching represents areas with no statistically detectable difference at the 95% confidence level according to the two-sample t-test.

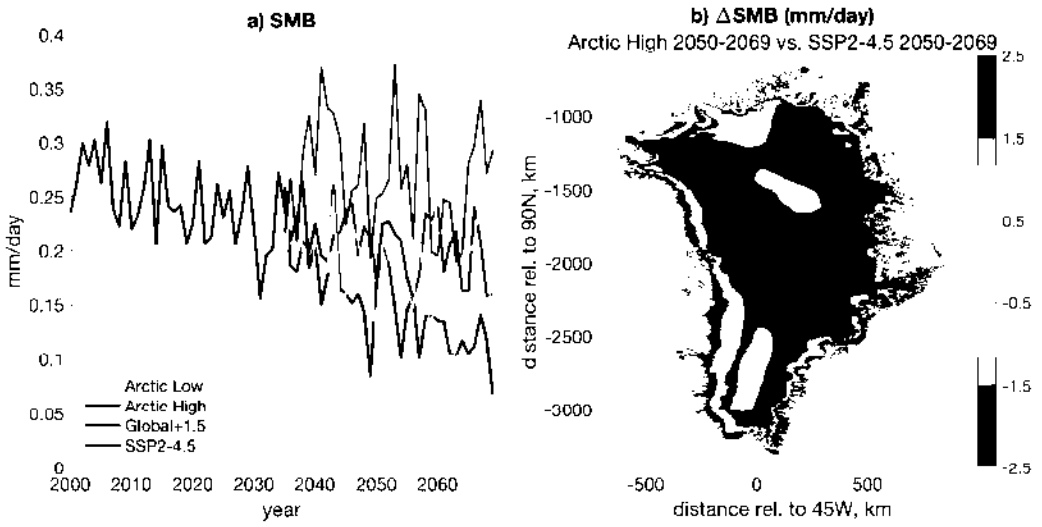

Figure 7. Changes in GrIS surface mass balance (SMB). Panel (a) plots annual mean SMB as a function of time: shading denotes ensemble spread. Panel (b) plots changes in SMB for Arctic High relative to SSP2-4.5 averaged over 2050-2069: shading denotes regions with no statistical change according to the two-sample t-test at a 95% significance level.

needed to provide a foundation for more robust assessment of the impacts of SAI. McGuire et al. (2018) also posits that climate-change-driven changes to soil and vegetation carbon will occur on different timescales: specifically, soil carbon stocks are projected to change more slowly than vegetation carbon stocks in the immediate future, and much of the soil carbon release from permafrost is expected to occur after 2100 regardless of scenario. Therefore, net CO_2-eq emissions up to 2070 may not be an accurate assessment of longer-term GHG commitments for a 35-year SAI simulation.

3.2.3 Greenland Ice Sheet

Surface mass balance (SMB) is the net change in mass at the surface of a glacier or ice sheet due to precipitation, evaporation, and runoff. Changes to SMB are likely responsible for an estimated 50-60% of the contribution of the GrIS to sea level rise over the past 30 years (van den Broeke et al., 2017; IMBIE, 2020). Globally-focused SAI has previously been found to increase GrIS SMB by reducing near-surface temperature and humidity (Moore et al., 2019), which Arctic-focused SAI also reduces (see Fig. 3c-d and 8c; maps of these variables over Greenland are contained in Fig. S5 of the SI). In Fig. 7, we present changes to GrIS SMB for Arctic High relative to SSP2-4.5. When injection begins in 2035, GrIS SMB is approximately 0.24 mm/day; in the SSP2-4.5 scenario, this value decreases to 0.132 ± 0.006 mm/day by the 2050-2069 period. The Arctic Low strategy increases this value to $0.19 \perp 0.01$ mm/day, statistically indistinguishable from

Global · 1.5 during 2024-2035 and 2070-2085 (0.198 ± 0.006) and slightly lower than SSP2-4.5 during the Arctic Low reference period (see 1 for reference periods) of 2020-2039 (0.229 ± 0.007). Arctic High further increases SMB to 0.27 ± 0.01 during the 2050-2069 period. slightly higher than its respective reference period of 2000-2019 (0.258 ⊥ 0.007). In these simulations, changes to SMB appear to be dominated by decreases in runoff (maps of runoff and other components for SMB are contained in Fig. S5). especially in the western ablation zone. which is consistent with the results of Moore et al. (2019) for globally-focused SAI. Although CESM2(WACCM) accounts for many important dynamic and thermodynamic processes governing surface mass balance, changes in ice dynamics processes such as glacial calving are not considered. so the ice sheet geometry is fixed with time. The relatively short duration of the simulations means that dynamic responses to ice sheet geometrical changes imposed by changing SMB are likely to be insignificant (Slater et al., 2019). but changes in ice elevation would contribute enhanced ablation as the surface lowers: this would likely be on the order of 10% for SSP2-4.5. while being less important for the SAI scenarios (Moore et al.. 2019). Further work is necessary to determine the effects of high-latitude SAI relative to global strategies on glacial calving and other dynamic processes.

3.3 Global Impacts

3.3.1 Surface Temperature

In Fig. 8. we present surface temperature output from our simulations. Also included is cooling efficiency in the Northern Hemisphere, defined as temperature change relative to SSP2-4.5 normalized by Tg of SO_2 injected. using the average of annual mean temperature and injection rates from 2050-2069. As expected. Arctic High produces less global cooling than Global+1.5 despite injecting slightly more: averaged over the 2050-2069 period. Arctic Low provides 0.23 + 0.03°C of cooling (0.041 + 0.005 K/Tg). Arctic High provides 0.66 − 0.04°C of cooling (0.062 + 0.004 K/Tg), and Global+1.5 provides 0.87 ± 0.02°C of cooling (0.102 ± 0.002 K/Tg). However. in the 60°N-90°N region, the Arctic-focused strategies provide more cooling per unit injection than Global + 1.5 (0.26 ± 0.02 K/Tg for Arctic Low, 0.29 ± 0.01 K/Tg for Arctic High, and 0.207 ± 0.009 K/Tg for Global+1.5). It is noteworthy that Arctic High provides more global cooling per unit injection than Arctic Low (about 50% more), as strategies with higher injection rates generally cool less efficiently due to the physics of aerosol coagulation (Visioni, MacMartin, et al., 2020; Kleinschmitt et al., 2018; Pierce et al.. 2010; Niemeier et al.. 2011). The two Arctic-focused strategies provide similar rates of high-latitude cooling per unit injection; the difference in global cooling efficiency comes from more efficient cooling by Arctic High at low and mid-latitudes in the Northern Hemisphere (Fig. 8d). This is likely due to memory in the climate system. as by 2050, Arctic High has been injecting of order 10 Tg/yr for 15 years, whereas Arctic Low ramped up from zero. On a year-by-year basis. Arctic Low provides more efficient cooling at the beginning of the simulation (see SI. Fig. S3b). which is in line with expectations. However. Arctic High becomes more efficient by the end of the simulation. Between the ocean, the land, and the atmosphere. the ocean has the highest heat capacity. and therefore the longest memory, and therefore we would expect memory-related effects to be ocean-related: while not conclusive. a map comparing the cooling efficiency of Arctic Low and Arctic High (Fig. S3a) does show that Arctic High and Arctic Low cool equally efficiently at the centers of land masses. such as central Asia, northern Africa. and North America, and many of the areas where Arctic High cools more efficiently than Arctic Low are in or near the oceans. We also find that Arctic High would cool much more efficiently at high latitudes (likely due to ice/snow-albedo feedbacks), but this is offset by a patch in the Northern Atlantic, which is likely related to the Atlantic Meridional Overturning Circulation (AMOC: Fig. S3c).

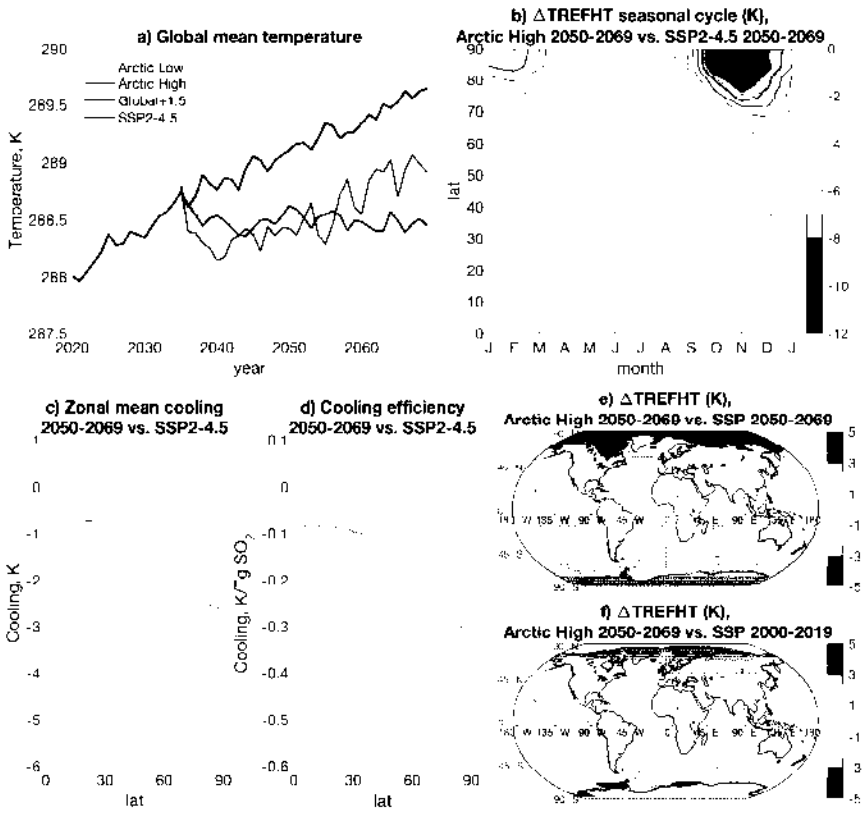

Figure 8. Surface temperature. Panel (a) plots globally averaged, annual mean surface temperature as a function of time; shading denotes ensemble spread. Panel (b) plots changes to the seasonal cycle of zonal mean temperature for Arctic High (2050-2069 average) relative to SSP2-4.5 during the same period. Panels (c) and (d) plot zonal mean cooling and zonal mean cooling per Tg of SO_2 injected, respectively; cooling is relative to SSP2-4.5 averaged over the 2050-2069 period, and injection rate is also averaged over the 2050-2069 period. Shading denotes standard error as described in Text S2. Panels (e) and (f) plot maps of surface temperature changes for Arctic High (2050-2069 average) relative to SSP2-4.5 (2050-2069 average and 2000-2019 average, respectively). Shading represents changes that are not statistically significant according to the two-sample t-test at the 95% confidence level.

The different distribution of cooling in different strategies have implications for how they affect the high-latitude climate. Global 1.5 and Arctic Low have similar rates of September sea ice recovery (Fig. 4a), and this may be because they provide similar cooling at very high latitudes where sea ice is present. However, Global+1.5 cools the middle latitudes, where large areas of permafrost or potential permafrost are located, more than Arctic Low, and permafrost recovery under Global+1.5 is higher than for Arctic Low (Fig. 5a). The detectable cooling from Arctic High covers most of the Northern Hemisphere, but very little cooling extends into the Southern Hemisphere; the cooling seen near Antarctica in Fig. 8c is likely due to natural variability, but it is possible that dynamical changes may also be responsible. As shown in panel 8b, the largest cooling effect at high latitudes from Arctic High occurs not during the period of maximum AOD in the early summer (see Fig. 1c) but rather in the autumn: this is likely because of avoided heat flux out of the ocean due to the larger extent of sea ice during this period (see 4b). For Arctic High, much of the surface temperature between 45°N-90°N is indistinguishable from the reference period of 2000-2019 (see Table 1 for reference periods) in the SSP2-4.5 scenario, but some spatial and temporal differences are present. For instance, the northeastern Pacific is warmer and the northern Atlantic is cooler under the Arctic High strategy than during the reference period, a response also seen in the temperature response of the globally-focused simulations of Richter et al. (2022). This is likely due at least in part to the behavior of AMOC: in CESM1, AMOC weakened under global warming but accelerated under GLENS, leaving a similar persistent warming in the north Atlantic (Fasullo et al., 2018). In CESM2(WACCM), the effects of globally-focused SAI on AMOC have the same sign but a smaller magnitude, reducing the weakening but not reversing it (Tilmes et al., 2020). The effects of Arctic-focused SAI are similar: the strength of the AMOC under SSP2-4.5 is 23.7 ⊥ 0.1 Sv in 2000-2019 and decreases to 17.2 ⊥ 0.2 Sv in 2050-2069, but only decreases to 19.1 ⊥ 0.2 Sv under Arctic Low and 21.1 ⊥ 0.2 Sv under Arctic High (see SI, Fig. S3c).

3.3.2 Precipitation

In Fig. 9, we present precipitation for Arctic High (2050-2069) relative to SSP2-4.5 during the same period and during the 2000-2019 reference period (see Table 1 for reference periods). Under global warming, the warmer atmosphere has a greater capacity to carry water: in the Historical and SSP2-4.5 simulations, global mean precipitation increases from 4.097 = 0.008 mm/day in 2000-2019 to 4.263 = 0.007 mm/day in 2050-2069. The cooling provided by SAI offsets this change: for Arctic Low (4.25 ⊥ 0.01 mm/day in 2050-2069), this reduction is indistinguishable from SSP2-4.5, but for Arctic High (4.20 ⊥ 0.02 mm/day), the reduction is detectable. As expected, high-latitude SAI pushes the ITCZ southward (Haywood et al., 2013; W. Lee et al., 2020), and this southward shift in tropical precipitation is clearly visible in Fig. 9. For SSP2-4.5, the 2050-2069 ITCZ location as measured by the centroid of tropical precipitation between 20°S and 20°N (Donohoe et al., 2013; Frierson & Hwang, 2012; W. Lee et al., 2020) is 1.07°N ⊥ 0.05°. During the same period, Arctic Low pushes the ITCZ southward to 0.8°N ⊥ 0.1°, and Arctic High to 0.54°N ⊥ 0.08°. Such a southward shift of the ITCZ could have consequences for people who rely on tropical precipitation patterns such as the African monsoon (Haywood et al., 2013; Krishnamohan & Bala, 2022); Robock et al. (2008) reported disruption to the Indian monsoon from 3 Tg/yr high-latitude injection, and similar changes are clearly visible here relative to SSP2-4.5 (Fig. 9c,e) and even more so relative to the reference period (Fig. 9d,f). Globally-focused strategies commonly inject in both hemispheres with the goal of avoiding such a result (Kravitz et al., 2017; MacMartin et al., 2022; Richter et al., 2022), and combining Arctic-focused SAI with injection in the Southern Hemisphere (either Antarctic or tropical) could reduce the risk of a change in the ITCZ. We note that climate models disagree on the expected sign of future ITCZ change (e.g., whether the ITCZ is expected to migrate north or south) due to global warming and changes to anthropogenic aerosols (Byrne et al., 2018), and should the ITCZ shift northward, a south-

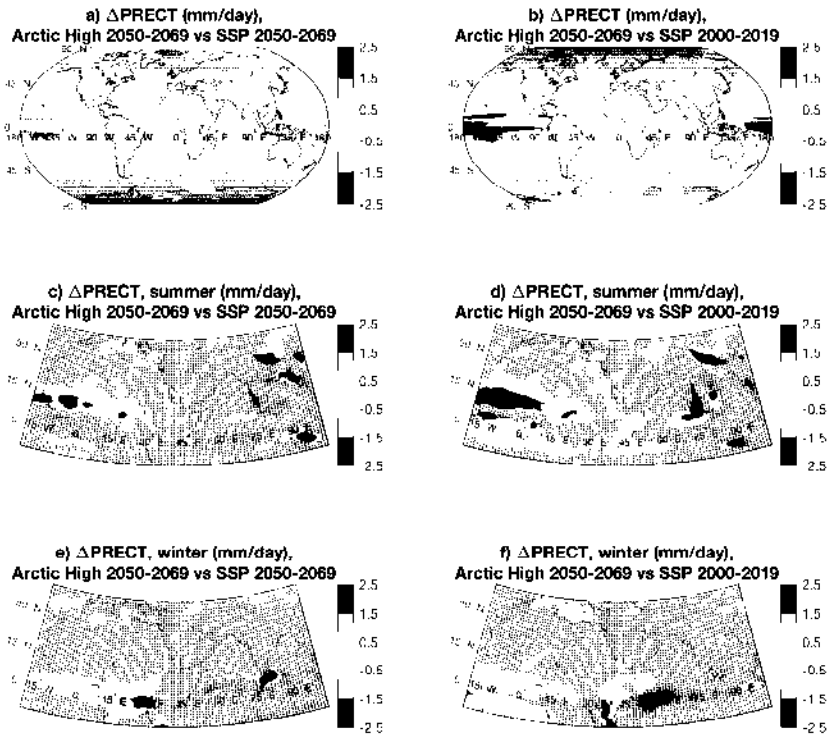

Figure 9. Precipitation, Arctic High 2050-2069 relative to SSP2-4.5 2050-2069 (left column) and Historical/SSP2-4.5 2000-2019 (right column). The top row shows changes to annual mean precipitation; the middle and bottom rows show changes to summer (JJA) and winter (DJF) precipitation over India and northern Africa, respectively. Shading indicates no statistically significant change at the 95% confidence level using the two-sample t-test.

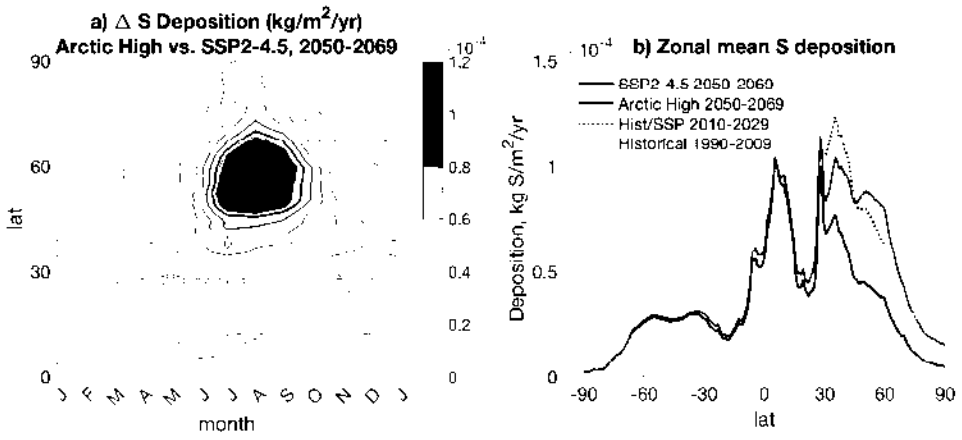

Figure 10. Changes to zonal mean sulfur deposition. Panel (a) displays the seasonal cycle of zonal mean sulfur deposition in kg/m^2/yr for Arctic High 2050-2069 relative to SSP2-4.5 2050-2069. Panel (b) shows zonal mean sulfur deposition for Arctic High and SSP2-4.5, both averaged over 2050-2069; shading denotes standard error as described in Text S2. Included for comparison are mid-latitude and high-latitude sulfur deposition for Historical/SSP2-4.5 in the 2010-2029 and 1990-2009 periods, respectively, which are similar to the increased deposition under Arctic High; these are indicated by dotted lines. (Note: sulfur deposition data for Historical/SSP2-4.5 is taken from runs using the full-atmosphere (TSMLT) configuration of WACCM (one ensemble member) instead of the MA configuration because deposition output was not saved for the MA simulations; emissions are the same for both configuration and tropospheric lifetime is short, so deposition should be similar).

ward shift in the ITCZ could be a goal of Arctic-focused SAI rather than an unwanted outcome; regardless, given the importance of tropical precipitation, the effects of SAI on the location of the ITCZ should remain a forefront concern for any future discussion of Arctic-focused SAI. Other possible influences to tropical precipitation also require further exploration; the latitudinal extent of the Hadley and Walker cells is expected to change in future GHG climates (Vallis et al., 2015), and the descending limbs of the Hadley circulation are associated with deserts. SAI tends to reverse these impacts (Guo et al., 2018), although the situation is complicated by stratospheric heating (Cheng et al., 2022).

3.3.3 Sulfur Deposition

In the Historical and SSP2-4.5 scenarios, sulfur pollution peaks in the late 1900s and decreases throughout the 21st century, averaging 21.69 ± 0.05 Tg/yr during the 2050-

2069 period, in[illegible] 14[illegible] Tg/yr[illegible]thern hemisphere. During this period, Arctic Low and Arctic High inject 5.57 Tg/yr and 10.66 Tg/yr of SO_2, or (dividing by molar weights) approximately 2.8 and 5.3 Tg/yr of sulfur (representing approximately 25% and 50% global increases), respectively. In Fig. 10, we present 2050-2069 changes to sulfur deposition from SO_4 for Arctic High relative to one ensemble member of SSP2-4.5 (SO_4 deposition model output was not saved for the second and third SSP2-4.5 ensemble members). The bulk of the increased sulfur deposition (Fig. 10a) is concentrated in the late summer between 45°N-60°N, although increased deposition is present throughout 30°N-60°N in all months of the year. Although the stratospheric Brewer-Dobson Circulation (BDC) tends poleward, it is less efficient at higher latitudes; additionally, deposition is also strongly dependent on precipitation, which is higher at lower latitudes (especially with the additional reduction in precipitation at higher latitudes due to more cooling at high latitudes; see Fig. 9a). Therefore, it is reasonable to see higher deposition rates south of the injection site despite the poleward direction of the BDC. Relative to SSP2-4.5, sulfur deposition in the 30°N-60°N latitude band increases from 5.19 $\pm$ 0.04 Tg/yr to 8.38 $\pm$ 0.09 Tg/yr, an increase of 60%; the increased deposition is comparable to Historical/SSP2-4.5 during the 2010-2029 period (Fig. 10b, dark blue dotted line), approximately 40 years earlier. While the absolute increase at high latitudes is smaller, the baseline deposition is also smaller, meaning that the relative increase in sulfur pollution is large. Pollution from mid latitudes has long been observed in the Arctic regions (Arctic Haze; Yang et al. (2018)) and is seasonally concentrated in the spring and composed primarily of sulfate aerosols, causing lake acidification during spring thaw. Arctic High increases the deposition north of 60°N from 0.63 $\pm$ 0.01 Tg/yr to 1.47 $\pm$ 0.02 Tg/yr, an increase of 133%. This increased deposition is comparable to Historical during the 1990-2009 period (Fig. 10b, light blue dotted line), approximately 60 years earlier. Both the large absolute increase in the mid-latitudes and the large relative change at high latitudes would likely impact ecosystems and the people who live in these regions (Visioni, Slessarev, et al., 2020; Zarnetske et al., 2021), and further study of the implications of increased sulfur deposition in these areas is necessary.

4 Conclusions and Discussion

Both Arctic-focused strategies restored and maintained September sea ice to within 10% of their targets, demonstrating that Arctic-focused SAI can reverse the loss of sea ice and that higher injection rates lead to greater restoration of sea ice. The results also show that Arctic-focused SAI could mitigate other high-latitude impacts of global warming: permafrost extent is higher relative to SSP2-4.5 under both strategies, and both strategies increased GrIS SMB by reducing runoff. Arctic Low and Arctic High cool the Arctic and increase September sea ice extent more efficiently than Global+1.5; this is in contrast to Robock et al. (2008), in which 5 Tg/yr of equatorial injection cooled the high latitudes and restored September sea ice much more effectively than 3 Tg/yr of injection at 68°N. However, the difference also reflects evolution of the injection strategies, as Global | 1.5 injected at multiple tropical and near-tropical locations (instead of just the equator) and Arctic Low and Arctic High injected in spring (instead of year-round). The Arctic-focused strategies also increase GrIS SMB more efficiently than Global+1.5. However, the Arctic-focused strategies and Global−1.5 all provide comparable amounts of cooling per unit injection in the mid-latitude and extrapolar regions (Arctic High is slightly more efficient in this region) and have comparable rates of permafrost area increase, indicating that tropical and Arctic injection may be comparably effective for mid-latitude impacts. Arctic-focused SAI also introduces other high-latitude effects, including changes to the seasonal cycle of high-latitude temperature and sea ice. Arctic High increases high-latitude sulfur deposition by more than double relative to the same period without SAI, equivalent to a backwards step of approximately 60 years for sulfur deposition rates in the Arctic. Lastly, in this model, Arctic High slows overall carbon uptake by the Arctic ecosystem via reduced storage in vegetation. While permafrost mod-

eling is highly uncertain, demonstrating this model's global warming produces a negative feedback by increasing plant uptake of CO_2 at high latitudes, and an intervention that reduces that warming could also dampen that feedback.

It was originally hypothesized that the effects of high-latitude injection could be largely confined to the Arctic due to the poleward direction of the stratospheric Brewer-Dobson circulation (Lane et al., 2007). However, Robock et al. (2008) concluded this was not the case, citing substantial impacts outside of the Arctic, including reductions to downward surface SW well south of the injection site and changes to tropical precipitation. Our results are similar, and we conclude that although Arctic-focused SAI gives the most cooling at high latitudes and in many cases affects high-latitude metrics (such as sea ice extent) more strongly than globally-focused SAI, it would be incorrect to categorize Arctic-focused SAI as a "local" intervention because of the effects outside the polar region. Arctic High causes detectable cooling nearly everywhere in the northern hemisphere, and although sulfur mixing ratio and AOD are highest near the pole, zonally-integrated sulfur burden and reduction in TOA incoming SW energy peak south of the injection location, and Arctic High increases sulfur deposition in the mid-latitudes by 60%. The hemispherically asymmetric forcing also causes a substantial southward shift in the ITCZ and disrupts the seasonal monsoons; this shift could be offset by combining Arctic-focused injection with injection in the southern hemisphere, either in the tropics or at the Antarctic. Similar studies in other models would greatly help to reduce uncertainty, including the quantification of both how Arctic-focused and globally-focused SAI impact the Arctic and also how Arctic-focused SAI impacts regions outside the Arctic (and how southern hemisphere injection might offset this). Simulations that include an evolving ice sheet would be especially useful in determining the effects of Arctic SAI on ice dynamics, and longer simulations would be useful in determining the effects of SAI on natural variability. Additionally, there is ample room for further in-depth exploration of SAI effects, such as changes to the circulation or analysis of the various radiative, humidity, and temperature feedbacks that govern Arctic amplification.

5 Open Research

Data used in this study is available through the Cornell eCommons repository at https://doi.org/10.7298/gnmp-q653. Additional data from the Global | 1.5, Global | 1.0, and Global | 0.5 simulations can be likewise be found through the Cornell eCommons repository at Visioni (2022), https://doi.org/10.7298/xr82-sv86.

Acknowledgments

The authors would like to thank two anonymous reviewers, as well as attendees of the 2022 Gordon Research Seminar and Gordon Research Conference for Climate Engineering who offered feedback on this project that substantially improved the quality of our manuscript. The authors would also like to acknowledge high-performance computing support from Cheyenne (https://doi.org/10.5065/D6RX99HX) provided by NCAR's Computational and Information Systems Laboratory, sponsored by the National Science Foundation. Support for WL and DM was provided by the National Science Foundation through agreement CBET-1818759. Support for DV was provided by the Atkinson Center for a Sustainable Future at Cornell University. Support for BK was provided in part by the National Sciences Foundation through agreement CBET-1931641, the Indiana University Environmental Resilience Institute, and the Prepared for Environmental Change Grand Challenge initiative. The Pacific Northwest National Laboratory is operated for the U.S. Department of Energy by Battelle Memorial Institute under contract DE-AC05-76RL01830. The CESM project is supported primarily by the National Science Foundation. This work was supported by the National Center for Atmospheric Research, which is a major facility sponsored by the National Science Foundation under Cooperative Agreement No. 1852977, and by SilverLining through its Safe Climate Research Initiative.

Armour, K. C., Eisenman, I., Blanchard-Wrigglesworth, E., McCusker, K. E., & Bitz, C. M. (2011). The reversibility of sea ice loss in a state-of-the-art climate model. *Geophysical Research Letters*, *38*(16). doi: https://doi.org/10.1029/2011GL048739

Bamber, J. L., Westaway, R. M., Marzeion, B., & Wouters, B. (2018). The land ice contribution to sea level during the satellite era. *Environmental Research Letters*, *13*. doi: 10.1088/1748-9326/aac2f0

Biskaborn, B. K., Smith, S. L., Noetzli, J., Matthes, H., Vieira, G., Streletskiy, D. A., ... Lantuit, H. (2019). Permafrost is warming at a global scale. *Nature Communications*, *10*. doi: 0.1038/s41467-018-08240-4

Boucher, O., Halloran, P. R., Burke, E. J., Doutriaux-Boucher, M., Jones, C. D., Lowe, J., ... Wu, P. (2012). Reversibility in an earth system model in response to co2 concentration changes. *Environmental Research Letters*, *7*(2). doi: 10.1088/1748-9326/7/2/024013

Byrne, M. P., Pendergrass, A. G., Rapp, A. D., & Wodzicki, K. R. (2018). Response of the Intertropical Convergence Zone to Climate Change: Location, Width, and Strength. *Current Climate Change Reports*, *4*, 355–370. doi: https://doi.org/10.1007/s40641-018-0110-5

Cai, S., Hsu, P.-C., & Liu, F. (2021). Changes in polar amplification in response to increasing warming in cmip6. *Atmospheric and Oceanic Science Letters*, *14*(3), 100043. doi: https://doi.org/10.1016/j.aosl.2021.100043

Chen, Y., Liu, A., & Moore, J. C. (2020). Mitigation of Arctic permafrost carbon loss through stratospheric aerosol geoengineering. *Nature Communications*, *11*(2430). doi: https://doi.org/10.1038/s41467-020-16357-8

Cheng, W., MacMartin, D. G., Kravitz, B., Visioni, D., Bednarz, E. M., Xu, Y., ... Deng, X. (2022). Changes in Hadley circulation and intertropical convergence zone under strategic stratospheric aerosol geoengineering. *npj Climate and Atmospheric Science*, *5*(32). doi: 10.1038/s41612-022-00254-6

Dai, A., Luo, D., Song, M., & Liu, J. (2019). Arctic amplification is caused by sea-ice loss under increasing co2. *Nature Communications*, *10*(121). doi: 0.1038/s41467-018-07954-9

Danabasoglu, G., Bates, S. C., Briegleb, B. P., Jayne, S. R., Jochum, M., Large, W. G., ... Yeager, S. G. (2012). The CCSM4 Ocean Component. *Journal of Climate*, *25*(5), 1361–1389. doi: 10.1175/JCLI-D-11-00091.1

Danabasoglu, G., Lamarque, J.-F., Bacmeister, J., Bailey, D. A., DuVivier, A. K., Edwards, J., ... Strand, W. G. (2020). The community earth system model version 2 (cesm2). *Journal of Advances in Modeling Earth Systems*, *12*(2). e2019MS001916. doi: https://doi.org/10.1029/2019MS001916

Donohoe, A., Marshall, J., Ferreira, D., & Mcgee, D. (2013, 05). The Relationship between ITCZ Location and Cross-Equatorial Atmospheric Heat Transport: From the Seasonal Cycle to the Last Glacial Maximum. *Journal of Climate*, *26*(11), 3597-3618. doi: 10.1175/JCLI-D-12-00467.1

DuVivier, A. K., Holland, M. M., Kay, J. E., Tilmes, S., Gettelman, A., & Bailey, D. A. (2020). Arctic and antarctic sea ice mean state in the community earth system model version 2 and the influence of atmospheric chemistry. *Journal of Geophysical Research: Oceans*, *125*(8), e2019JC015934. doi: https://doi.org/10.1029/2019JC015934

England, M. R., Eisenman, I., Lutsko, N. J., & Wagner, T. J. W. (2021). The recent emergence of arctic amplification. *Geophysical Research Letters*, *48*(15). e2021GL094086. (e2021GL094086 2021GL094086) doi: https://doi.org/10.1029/2021GL094086

Fasullo, J. T., Tilmes, S., Richter, J. H., Kravitz, B., MacMartin, D. G., Mills, M. J., & Simpson, I. R. (2018). Persistent polar ocean warming in a strategically geoengineered climate. *Nature Geoscience*, *11*, 910–914. doi:

https://doi.org/10.1038/s41561-018-0131-9
Fox-Kemper, B., Hewitt, H., Xiao, C., Adalgeirsdottir, G., Drijfhout, S., Edwards, T., ... Yu, Y. (2021). Ocean, cryosphere and sea level change. In V. Masson-Delmotte et al. (Eds.), *Climate change 2021: The physical science basis. contribution of working group i to the sixth assessment report of the intergovernmental panel on climate change* (pp. 1211–1362). Cambridge University Press.

Frierson, D. M. W., & Hwang, Y.-T. (2012, 01). Extratropical Influence on ITCZ Shifts in Slab Ocean Simulations of Global Warming. *Journal of Climate*, *25*(2), 720-733. doi: 10.1175/JCLI-D-11-00116.1

Gettelman, A., Mills, M. J., Kinnison, D. E., Garcia, R. R., Smith, A. K., Marsh, D. R., ... Randel, W. J. (2019). The whole atmosphere community climate model version 6 (waccm6). *Journal of Geophysical Research: Atmospheres*, *124*(23), 12380-12403. doi: https://doi.org/10.1029/2019JD030943

Guo, A., Moore, J. C., & Ji, D. (2018). Tropical atmospheric circulation response to the g1 sunshade geoengineering radiative forcing experiment. *Atmospheric Chemistry and Physics*, *18*(12), 8689–8706. doi: 10.5194/acp-18-8689-2018

Haywood, J. M., Jones, A., Bellouin, N., & Stephenson, D. (2013). Asymmetric forcing from stratospheric aerosols impacts Sahelian rainfall. *Nature Climate Change*, *3*, 660–665. (doi:10.1038/nclimate1857) doi: 10.1038/nclimate1857

Hugelius, G., Strauss, J., Zubrzycki, S., Harden, J. W., Schuur, E. A. G., Ping, C.-L., ... Kuhry, P. (2014). Estimated stocks of circumpolar permafrost carbon with quantified uncertainty ranges and identified data gaps. *Biogeosciences*, *11*(23), 6573–6593. doi: 10.5194/bg-11-6573-2014

Hunke, E. C., Lipscomb, W. H., Turner, A. K., Jeffery, N., & Elliott, S. (2015). Cice: The los alamos sea ice model, documentation and software user's manual (5.1 ed.) [Computer software manual].

IMBIE. (2020). Mass balance of the greenland ice sheet from 1992 to 2018. *Nature*, *579*, 233–239. doi: 0.1038/s41586-019-1855-2

Jackson, L. S., Crook, J. A., Jarvis, A., Leedal, D., Ridgwell, A., Vaughan, N., & Forster, P. M. (2015). Assessing the controllability of Arctic sea ice extent by sulfate aerosol geoengineering. *Geophysical Research Letters*, *42*(4), 1223-1231. doi: 10.1002/2014GL062240

Jiang, J., Cao, L., MacMartin, D. G., Simpson, I. R., Kravitz, B., Cheng, W., ... Mills, M. J. (2019). Stratospheric Sulfate Aerosol Geoengineering Could Alter the High-Latitude Seasonal Cycle. *Geophysical Research Letters*, *46*(23), 14153-14163. doi: 10.1029/2019GL085758

Kleinschmitt, C., Boucher, O., & Platt, U. (2018). Sensitivity of the radiative forcing by stratospheric sulfur geoengineering to the amount and strategy of the so_2 injection studied with the lmdz-s3a model. *Atmospheric Chemistry and Physics*, *18*(4), 2769–2786. doi: 10.5194/acp-18-2769-2018

Kravitz, B., MacMartin, D. G., Mills, M. J., Richter, J. H., Tilmes, S., Lamarque, J.-F., ... Vitt, F. (2017). First Simulations of Designing Stratospheric Sulfate Aerosol Geoengineering to Meet Multiple Simultaneous Climate Objectives. *Journal of Geophysical Research: Atmospheres*, *122*(23), 12,616-12,634. doi: 10.1002/2017JD026874

Krishnamohan, K. S., & Bala, G. (2022). Sensitivity of tropical monsoon precipitation to the latitude of stratospheric aerosol injections. *Climate Dynamics*(59), 151–168. doi: 10.1007/s00382-021-06121-z

Lane, L., Caldeira, K., Chatfield, R., & Langhoff, S. (Eds.). (2007). *Workshop report on managing solar radiation* (Vol. NASA/CP–2007-214558). NASA. Retrieved from `https://ntrs.nasa.gov/citations/20070031204`

Lawrence, D. M., Fisher, R. A., Koven, C. D., Oleson, K. W., Swenson, S. C., Bonan, G., ... Zeng, X. (2019). The community land model version 5: Description of new features, benchmarking, and impact of forcing uncertainty.

Journal of Advances in Modeling Earth Systems, *11*(12), 4245-4287. doi: https://doi.org/10.1029/2018MS001583

Lawrence, D. M., Koven, C. D., Swenson, S. C., Riley, W. J., & Slater, A. G. (2015). Permafrost thaw and resulting soil moisture changes regulate projected high-latitude co2 and ch4 emissions. *Environmental Research Letters*, *10*(9). doi: 10.1088/1748-9326/10/9/094011

Lee, H., Ekici, A., Tjiputra, J., Muri, H., Chadburn, S. E., Lawrence, D. M., & Schwinger, J. (2019). The response of permafrost and high-latitude ecosystems under large-scale stratospheric aerosol injection and its termination. *Earth's Future*, 7(6), 605-614. doi: https://doi.org/10.1029/2018EF001146

Lee, W., MacMartin, D., Visioni, D., & Kravitz, B. (2020). Expanding the design space of stratospheric aerosol geoengineering to include precipitation-based objectives and explore trade-offs. *Earth System Dynamics*, *11*(4), 1051–1072. doi: 10.5194/esd-11-1051-2020

Lee, W., MacMartin, D., Visioni, D., & Kravitz, B. (2021). High-Latitude Stratospheric Aerosol Geoengineering Can Be More Effective if Injection Is Limited to Spring. *Geophysical Research Letters*, *48*(9). doi: 10.1029/2021GL092696

Lipscomb, W. H., Price, S. F., Hoffman, M. J., Leguy, G. R., Bennett, A. R., Bradley, S. L., ... Worley, P. H. (2019). Description and evaluation of the community ice sheet model (cism) v2.1. *Geoscientific Model Development*, *12*(1), 387–424. doi: 10.5194/gmd-12-387-2019

Liu, X., Ma, P.-L., Wang, H., Tilmes, S., Singh, B., Easter, R. C., ... Rasch, P. J. (2016). Description and evaluation of a new four-mode version of the modal aerosol module (mam4) within version 5.3 of the community atmosphere model. *Geoscientific Model Development*, *9*(2), 505–522. doi: 10.5194/gmd-9-505-2016

MacMartin, D. G., & Kravitz, B. (2019). The Engineering of Climate Engineering. *Annual Review of Control, Robotics, and Autonomous Systems*, *2*(1), 445-467. doi: 10.1146/annurev-control-053018-023725

MacMartin, D. G., Kravitz, B., Keith, D. W., & Jarvis, A. (2014). Dynamics of the coupled human-climate system resulting from closed-loop control of solar geoengineering. *Climate Dynamics*, *43*(1-2), 243-258. doi: 10.1007/s00382-013-1822-9

MacMartin, D. G., Visioni, D., Kravitz, B., Richter, J. H., Felgenhauer, T., Lee, W. R., ... Sugiyama, M. (2022). Scenarios for modeling solar radiation modification. *Proceedings of the National Academy of Sciences of the United States of America*.

McGuire, A. D., Lawrence, D. M., Koven, C., Clein, J. S., Burke, E., Chen, G., ... Zhuang, Q. (2018). Dependence of the evolution of carbon dynamics in the northern permafrost region on the trajectory of climate change. *Proceedings of the National Academy of Sciences*, *115*(15), 3882-3887. doi: 10.1073/pnas.1719903115

Mills, M. J., Richter, J. H., Tilmes, S., Kravitz, B., MacMartin, D. G., Glanville, A. A., ... Kinnison, D. E. (2017). Radiative and Chemical Response to Interactive Stratospheric Sulfate Aerosols in Fully Coupled CESM1(WACCM). *Journal of Geophysical Research: Atmospheres*, *122*(23), 13,061-13,078. doi: 10.1002/2017JD027006

Moore, J. C., Rinke, A., Yu, X., Ji, D., Cui, X., Li, Y., ... Yang, S. (2014). Arctic sea ice and atmospheric circulation under the geomip g1 scenario. *Journal of Geophysical Research: Atmospheres*, *119*(2), 567-583. doi: https://doi.org/10.1002/2013JD021060

Moore, J. C., Yue, C., Zhao, L., Guo, X., Watanabe, S., & Ji, D. (2019). Greenland Ice Sheet Response to Stratospheric Aerosol Injection Geoengineering. *Earth's Future*, 7(12), 1451-1463. doi: https://doi.org/10.1029/2019EF001393

Mouginot, J., Rignot, E., Bjørk, A. A., van den Broeke, M., Millan, R., Morlighem,

M., ... Velicogna, I. (2019). Forty-six years of Greenland Ice Sheet mass balance from 1972 to 2018. *Proceedings of the National Academy of Sciences*, *116*(19), 9239-9244. doi: 10.1073/pnas.1904242116

National Academies of Sciences, Engineering, and Medicine. (2021). *Reflecting Sunlight: Recommendations for Solar Geoengineering Research and Research Governance*. Washington, DC: The National Academies Press. doi: 10.17226/25762

Niemeier, U., Schmidt, H., & Timmreck, C. (2011). The dependency of geoengineered sulfate aerosol on the emission strategy. *Atmospheric Science Letters*, *12*(2), 189-194. doi: https://doi.org/10.1002/asl.304

Notz, D., & SIMIP. (2020). Arctic sea ice in cmip6. *Geophysical Research Letters*, *47*(10), e2019GL086749. doi: https://doi.org/10.1029/2019GL086749

Notz, D., & Stroeve, J. C. (2018). The Trajectory Towards a Seasonally Ice-Free Arctic Ocean. *Current Climate Change Reports*, *4*, 407–416. doi: 10.1007/s40641-018-0113-2

Pierce, J. R., Weisenstein, D. K., Heckendorn, P., Peter, T., & Keith, D. W. (2010). Efficient formation of stratospheric aerosol for climate engineering by emission of condensible vapor from aircraft. *Geophysical Research Letters*, *37*(18). doi: https://doi.org/10.1029/2010GL043975

Pithan, F., & Mauritsen, T. (2014). Arctic amplification dominated by temperature feedbacks in contemporary climate models. *Nature Geoscience*, *7*, 181–184. doi: https://doi.org/10.1038/ngeo2071

Plaza, C., Pegoraro, E., Bracho, R., Celis, G., Crummer, K. G., Hutchings, J. A., ... Schuur, E. A. G. (2019). Direct observation of permafrost degradation and rapid soil carbon loss in tundra. *Nature Geoscience*, *12*, 627–631. doi: 10.1038/s41561-019-0387-6

Previdi, M., Smith, K. L., & Polvani, L. M. (2021, sep). Arctic amplification of climate change: a review of underlying mechanisms. *Environmental Research Letters*, *16*(9), 093003. Retrieved from `https://doi.org/10.1088/1748-9326/ac1c29` doi: 10.1088/1748-9326/ac1c29

Richter, J., Visioni, D., MacMartin, D., Bailey, D., Rosenbloom, N., Lee, W., ... Lamarque, J.-F. (2022). Assessing responses and impacts of solar climate intervention on the earth system with stratospheric aerosol injection (arise-sai). *EGUsphere*, *2022*, 1–35. doi: 10.5194/egusphere-2022-125

Ridley, J. K., Lowe, J. A., & Hewitt, H. T. (2012). How reversible is sea ice loss? *The Cryosphere*, *6*(1), 193–198. doi: 10.5194/tc-6-193-2012

Robock, A., Oman, L., & Stenchikov, G. L. (2008). Regional climate responses to geoengineering with tropical and Arctic SO2 injections. *Journal of Geophysical Research: Atmospheres*, *113*(D16). doi: 10.1029/2008JD010050

Samanta, A., Anderson, B. T., Ganguly, S., Knyazikhin, Y., Nemani, R. R., & Myneni, R. B. (2010). Physical climate response to a reduction of anthropogenic climate forcing. *Earth Interactions*, *14*(7), 1 - 11. doi: 10.1175/2010EI325.1

Schaefer, K., Lantuit, H., Romanovsky, V. E., Schuur, E. A. G., & Witt, R. (2014). The impact of the permafrost carbon feedback on global climate. *Environmental Research Letters*, *9*(8). doi: 10.1088/1748-9326/9/8/085003

Schuur, E. A. G., McGuire, A. D., Schädel, C., Grosse, G., Harden, J. W., Hayes, D. J., ... E., V. J. (2015). Climate change and the permafrost carbon feedback. *Nature*, *520*, 171–179. doi: 10.1038/nature14338

Slater, D. A., Straneo, F., Felikson, D., Little, C. M., Goelzer, H., Fettweis, X., & Holte, J. (2019). Estimating greenland tidewater glacier retreat driven by submarine melting. *The Cryosphere*, *13*(9), 2489–2509. doi: 10.5194/tc-13-2489-2019

Smith, R., Jones, P., Briegleb, B., Bryan, F., Danabasoglu, G., Dennis, J., ... Yeager, S. (2010). The parallel ocean program (pop) reference manual, ocean component of the community climate system model (ccsm) Computer software

Stocker, T., et al. (Eds.). (2013). *Climate change 2013: The physical science basis. contribution of working group i to the fifth assessment report of the intergovernmental panel on climate change*. Cambridge University Press.

Stroeve, J. C., & Notz, D. (2018, sep). Changing state of Arctic sea ice across all seasons. *Environmental Research Letters*, *13*(10), 103001. doi: 10.1088/1748-9326/aade56

Tarnocai, C., Canadell, J. G., Schuur, E. A. G., Kuhry, P., Mazhitova, G., & Zimov, S. (2009). Soil organic carbon pools in the northern circumpolar permafrost region. *Global Biogeochemical Cycles*, *23*(2). doi: https://doi.org/10.1029/2008GB003327

Tilmes, S., MacMartin, D. G., Lenaerts, J. T. M., van Kampenhout, L., Muntjewerf, L., Xia, L., ... Robock, A. (2020). Reaching 1.5 and 2.0°C global surface temperature targets using stratospheric aerosol geoengineering. *Earth System Dynamics*, *11*(3), 579–601. doi: 10.5194/esd-11-579-2020

Tilmes, S., Richter, J. H., Kravitz, B., MacMartin, D. G., Mills, M. J., Simpson, I. R., ... Ghosh, S. (2018, 12). CESM1(WACCM) Stratospheric Aerosol Geoengineering Large Ensemble Project. *Bulletin of the American Meteorological Society*, *99*(11), 2361-2371. doi: 10.1175/BAMS-D-17-0267.1

Vallis, G. K., Zurita-Gotor, P., Cairns, C., & Kidston, J. (2015). Response of the large-scale structure of the atmosphere to global warming. *Quarterly Journal of the Royal Meteorological Society*, *141*(690), 1479-1501. doi: https://doi.org/10.1002/qj.2456

van den Broeke, M., Box, J., Fettweis, X., Hanna, E., Noël, B., Tedesco, M., ... van Kampenhout, L. (2017). Greenland Ice Sheet Surface Mass Loss: Recent Developments in Observation and Modeling. *Current Climate Change Reports*, *3*, 345–356. doi: 10.1007/s40641-017-0084-8

Visioni, D. (2022). *Data from: Scenarios for modeling solar radiation modification*. Cornell eCommons Library. Retrieved from `https://doi.org/10.7298/xr82-sv86`

Visioni, D., MacMartin, D. G., Kravitz, B., Lee, W., Simpson, I. R., & Richter, J. H. (2020). Reduced Poleward Transport Due to Stratospheric Heating Under Stratospheric Aerosols Geoengineering. *Geophysical Research Letters*, *47*(17), e2020GL089470. (e2020GL089470 10.1029/2020GL089470) doi: 10.1029/2020GL089470

Visioni, D., Slessarev, E., MacMartin, D. G., Mahowald, N. M., Goodale, C. L., & Xia, L. (2020, sep). What goes up must come down: impacts of deposition in a sulfate geoengineering scenario. *Environmental Research Letters*, *15*(9), 094063. doi: 10.1088/1748-9326/ab94eb

Xie, M., Moore, J. C., Zhao, L., Wolovick, M., & Muri, H. (2022). Impacts of three types of solar geoengineering on the atlantic meridional overturning circulation. *Atmospheric Chemistry and Physics*, *22*(7), 4581–4597. doi: 10.5194/acp-22-4581-2022

Yang, Y., Wang, H., Smith, S. J., Easter, R. C., & Rasch, P. J. (2018). Sulfate aerosol in the arctic: Source attribution and radiative forcing. *Journal of Geophysical Research: Atmospheres*, *123*(3), 1899-1918. doi: https://doi.org/10.1002/2017JD027298

Zarnetske, P. L., Gurevitch, J., Franklin, J., Groffman, P. M., Harrison, C. S., Hellmann, J. J., ... Yang, C.-E. (2021). Potential ecological impacts of climate intervention by reflecting sunlight to cool earth. *Proceedings of the National Academy of Sciences*, *118*(15), e1921854118. doi: 10.1073/pnas.1921854118

NATIONAL SCIENCE FOUNDATION

Award:2038246 **PI Name:**MacMartin, Douglas

Notification Type	Grantee Approved No Cost Extension
Award Number	2038246
Award Title	Fundamental limits and trade-offs of stratospheric aerosol geoengineering
NSF Status	Reviewed by PO.
NSF Status Updated By	bhamilto
NSF Status Date	10/20/23
Prepared By	
Submitted By	
Submitted Date	10/20/23
Submitter Email	tjb3@cornell.edu
Revised End Date	12/31/24
Justification	The research associated with this award has been largely completed but the final results not yet submitted to a journal (because the PhD student graduated and is working, so completing the final paper is likely to take extra time). Further, the proposal requested funding for a final workshop with policy experts to discuss results and future directions and we haven't scheduled that workshop yet as we were waiting on finishing the optimization paper!

NATIONAL SCIENCE FOUNDATION

Award Notice

Award Number (FAIN): 2038246
Managing Division Abbreviation: CBET **Amendment Number:** 000

AWARDEE INFORMATION

Award Recipient: Cornell University
Awardee Address: 373 Pine Tree Road Ithaca, NY 148502820
Official Awardee Email Address:cu_awds@cornell.edu
Unique Entity Identifier (DUNS ID): 872612445

AMENDMENT INFORMATION

Amendment Type: New Project
Amendment Date: 10/30/2020
Amendment Number: 000
Proposal Number: 2038246
Amendment Description:

The National Science Foundation hereby awards a Standard Grant for support of the project described in the proposal referenced above .

The Foundation authorizes the awardee to enter into the proposed subaward arrangement and to fund the subaward with award funds up to the amount indicated in the approved budget or NSF-approved post award request. The subaward should contain appropriate provisions consistent with Appendix B of the Research Terms and Conditions (RTC) dated December 10, 2018, or Articles 8.a.4. and 9 of the NSF Grant General Conditions (GC-1) dated February 25, 2019 (as appropriate), as well as any special conditions included in this award.

AWARD INFORMATION

Award Number (FAIN): 2038246
Award Instrument: Standard Grant
Award Date: 10/30/2020
Award Period of Performance: Start Date: 01/01/2021 End Date: 12/31/2023
Project Title: Fundamental limits and trade-offs of stratospheric aerosol geoengineering
Managing Division Abbreviation: CBET
Research and Development Award: Yes
Funding Opportunity: PD 20-7643 Environmental Sustainability
CFDA Number and Name: 47.041 Engineering Grants

FUNDING INFORMATION

Amount Obligated by this Amendment: $398,143
Total Intended Award Amount: $398,143
Total Approved Cost Share or Matching Amount: $0
Total Amount Obligated to Date: $398,143
Expenditure Limitation: Not Applicable

PROJECT PERSONNEL

Principal Investigator: Douglas G MacMartin	**Email:** dgm224@cornell.edu	**Institution:** Cornell University
Co-Principal Investigator: Benjamin Kravitz	**Email:** bkravitz@iu.edu	**Institution:** Indiana University

NSF CONTACT INFORMATION

Managing Grants Official (Primary Contact) **Name:** Denise B. Robinson **Email:** drobinso@nsf.gov	**Awarding Official** **Name:** Denise B. Robinson **Email:** drobinso@nsf.gov	**Managing Program Officer** **Name:** Bruce K. Hamilton **Email:** bhamilto@nsf.gov

GENERAL TERMS AND CONDITIONS

This is awarded pursuant to the authority of the National Science Foundation Act of 1950, as amended (42 U.S.C. 1861-75) and is subject to Research Terms and Conditions (RTCs) dated 03/14/2017, and NSF Agency Specific Requirements, dated 10/05/2020, available at https://www.nsf.gov/awards/managing/rtc.jsp.

This institution is a signatory to the Federal Demonstration Partnership (FDP) Phase VI Agreement which requires active institutional participation in new or ongoing FDP demonstrations and pilots.

In addition, this award incorporates the following terms and conditions that implement Sections §§ 200.216 and 200.340 of the revised 2 CFR § 200 which was published in the Federal Register on August 13, 2020. The revised 2 CFR § 200 is effective on November 12, 2020, except for sections § 200.216 and § 200.340, which are effective on August 13, 2020:

1. Section 889 of the John S. McCain National Defense Authorization Act for Fiscal Year 2019

Section 889 of the National Defense Authorization Act (NDAA) for Fiscal Year (FY) 2019 (Public Law 115-232) prohibits the head of an executive agency from obligating or expending loan or grant funds to procure or obtain, extend, or renew a contract to procure or obtain, or enter into a contract (or extend or renew a contract) to procure or obtain the equipment, services, or systems prohibited systems as identified in section 889 of the NDAA for FY 2019.

(a) In accordance with 2 CFR 200.216 and 200.471, all awards that are issued on or after August 13, 2020, recipients and subrecipients are prohibited from obligating or expending loan or grant funds to:

(1) Procure or obtain;

(2) Extend or renew a contract to procure or obtain; or

(3) Enter into a contract (or extend or renew a contract) to procure or obtain equipment, services, or systems that uses covered telecommunications equipment or services as a substantial or essential component of any system, or as critical technology as part of any system. As described in Public Law 115-232, section 889, covered telecommunications equipment is telecommunications equipment produced by Huawei Technologies Company or ZTE Corporation (or any subsidiary or affiliate of such entities).

(i) For the purpose of public safety, security of government facilities, physical security surveillance of critical infrastructure, and other national security purposes, video surveillance and telecommunications equipment produced by Hytera Communications Corporation, Hangzhou Hikvision Digital Technology Company, or Dahua Technology Company (or any subsidiary or affiliate of such entities).

(ii) Telecommunications or video surveillance services provided by such entities or using such equipment.

(iii) Telecommunications or video surveillance equipment or services produced or provided by an entity that the Secretary of Defense, in consultation with the Director of the National Intelligence or the Director of the Federal Bureau of Investigation, reasonably believes to be an entity owned or controlled by, or otherwise connected to, the government of a covered foreign country.

(b) In implementing the prohibition under Public Law 115-232, section 889, subsection (f), paragraph (1), heads of executive agencies administering loan, grant, or subsidy programs shall prioritize available funding and technical support to assist affected businesses, institutions and organizations as is reasonably necessary for those affected entities to transition from covered communications equipment and services, to procure replacement equipment and services, and to ensure that communications service to users and customers is sustained.

(c) See Public Law 115-232, section 889 for additional information.

COVERED FOREIGN COUNTRY means the People's Republic of China.

2. Implementation of the newly revised section 2 CFR § 200.340

The following language replaces paragraph b. of the Termination article contained in the applicable set of NSF general conditions referenced in the award notice:

b. The award may be suspended or terminated in whole or in part in any of the following situations:

1. By NSF, if the awardee fails to comply with the terms and conditions of a Federal award;

2. By NSF, to the greatest extent authorized by law, if an award no longer effectuates the program goals or agency priorities;

3. By NSF, with the consent of the awardee, in which case the two parties must agree upon the

termination conditions, including the effective date and, in the case of partial termination, the portion to be terminated;

4. By the awardee upon sending to NSF written notification setting forth the reasons for such termination, the effective date, and, in the case of partial termination, the portion to be terminated. However, if NSF determines in the case of partial termination that the reduced or modified portion of the NSF award will not accomplish the purposes for which the NSF award was made, NSF may terminate the Federal award in its entirety;

5. By NSF, pursuant to termination provisions included in the NSF award; or

6. By NSF, when ordered by the Deputy Director under NSF's Regulation on Research Misconduct [45 CFR Part 689].

BUDGET

A. Senior Personnel	
Senior Personnel Count	(b)(4)
Senior Personnel Calendar Months	
Senior Personnel Academic Months	
Senior Personnel Summer Months	
Senior Personnel Amount	
B. Other Personnel	
Post Doctoral Scholars	
Post Doctoral Count	0.00
Post Doctoral Calendar Months	0.00
Post Doctoral Academic Months	0.00
Post Doctoral Summer Months	0.00
Post Doctoral Amount	$0
Other Professionals	
Other Professionals Count	0.00
Other Professionals Calendar Months	0.00
Other Professionals Academic Months	0.00
Other Professionals Summer Months	0.00
Other Professionals Amount	$0
Graduate Students	

Graduate Students Count	(b)(4)
Graduate Students Amount	
Undergraduate Students	
Undergraduate Students Count	0.00
Undergraduate Students Amount	$0
Secretarial - Clerical	
Secretarial - Clerical Count	0.00
Secretarial - Clerical Amount	$0
Other	
Other Count	0.00
Other Amount	$0
Total Salaries and Wages (A+B)	(b)(4)
C. Fringe Benefits	
Total Salaries, Wages, Fringe Benefits (A + B + C)	
D. Equipment	
E. Travel	
Domestic	
International	
F. Participant Support Costs	
Participant Support Costs Stipends	$0
Participant Support Costs Travel	$0
Participant Support Costs Subsistence	$0
Participant Support Costs Other	$0
Total Number of Participants	0.00
Total Participant Costs (F)	$0
G. Other Direct Costs	
Materials Supplies	(b)(4)
Publication Costs	
Consultant Services	
Computer Services	
Subawards	
Other	
Total Other Direct Costs (G)	
H. Total Direct Costs (A Through G)	
I. Indirect Costs*	
J. Total Direct and Indirect Costs (H + I)	$398,143
K. Fees	$0
L. Total Amount of Request (J) OR (J + K)	**$398,143**

M. Cost Sharing Proposed Level	2024-256F	00000000866	"UNCLASSIFIED"	7/16/2025
	$0			

*Indirect Cost Rates

Item Name	Indirect Cost Rate
Facilities and Administrative	(b)(4)

These rates are at the time of award and are based upon the budget submitted to the NSF. It does not include any out-year adjustments. The NSF will not modify awards simply to correct indirect cost rates cited in the award notice. See the Proposal & Award Policies & Procedures Guide (PAPPG) Chapter X.A.3.a. for guidance on re-budgeting authority.

Project Report Printer Friendly Version 2024-2565 [illegible] "UNCLASSIFIED" 7/16/2025 Click here to print

Preview of Award 2038246 - Final Annual Project Report

Cover

Federal Agency and Organization Element to Which Report is Submitted:	**4900**
Federal Award or Other Identifying Number Assigned by Agency:	**2038246**
Project Title:	**Fundamental limits and trade-offs of stratospheric aerosol geoengineering**
PD/PI Name:	**Douglas G MacMartin, Principal Investigator** **Benjamin Kravitz, Co-Principal Investigator**
Recipient Organization:	**Cornell University**
Project/Grant Period:	**01/01/2021 - 12/31/2024**
Reporting Period:	**01/01/2024 - 12/31/2024**
Submitting Official (if other than PD\PI):	**Douglas G MacMartin** **Principal Investigator**
Submission Date:	**03/06/2025**
Signature of Submitting Official (signature shall be submitted in accordance with agency specific instructions)	**Douglas G MacMartin**

Accomplishments

*** What are the major goals of the project?**

Geoengineering (in particular we focus on stratospheric aerosol injection) would cool the climate, reducing some impacts from climate change, but it would not simply reverse changes due to increased atmospheric greenhouse gas concentrations, leading to residual changes. These changes, however, depend on how it is done – particularly what latitudes or seasons that aerosols are added to the stratosphere. The main goal of the project is to understand what geoengineering can and cannot do. This will help us understand which decisions matter, which uncertainties need to be resolved or managed, fundamental limits to how well it can compensate for climate change, and where any trade-offs might be. All of these are essential for informing future decisions about whether and how to deploy geoengineering.

*** What was accomplished under these goals and objectives (you must provide information for at least one of the 4 categories below)?** 2024-256F 00000000870 "UNCLASSIFIED" 7/16/2025

Major Activities:

There are a number of significant activities from this project. (i) We have integrated previously conducted geoengineering simulations that use different combinations of locations (latitudes) and times of year (season) to achieve different sets of climate objectives with simulations at many different latitudes and seasons to estimate the total number of independent "design" degrees of freedom available; (ii) building on that, we have designed and conducted a set of simulations that collectively span a complete range of independent strategies; these include four different hemispherically-symmetric strategies including one more polar-focused, as well as an Arctic-focused strategy, and a default multi-objective strategy considered in previous model version, as well as an updated and longer set of fixed-injection-rate cases (iii) we have also designed and completed simulations that consider a range of different plausible future deployment scenarios, involving in particular different amounts of cooling, but also different start dates and inconsistencies in deployment; this both helps assess nonlinearities and transients as well as being valuable on its own for informing dependence of impacts on scenario, (iv) we have conducted optimization for different climate metrics to assess both how much the strategy depends on the metric chosen as well as how much "better" one might be able to achieve than with current strategies (completed in the final year), (v) the simulations conducted have been used already to look at some impact analyses (such as risks from Antarctic ice melt), and finally (vi) we have collaborated with other climate modeling centers to conduct similar analyses, resulting in several papers with U. Exeter; simulations conducted as part of this project have motivated the design of both scenarios and strategies for the next set of Geoengineering Model Intercomparison Project (GeoMIP) simulations.

Specific Objectives:

Significant Results:

(1) For global cooling of up to 1.5°C, there are approximately 6-8 independent degrees of freedom for SAI that would lead to detectably different climate outcomes. These include injection at 30N, 15N, equator, 15S, 30S, as well as spring injection at 60N and 60S. This also means that as many as 6-8 independent climate objectives might be simultaneously managed; previous studies have considered at most 3, suggesting both that there is considerable scope for exploring distinct strategies, and that this scope is "small" enough that this exploration is feasible. (2) Different strategies involving different combinations of these latitudes yield different outcomes not only in surface temperature and precipitation, but on Arctic sea ice, hurricane indices, ITCZ, Antarctic sea ice risks, etc. (3) Arctic-focused and polar-focused strategies are plausible, with injection at lower altitude but high latitude; these preferentially cool at higher latitude with less tropical cooling, yielding greater efficiency for some impacts but different trade-offs relative to other strategies. (This last one is also particularly noteworthy because it would be easier to deploy at lower altitude, and many risks people care about are at high latitude) (4) A hemispherically-symmetric strategy that injects equal amounts at roughly 30N and 30S (15N and 15S might do as well) is simpler to implement in other models and is not too sub-optimal relative to more complicated strategies for many metrics (in particular, it roughly maintains equator-to-pole temperature gradients without formally needing to control for them), and finally (5), optimizing across the available degrees of freedom can be used to explore Pareto-optimal front; e.g. what strategies do best trading off temperature and precipitation changes. The optimum solutions clearly do "better" than any existing strategies. For minimizing temperature alone, then for modest cooling the differences are not large relative to existing strategies that have been simulated. However, there is some potential to find strategies that do a better job of balancing changes in temperature and precipitation (in this climate model).

Key outcomes or Other achievements:

Results from this project have led to collaboration with U. Exeter to conduct a subset of similar simulations in the UKESM model, and are serving as the basis for designing the next round of GeoMIP simulations. Preliminary analyses are also being conducted with policy experts on different scenarios using these simulations. Two PhD theses were supported or partially supported by this award; Yan Zhang and Walker Lee; this award also partially supported a third PhD student, Ezra Brody.

*** What opportunities for training and professional development has the project provided?**

The project has directly supported the research of two graduate students in engineering and one term of a third student; work related to this project has also involved two postdoctoral research associates with a background in climate science (one of whom is now faculty at Cornell in Atmospheric Science, the other a researcher at NOAA). This provides a learning experience for both; the graduate students benefit from the expertise of the postdocs, and the postdocs gain an appreciation for engineering design principles, as well as some experience in mentoring graduate students. The graduate students have learned how to run CESM(WACCM), analyze the output, write papers, and prepare the results for presentations at conferences. Both students have graduated; Walker Lee is currently at NCAR working on design and feedback for Marine Cloud Brightening

*** Have the results been disseminated to communities of interest? If so, please provide details.**

The first paper from this award (partly supported by a previous NSF award) was published early in 2022 in Earth Systems Dynamics; a paper on scenarios was published in PNAS in 2022; a paper on Arctic-focused approach published in Earth's Future in 2023, two papers comparing multiple strategies published, one in Atm. Chem. Phys. and another in Earth System Dynamics (which was selected as a highlight paper!); a final paper on optimization is currently under review. Results using simulations that were generated as part of this research have been published in several papers, and there are a further two papers published with the UKESM climate model. All work is being presented at conferences, e.g., at AGU fall meeting in 2021 and 2022, and Gordon Research Conference (GRC) on Climate Engineering in 2022 and in two talks at the 2024 GRC (one of which was almost entirely based on this NSF award); some results have been used in a presentation at Arctic Circle meeting, as well as in GeoMIP meetings. Work on scenarios and strategies was discussed in a meeting held at NCAR focusing on scenario design; this research was also discussed at an IAI-sponsored international meeting in Jamaica. Research results are also disseminated to the research community through geoengineering email lists. Simulations have been made available and are being used by other researchers exploring impacts, including those in the developing world. And maybe in the long term most important; the results of this research were the driving influence on selecting the strategy and scenario used in the next round of GeoMIP simulations, which in turn will support the ability to write a coherent assessment of SAI for the IPCC AR7.

Finally, in 2024 we held a small workshop (adjacent to the GeoMIP meeting that was held at Cornell) building off of the research conducted in this grant, with a particular emphasis on what could be done with higher-latitude and thus lower-altitude deployment; this follows from the "polar" strategy (60N and 60S, with each conducted only in spring) that was simulated as part of this grant.

Products

Books

Book Chapters

Inventions

Journals or Juried Conference Papers

View all journal publications currently available in the for this award.

The results in the NSF Public Access Repository will include a comprehensive listing of all journal publications recorded to date that are associated with this award.

Kravitz, Ben and MacMartin, Douglas G. and Butler, Amy H. and Bednarz, Ewa M. and Visioni, Daniele. (2023). Potential Nonâ€ Linearities in the High Latitude Circulation and Ozone Response to Stratospheric Aerosol Injection. *Geophysical Research Letters*. 50 (22) . Status = Added in NSF-PAR Federal Government's License = Acknowledged. (Completed by MacMartin, on 01/04/2024)

Bednarz, E. M. and Visioni, D. and Kravitz, B. and Goddard, P. B. and MacMartin, D. G.. (2023). Stratospheric Aerosol Injection Can Reduce Risks to Antarctic Ice Loss Depending on Injection Location and Amount. *Journal of Geophysical Research: Atmospheres*. 128 (22) . Status = Added in NSF-PAR Federal Government's License = Acknowledged. (Completed by MacMartin, Benjamin on 01/04/2024)

Visioni, D. and Goddard, P. B. and Kravitz, B. and Bednarz, E. M. and MacMartin, D. G.. (2023). The Choice of Baseline Period Influences the Assessments of the Outcomes of Stratospheric Aerosol Injection. *Earth's Future*. 11 (8) . Status = Added in NSF-PAR Federal Government's License = Acknowledged. (Completed by MacMartin, Benjamin on 01/04/2024)

Kravitz, Ben and Chen, Yating and Lee, Walker Raymond and MacMartin, Douglas G. and Visioni, Daniele. (2023). Highâ€ Latitude Stratospheric Aerosol Injection to Preserve the Arctic. *Earth's Future*. 11 (1) . Status = Added in NSF-PAR Federal Government's License = Acknowledged. (Completed by MacMartin, Douglas on 01/04/2024)

Kravitz, Ben and Visioni, Daniele and Butler, Amy H. and Zhang, Yan and Bednarz, Ewa M.. (2023). Injection strategy â€“ a driver of atmospheric circulation and ozone response to stratospheric aerosol geoengineering. *Atmospheric Chemistry and Physics*. 23 (21) 13665 to 13684. Status = Added in NSF-PAR Federal Government's License = Acknowledged. (Completed by MacMartin, Douglas on 01/04/2024)

Henry, Matthew and Haywood, Jim and Dalvi, Mohit and Wells, Alice and Jones, Andy. (2023). Comparison of UKESM1 and CESM2 simulations using the same multi-target stratospheric aerosol injection strategy. *Atmospheric Chemistry and Physics*. 23 (20) 13369 to 13385. Status = Added in NSF-PAR Federal Government's License = Acknowledged. (Completed by MacMartin, on 01/04/2024)

MacMartin, D. G. and Richter, J.H. and Kravitz, B. and Felgenhauer, T. and Visioni, D.. (2022). Scenarios for modeling solar radiation modification. *Proceedings of the National Academy of Sciences*. 119 (33) . Status = Added in NSF-PAR Federal Government's License = Acknowledged. (Completed by MacMartin, Douglas on 12/07/2022)

Braesicke, Peter and Visioni, Daniele and Bednarz, Ewa M. and Banerjee, Antara and Kravitz, Ben. (2022). The Overlooked Role of the Stratosphere Under a Solar Constant Reduction. *Geophysical Research Letters*. 49 (12) . Status = Added in NSF-PAR Federal Government's License = Acknowledged. (Completed by MacMartin, Douglas on 12/07/2022)

MacMartin, Douglas G. and Visioni, Daniele and Zhang, Yan and Kravitz, Ben. (2022). How large is the design space for stratospheric aerosol geoengineering?. *Earth System Dynamics*. 13 (1) 201 to 217. Status = Added in NSF-PAR Federal Government's License = Acknowledged. (Completed by MacMartin, Douglas on 12/07/2022)

Brody, E., Y. Zhang, D. G. MacMartin, D. Visioni, B. Kravitz, and E. M. Bednarz, â€œUsing Optimization Tools to Explore Stratospheric Aerosol Injection Strategiesâ€ , submitted, Earth System Dynamics. Status = UNDER_REVIEW.

Bednarz, E.M., P.B. Goddard., D.G. MacMartin, D. Visioni, D. Bailey, and G. Danabasoglu, â€œStratospheric Aerosol Injection could prevent future Atlantic Meridional Overturning Circulation decline, but injection location is keyâ€ , submitted, Earthâ€™s Future. Status = UNDER_REVIEW.

Licenses

Other Conference Presentations / Papers

Other Products

Other Publications

Patent Applications

Technologies or Techniques

Thesis/Dissertations

Yan Zhang. *DESIGN SPACE EXPLORATION FOR STRATOSPHERIC AEROSOL INJECTION*. (2023). Cornell University. Acknowledgement of Federal Support = No

Walker Lee. *Exploring, Mapping, and Expanding the Design Space of Climate Intervention via Stratospheric Aerosol Injection*. (2023). Cornell University. Acknowledgement of Federal Support = No

Websites or Other Internet Sites

Participants/Organizations

What individuals have worked on the project?

Name	Most Senior Project Role	Nearest Person Month Worked
(b)(6)	Faculty	(b)(4): (b)(6)
	Graduate Student (research assistant)	
	Graduate Student (research assistant)	
	Graduate Student (research assistant)	
	Co PD/PI	
	PD/PI	

Full details of individuals who have worked on the project:

Daniele Visioni
Email: dv224@cornell.edu
Most Senior Project Role: Faculty
Nearest Person Month Worked: (b)(4): (b)(6)
Contribution to the Project: Assisted graduate students in running climate models, assisted graduate students in writing papers, but was only supported by NSF funding early in the project
Funding Support: Cornell Atkinson Center for a Sustainable Future
International Collaboration: No
International Travel: No

(b)(6)
Most Senior Project Role: Graduate Student (research assistant)
Nearest Person Month Worked: (b)(4): (b)(6)
Contribution to the Project: Developing simulations of Arctic injection in particular (and Arctic+Antarctic), analyzing, and writing papers. No effort in final year.
Funding Support: Also supported by Cornell Atkinson Center for a Sustainable Future for related research on Arctic impacts and processes
International Collaboration: Yes, United Kingdom
International Travel: No

(b)(6)
Most Senior Project Role: Graduate Student (research assistant)
Nearest Person Month Worked: (b)(4): (b)(6)
Contribution to the Project: Designing simulations, conducting simulations, analyzing simulations, writing papers. No effort in final year.
Funding Support: Summer salary came from Cornell Atkinson Center for Sustainable Futures

International Collaboration: No
International Travel: No

(b)(6)

Most Senior Project Role: Graduate Student (research assistant)
Nearest Person Month Worked (b)(4): (b)(6)
Contribution to the Project: Completed optimization work to determine whether there are "better" SAI strategies and identify dependence on the choice of metric and trade-offs, and wrote paper documenting optimization
Funding Support: Supported for one term on this award.
International Collaboration: No
International Travel: No

Benjamin Kravitz
Email: bkravitz@iu.edu
Most Senior Project Role: Co PD/PI
Nearest Person Month Worked (b)(4): (b)(6)
Contribution to the Project: Helped in overall guidance and assisting grad students in writing papers.
Funding Support: No additional support
Change in active other support: Yes
International Collaboration: No
International Travel: No

Douglas G MacMartin
Email: dgm224@cornell.edu
Most Senior Project Role: PD/PI
Nearest Person Month Worked: (b)(4):
Contribution to the Project: Overall project management, supervising postdocs and students
Funding Support: None
Change in active other support: Yes
International Collaboration: No
International Travel: No

What other organizations have been involved as partners?

Nothing to report.

Were other collaborators or contacts involved? If so, please provide details.

Yaga Richter (NCAR), Ewa Bednarz (NOAA), Amy Butler (NOAA), Simone Tilmes (NCAR), Paul Goddard (Indiana U.), Jim Haywood, Andy Jones, Matthew Henry, Alice Wells (all U. Exeter, UK), and for permafrost and ice analysis, Y. Chen (BNU), John Moore (Arctic) and G. Leguy, Dave Lawrence and Dave Bailey (NCAR)

Impacts

What is the impact on the development of the principal discipline(s) of the project?

We have demonstrated the importance of strategy (and the scenario as well) for influencing outcomes from SAI – that it cannot meaningfully be considered as “one thing” and that one cannot simply pick some ad hoc choice for injection strategy; this then provides guidance for how geoengineering can/should be simulated. One clear metric defining success of the project is that it is now well recognized within the research community that outcomes depend on strategy, and that there are multiple plausible approaches for a hypothetical future deployment of SAI with different sets of outcomes. This recognition is critical for research not only into outcomes, but also uncertainty. Other modeling groups have started looking at design aspects, duplicating strategies we developed in UKESM for example. In addition

to understanding strategies that optimize for different metrics, it is also important to evaluate how much penalty there is for considering simpler strategies that would be easier to simulate in a large multi-model intercomparison. Based on this, strategies developed herein have been used to define the next set of GeoMIP simulations, which in turn will be used as an important element contributing to the next IPCC report. The design-based approach is also being planned for research into marine cloud brightening and has already influenced simulation design for MCB.

What is the impact on other disciplines?

We have created a dataset of geoengineering simulations that can and are being used by numerous other disciplines (for example, to assess various impacts). Understanding the extent to which there are inherent trade-offs between different objectives, or to what extent there are broadly "best" ways of deploying that would simultaneously satisfy many actors, is essential for informing the development of governance in this area. Understanding the range of different plausible strategies is similarly essential, e.g., the potential for an "Arctic-focused" strategy that could be deployed without requiring development of new aircraft, or more "polar-focused" strategies that could target Antarctic impacts more effectively.

What is the impact on the development of human resources?

Graduate students trained in engineering are being cross-trained in climate science; similarly postdocs (not supported by this award but part of our research group) trained in climate science are exposed to engineering design ideas; this thus builds interdisciplinary expertise. (Indeed, this extends beyond our research group as well!)

What was the impact on teaching and educational experiences?

Results will be incorporated into courses on geoengineering in the future, and examples from this research have been presented in engineering courses on feedback. Research ideas from this award have already led to one senior design project in Mechanical and Aerospace Engineering at Cornell and will likely lead to others.

What is the impact on physical resources that form infrastructure?

Nothing to report.

What is the impact on institutional resources that form infrastructure?

Nothing to report.

What is the impact on information resources that form infrastructure?

Nothing to report.

What is the impact on technology transfer?

Nothing to report.

What is the impact on society beyond science and technology?

This project is ultimately aimed at providing decision support for geoengineering. The limits and tradeoffs in geoengineering are essential pieces of information for deciding if, when, where, and how geoengineering might be done in the future. The results from our project could directly inform that decision process, as well as the development of international governance capacity to support that decision process, and the methods we are demonstrating will enable other researchers to pursue similar lines of investigation.

What percentage of the award's budget was spent in a foreign country?

None.

Changes/Problems

Changes in approach and reason for change

Nothing to report.

Actual or Anticipated problems or delays and actions or plans to resolve them

Nothing to report.

Changes that have a significant impact on expenditures

Nothing to report.

Significant changes in use or care of human subjects

Nothing to report.

Significant changes in use or care of vertebrate animals

Nothing to report.

Significant changes in use or care of biohazards

Nothing to report.

Change in primary performance site location

Nothing to report.

COVER SHEET FOR PROPOSAL TO THE NATIONAL SCIENCE FOUNDATION

PROGRAM ANNOUNCEMENT/SOLICITATION NO./DUE DATE
PD 20-7643

☐ Special Exception to Deadline Date Policy

FOR NSF USE ONLY
NSF PROPOSAL NUMBER
2038246

FOR CONSIDERATION BY NSF ORGANIZATION UNIT(S) (Indicate the most specific unit known, i.e. program, division, etc.)
CBET - EnvS-Environmtl Sustainability

DATE RECEIVED	NUMBER OF COPIES	DIVISION ASSIGNED	FUND CODE	DUNS# (Data Universal Numbering System)	FILE LOCATION
06/18/2020	1	07020000 CBET	7643	872612445	06/19/2020 2:01am

EMPLOYER IDENTIFICATION NUMBER (EIN) OR TAXPAYER IDENTIFICATION NUMBER (TIN)
150532082

SHOW PREVIOUS AWARD NO. IF THIS IS
☐ A RENEWAL
☐ AN ACCOMPLISHMENT-BASED RENEWAL

IS THIS PROPOSAL BEING SUBMITTED TO ANOTHER FEDERAL AGENCY? (b)(4); (b)(6)

NAME OF ORGANIZATION TO WHICH AWARD SHOULD BE MADE
Cornell University

AWARDEE ORGANIZATION CODE (IF KNOWN)
0027110000

ADDRESS OF AWARDEE ORGANIZATION, INCLUDING 9 DIGIT ZIP CODE
373 Pine Tree Road
Ithaca, NY 148502820
US

NAME OF PRIMARY PLACE OF PERF
Cornell University

ADDRESS OF PRIMARY PLACE OF PERF, INCLUDING 9 DIGIT ZIP CODE
Cornell University
124 Hoy Rd
Ithaca ,NY ,148537501 ,US.

IS AWARDEE ORGANIZATION (Check All That Apply)
☐ SMALL BUSINESS ☐ MINORITY BUSINESS
☐ FOR-PROFIT ORGANIZATION ☐ WOMAN-OWNED BUSINESS

☐ IF THIS IS A PRELIMINARY PROPOSAL THEN CHECK HERE

TITLE OF PROPOSED PROJECT **What are the fundamental limits / trade-offs of stratospheric aerosol geoengineering?**

REQUESTED AMOUNT	PROPOSED DURATION (1-60 MONTHS)	REQUESTED STARTING DATE	SHOW RELATED PRELIMINARY PROPOSAL NO. IF APPLICABLE
$ 398,143	36 months	01/01/21	

THIS PROPOSAL INCLUDES ANY OF THE ITEMS LISTED BELOW
☐ BEGINNING INVESTIGATOR
☐ DISCLOSURE OF LOBBYING ACTIVITIES
☐ PROPRIETARY & PRIVILEGED INFORMATION
☐ HISTORIC PLACES
☐ VERTEBRATE ANIMALS IACUC App. Date _____
PHS Animal Welfare Assurance Number _____
☒ TYPE OF PROPOSAL **Research**

☐ HUMAN SUBJECTS Human Subjects Assurance Number _____
Exemption Subsection _____ or IRB App. Date _____
☐ FUNDING OF INT'L BRANCH CAMPUS OF U.S IHE ☐ FUNDING OF FOREIGN ORG
☒ INTERNATIONAL ACTIVITIES: COUNTRY/COUNTRIES INVOLVED
XX
☒ COLLABORATIVE STATUS
Not a collaborative proposal

PI/PD DEPARTMENT
Mechanical and Aerospace Engineering

PI/PD FAX NUMBER
626-395-6170

PI/PD POSTAL ADDRESS
Hoy Road
Upson Hall
Ithaca,NY 14850
United States

NAMES (TYPED)	High Degree	Yr of Degree	Telephone Number	Email Address
PI/PD NAME **Douglas G MacMartin**	**PhD**	**1992**	**650-619-9341**	**dgm224@cornell.edu**
CO-PI/PD **Benjamin Kravitz**	**PhD**	**2011**	**812-855-4334**	**bkravitz@iu.edu**
CO-PI/PD				
CO-PI/PD				
CO-PI/PD				

Certification for Authorized Organizational Representative (or Equivalent)

By electronically signing and submitting this proposal, the Authorized Organizational Representative (AOR) is: (1) certifying that statements made herein are true and complete to the best of his/her knowledge; and (2) agreeing to accept the obligation to comply with NSF award terms and conditions if an award is made as a result of this application. Further, the applicant is hereby providing certifications regarding conflict of interest (when applicable), flood hazard insurance (when applicable), responsible conduct of research and organizational support as set forth in the NSF Proposal & Award Policies & Procedures Guide (PAPPG). Willful provision of false information in this application and its supporting documents or in reports required under an ensuing award is a criminal offense (U.S. Code, Title 18, Section 1001).

Certification Regarding Conflict of Interest

The AOR is required to complete certifications stating that the organization has implemented and is enforcing a written policy on conflicts of interest (COI), consistent with the provisions of PAPPG Chapter IX.A.; that, to the best of his/her knowledge, all financial disclosures required by the conflict of interest policy were made; and that conflicts of interest, if any, were, or prior to the organization's expenditure of any funds under the award, will be, satisfactorily managed, reduced or eliminated in accordance with the organization's conflict of interest policy. Conflicts that cannot be satisfactorily managed, reduced or eliminated and research that proceeds without the imposition of conditions or restrictions when a conflict of interest exists, must be disclosed to NSF via use of the Notifications and Requests Module in FastLane.

Certification Regarding Flood Hazard Insurance

Two sections of the National Flood Insurance Act of 1968 (42 USC §4012a and §4106) bar Federal agencies from giving financial assistance for acquisition or construction purposes in any area identified by the Federal Emergency Management Agency (FEMA) as having special flood hazards unless the:

(1) community in which that area is located participates in the national flood insurance program; and
(2) building (and any related equipment) is covered by adequate flood insurance.

By electronically signing the Certification Pages, the Authorized Organizational Representative (or equivalent) located in FEMA-designated special flood hazard areas is certifying that adequate flood insurance has been or will be obtained in the following situations:

(1) for NSF grants for the construction of a building or facility, regardless of the dollar amount of the grant; and
(2) for other NSF grants when more than $25,000 has been budgeted in the proposal for repair, alteration or improvement (construction) of a building or facility.

Certification Regarding Responsible Conduct of Research (RCR)

(This certification is not applicable to proposals for conferences, symposia, and workshops.)

By electronically signing the Certification Pages, the Authorized Organizational Representative is certifying that, in accordance with the NSF Proposal & Award Policies & Procedures Guide, Chapter IX.B. , the institution has a plan in place to provide appropriate training and oversight in the responsible and ethical conduct of research to undergraduates, graduate students and postdoctoral researchers who will be supported by NSF to conduct research. The AOR shall require that the language of this certification be included in any award documents for all subawards at all tiers.

Certification Regarding Organizational Support

By electronically signing the Certification Pages, the Authorized Organizational Representative (or equivalent) is certifying that there is organizational support for the proposal as required by Section 526 of the America COMPETES Reauthorization Act of 2010. This support extends to the portion of the proposal developed to satisfy the Broader Impacts Review Criterion as well as the Intellectual Merit Review Criterion, and any additional review criteria specified in the solicitation. Organizational support will be made available, as described in the proposal, in order to address the broader impacts and intellectual merit activities to be undertaken.

Certification Regarding Dual Use Research of Concern

By electronically signing the certification pages, the Authorized Organizational Representative is certifying that the organization will be or is in compliance with all aspects of the United States Government Policy for Institutional Oversight of Life Sciences Dual Use Research of Concern.

AUTHORIZED ORGANIZATIONAL REPRESENTATIVE	SIGNATURE	DATE
NAME **Tammy J Custer**	**Electronic Signature**	**Jun 18 2020 9:31AM**

TELEPHONE NUMBER	EMAIL ADDRESS	FAX NUMBER
607-255-5066	**tjb3@cornell.edu**	**607-255-5058**

PROJECT SUMMARY

Overview:

Reducing net emissions of CO2 and other greenhouse gas (GHG) is an essential part of any response to climate change, but is unlikely to occur fast enough to avoid significant climate impacts, leaving open the possibility of significant future climate impacts. Model projections of stratospheric aerosol geoengineering suggest that it could reduce some climate impacts, and thus could potentially become an additional element of a comprehensive climate change strategy. However, current knowledge is insufficient to support informed decisions. A key issue is that geoengineering would not affect the climate the same way as increased atmospheric GHG, leading to residual differences. However, these differences depend strongly on how geoengineering is deployed, making analysis of geoengineering fundamentally different in character from analysis of GHG-driven climate change as it necessitates an engineering-design perspective. A critical question in evaluating geoengineering is thus, what are the fundamental limits or trade-offs in how well geoengineering can manage the climate response from increased GHG? That is, what can geoengineering do, and what can it not do? Building on recent research, we propose to address this essential question. Specifically, we will generate a set of climate model simulations that each make different choices for which climate goals to prioritize relative to others, and use this to identify potential tradeoffs (sets of objectives that are mutually exclusive) and boundaries (which objectives are achievable and which are not). Throughout this process, we will engage policy and governance experts, regarding the potential range of climate goals that might motivate different actors, and on the governance implications of identified trade-offs.

Intellectual Merit:

The full range of possible strategies has never been explored, in part because optimization over the space of available degrees of freedom – primarily latitudes and seasons of aerosol injection – is complicated by uncertainty and nonlinear interactions (from both microphysics and aerosol-heating-induced changes in stratospheric circulation), and compounded by combinatorial computational complexity. To address these challenges, we combine three innovations. First, the key enabler to this research is an initial assessment on the "size" of the design space; how many usefully-independent degrees of freedom are there? This reduces the combinatorial problem. Second, the computational burden can be reduced by separating the simulations needed to understand the spatial- and seasonal- distribution of stratospheric aerosol optical depth (AOD), which can be short but require a complete stratosphere model, from those needed to assess the climate response to a specified aerosol distribution, which require multi-decadal simulations but not an accurate stratosphere. And third, nonlinearities and uncertainty can be managed through feedback that adjusts injection rates; this enables comparing simulations based on specified objectives rather than specified injection rates. We will design a suite of simulations that individually meet different objectives and collectively span the space of possible outcomes. From this, the key tool in evaluating and visualizing trade-offs is through Pareto-optimal surfaces: how do strategies and their responses change as a function of the optimization criteria. By combining these novel contributions, we can begin down a path toward a "holy grail" of geoengineering research: assessing what geoengineering can and cannot do.

Broader Impacts:

The fundamental motivation for this research is to understand a potential option to reduce future climate impacts. Better information is needed both to support future decisions around deployment, and support the development of governance capacity that will be needed to make these decisions. This research will enable a more complete view of the impacts of deploying geoengineering than has previously been possible, by generating simulations that capture a more comprehensive set of deployment options rather than just one or two; and furthermore will assess the extent to which different objectives can or cannot be simultaneously met. Although our simulations are focused on understanding physical science tradeoffs, the social and governance dimensions play a critical role in understanding which objectives may be most important to achieve or which strategies are simply politically infeasible, thus limiting the space in ways not revealed by climate modeling. We will interface with governance experts throughout to ensure research informs policy. Simulations will also be made available to the wider international community, including developing world researchers funded through DECIMALS. Finally, integrating an engineering design perspective into climate science can broaden both communities and spark new insights.

TABLE OF CONTENTS

For font size and page formatting specifications, see PAPPG section II.B.2.

*Proposers may select any numbering mechanism for the proposal. The entire proposal however, must be paginated. Complete both columns only if the proposal is numbered consecutively.

What are the fundamental limits / trade-offs of stratospheric aerosol geoengineering?

1 Introduction and motivation

Reducing CO_2 and other greenhouse gas (GHG) emissions is an essential part of any response to climate change, but it is unlikely that this will occur fast enough to avoid significant climate impacts [41, 49]. Negative emissions technologies may be able to reduce long-term warming [13, 35], but there is no guarantee that these largely untested ideas can be developed and scaled up quickly enough [10, 9], leaving open the possibility of significant future climate impacts. Model projections of stratospheric aerosol geoengineering suggest that it could reduce some climate impacts [34, 14], and thus future decision-makers might consider this as an additional element of a comprehensive climate change strategy [30]. However, current knowledge is insufficient to support informed decisions about whether to deploy geoengineering (hereafter, geoengineering is used interchangeably with stratospheric sulfate aerosol geoengineering) and, if so, what it can be relied upon to do [27].

Geoengineering would not affect the climate the same way as increased atmospheric GHGs affect the climate, leading to residual differences. However, these differences depend strongly on how geoengineering is deployed [19, 50], meaning that the climate effects of geoengineering have an important engineering-design component [23, 26]. This makes analysis of geoengineering fundamentally different in character from analysis of GHG-driven climate change. Given this potential for making deliberate choices based on desired outcomes, one of the critical questions in evaluating geoengineering is thus: what are the fundamental limits or trade-offs in how well geoengineering can manage the climate response from increased GHG? That is, ***what can geoengineering do, and what can it not do***? Building on recent research, we propose here to provide an answer to this long-standing essential question, focusing exclusively on stratospheric aerosol geoengineering.

This design perspective is important for interpreting past conclusions and making new ones. For example, from energetic arguments, it is not possible to simultaneously maintain global mean temperature and global mean precipitation [2, 17, 43, 16]. However, other early simulations suggested geoengineering would overcool the tropics and undercool the poles, which we now know is due to how geoengineering was simulated in those studies [19]. Similarly, several past studies have shown that geoengineering reduced monsoonal rain in India, but it appears that this depends on the season of stratospheric aerosol injection [50]. These last two examples involve introducing additional *degrees of freedom*. Rather than just injecting SO_2 into the stratosphere at the equator, as in many early simulations, one can inject at different latitudes [47, 6], and combine injection at different latitudes to simultaneously achieve multiple climate goals [29, 22]. Rather than injecting the same amount every day of the year, adjusting the injection rate seasonally can also alter climate outcomes [51, 50]. However, we don't yet fully understand the limits of these sorts of activities: how big is the space of achievable climates? A crucial barrier to answering these questions is that just because one can choose different latitudes and seasons, those different choices may not yield usefully different outcomes. We have started down the path of addressing that question (Section 2.2 below); this is a fundamental enabler to addressing what can and cannot be achieved.

The space of available degrees of freedom can be described by the latitudes and seasons of aerosol injection, or equivalently the resulting spatiotemporal patterns of stratospheric aerosol optical depth (AOD). Our ultimate vision is to learn how to achieve particular climate objectives by adjusting these degrees of freedom. Understanding this design space is complicated by uncertainty and by nonlinear interactions arising from both microphysics (e.g., [37, 8, 36]) and aerosol-heating induced changes in stratospheric circulation [1, 42]. Moreover, simulating every combination of these degrees of freedom in expensive, state-of-the-art models is computationally infeasible. To address this challenge, our proposal combines three innovations/observations:

1. The computational burden can be greatly reduced by observing that the problem can be separated into two pieces: which injection strategies lead to which spatial- and seasonal- distributions of stratospheric AOD, and which AOD distributions lead to which climate effects? The first part can be done with short simulations but requires a complete stratosphere model, whereas the second requires multi-decadal simulations but not as accurate a stratosphere.
2. Not all combinations of degrees of freedom are independent — some combinations may achieve the same climate impacts as others (see Section 2.2).
3. Nonlinearities and uncertainty can be managed through feedback that adjusts injection rates (associated with the degrees of freedom) to achieve some set of desired outcomes [28, 23] (see Section 2.4).

Ultimately there are more climate variables that "matter" than there are degrees of freedom that can be adjusted, and there will inevitably be trade-offs - not all objectives can be simultaneously met by any given strategy. An important tool in evaluating and visualizing trade-offs is Pareto-optimal surfaces, which describes how strategies and their responses change as a function of the optimization criteria (Section 2.3).

By combining these novel innovations, we can begin down the pathway toward a "holy grail" of geoengineering research - assessing what geoengineering can and cannot do.

Specific Objectives

We will generate a set of climate model simulations that, taken collectively, describes the space of achievable climate goals. This will be a set of case studies that each make different choices for which climate goals to prioritize relative to others, and which degrees of freedom to use in doing so. These simulations will be made available to the broader community for impact analysis.

We will use this set of simulations to (a) identify potential tradeoffs (sets of objectives that are mutually exclusive) and (b) boundaries (which objectives are achievable and which are not). This will provide an initial answer to a central question in geoengineering research: what can geoengineering do, and what can it not do?

Throughout this process, we will engage policy and governance experts, first regarding the potential range of climate goals that might motivate different actors, and then on the governance implications of identified trade-offs. Although our simulations are focused on understanding physical/natural science tradeoffs, the social and governance dimensions play a critical role in understanding which objectives may be most important to achieve or which strategies are simply politically infeasible, thus limiting the space in ways not revealed by climate modeling.

Achieving these objectives will significantly advance our understanding of the range of plausible

geoengineering strategies and their trade-offs, feeding into a more holistic impacts assessment than has previously been possible, and informing governance and ultimately policy in this area.

2 Technical Background

There are a number of elements on which the proposed effort builds; many of these have only recently been demonstrated through an NSF EAGER award.

2.1 Climate model and simulations to date

The ability to assess different injection strategies rests in part on having a climate model that captures stratospheric dynamics, aerosol microphysics and chemistry. The prior research that enables the proposed work was conducted with the Community Earth System Model version 1, with the Whole Atmosphere Community Climate Model as its atmospheric component; CESM1(WACCM). This model has been validated against observations after volcanic eruptions [32] and used in a number of subsequent geoengineering studies (e.g., [47, 46, 29, 22, 19, 42, 51, 50]. Research conducted herein will use the updated version CESM2(WACCM6) [7, 11, 44].

Simulations exploring different injection strategies were originally conducted with annually-constant injection rates at 30°N, 15°N, 0°, 15°S, and 30°S, as well as 50°N and 50°S, all ∼5km above the annual mean tropopause [47]. (The effect of altitude will not be explored herein both to bound scope and because it is expected from past work to primarily affect efficiency [48, 6].) Early analysis discarded the higher-latitude 50°N/50°S cases because the annually-averaged AOD was similar to the 30°N and 30°S cases but with lower efficiency. Ref. [51] repeated the cases from 30°N to 30°S, but also simulated cases in which injection was restricted to a single season; March-April-May (MAM), June-July-August (JJA), September-October-November (SON), and December-January-February (DJF). In addition, we have now simulated injection at 45°N, 60°N, 45°S, and 60°S: while annually-constant injection at these latitudes is not very efficient in terms of AOD produced per unit injection, injection in spring (MAM in Northern Hemisphere, SON in Southern) produces a peak in AOD at high latitudes aligned with the summer peak in insolation; this is indicative of higher efficiency in affecting Arctic sea ice for example [50]. Furthermore, injection at 60°N/60°S is poleward of the stratospheric polar jet that acts as a transport barrier to aerosols. These additional cases thus provide potentially valuable additional degrees of freedom that expand the design space.

2.2 Degrees of freedom

The total number of simulations described above is 35; see Figure 1. However, due to the aerosol lifetime and the constraints imposed by stratospheric circulation, the number of usefully independent degrees of freedom is considerably less than that. For example, the spatial- and seasonal-pattern of AOD of all of the simulations described previously can be represented as a linear combination of the following nine simulations (indicated in yellow in Figure 1) with a residual of only 2.5%:

1. Annually-constant equatorial injection
2. Summer injection in each hemisphere at 15°N and 15°S (JJA and DJF respectively)
3. Spring/fall injection (MAM and SON) in each hemisphere at 30°N and 30°S, and
4. Spring injection at 60°N and 60°S (MAM and SON respectively)

This set is not necessarily "optimal", in that there are other choices of 9 that yield similar results and a similar resulting subspace of achievable spatiotemporal AOD patterns. This set has the advantage that spring/fall injections have been demonstrated to have significantly distinct outcomes for Arctic sea ice, for Indian monsoon precipitation, and for Amazon dry-season precipitation [50], but different choices of degrees of freedom may better target different objectives.

Conclusions from these simulations indicate that, at least in this model,

1. Choosing alternate seasons at 30°N and 30°S introduces significant seasonal dependence to the resulting mid-latitude AOD, with potentially important surface climate responses [50].
2. The effect of injection season is less important at lower latitudes: a second season at 15°N, 15°S, or at the equator, provides less "new" capability than at 30°N and 30°S.
3. Adding high latitude injection of the appropriate season provides significantly unique spatiotemporal patterns of AOD, introducing the potential to increase summer AOD poleward of the stratospheric transport barrier that otherwise limits high-latitude AOD (see e.g., [47]): increased summer AOD increases Arctic sea-ice extent [50]. Most patterns of AOD introduced by high latitude injection are not expected to have significant advantages in climate response due to the timing of the high-latitude AOD peak relative to the peak in summer insolation.
4. 45°N and 45°S injection do not provide significantly "new" capability relative to 60°N/S.

The spatiotemporal patterns of AOD for each of the 9 injection choices described above are shown in Figure 2, along with a spider-plot that illustrates the additional flexibility in choosing the AOD that increasing sets of injection choices achieves. The AOD metrics shown include the achievable projection onto each of the first three Legendre polynomials L0, L1, L2 that have been used in many prior multi-degree-of-freedom studies [3, 23, 29, 22], as well as summer high-latitude AOD in each hemisphere, and seasonal modulation of the mid-latitude AOD. Not all of these may be important for achieving any particular climate objective, but each capability may expand the space of achievable objectives.

2.3 Pareto-optimality

The design space of SAI is spanned by all possible combinations of all available degrees of freedom. In CESM1(WACCM), we have quantified a portion of this space via five different simulations. These include (i) the 20-member ensemble of the Geoengineering Large Ensemble (GLENS), that used injection at 30°N, 15°N, 15°S, and 30°S to maintain three large-scale patterns of temperature change [22, 46], (ii) an equatorial-injection strategy [19], (iii,iv) two strategies employing different seasons of injection and similar goals to GLENS [50], and (v) a simulation using the same latitudes as GLENS but different objectives and thus different distribution of injection across the 4 latitudes (not yet published; see Fig. 4).

While these simulations do not span the full design-space, they are sufficient to illustrate the potential for trade-offs (see also [25]). Any objective, or set of objectives, will have a minimum set of usefully-independent degrees of freedom that meet that objective, or come as close as physically possible. Some objectives may be mutually exclusive – we already have the example of global mean temperature and global mean precipitation [43], and Figure 3 shows how SAI in the previously described simulations has different effects on precipitation over northern India vs Amazon.

This illustrates a fundamental purpose of the proposed research – to understand whether there are trade-offs such as this one that persist when considering the entire design space for SAI. Iden-

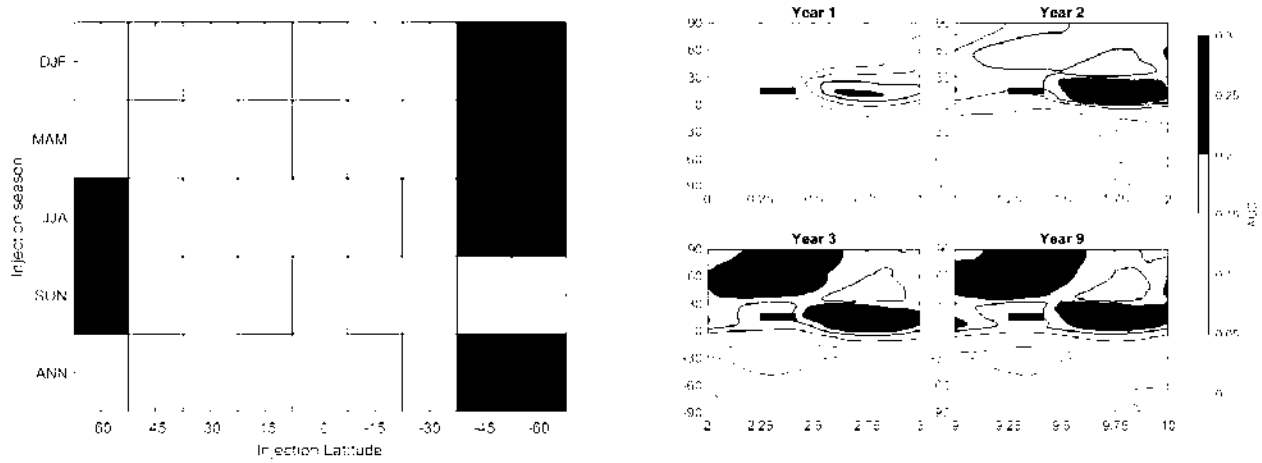

Figure 1: Left: Injection latitudes and seasons that have been simulated, with those considered in Section 2.2 highlighted in yellow. Right: An example showing convergence of the spatial- and seasonal- pattern of AOD (for injection at 15°N in MAM, indicated by the thick black line in each panel); by year 3 the pattern is established.

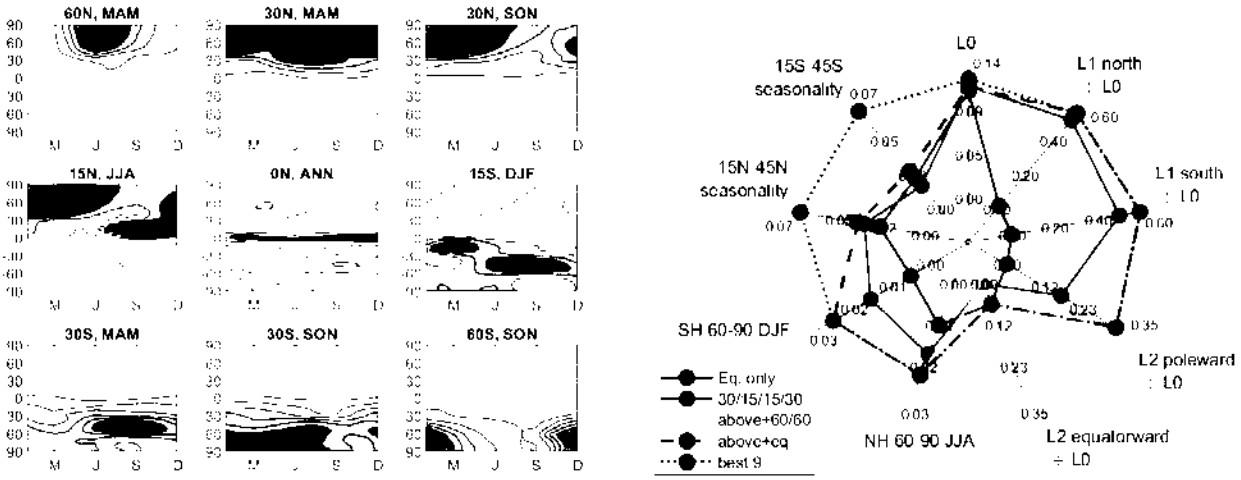

Figure 2: Left: the spatiotemporal patterns of AOD for each of the 9 injection cases included in the set described in Section 2.2. Right, the influence of different choices on different AOD metrics, where a larger radius for some particular set of injection options implies greater flexibility in choosing characteristics of the AOD that may be relevant for different climate objectives. Cases shown are (i) annually-constant injection at the equator (blue), (ii) annually-constant injection at 30°S, 15°S, 15°N, and 30°N as in [29] (orange); this adds the ability to obtain annually-averaged L1 increasing either northward or southward, and some ability to achieve a poleward-increasing projection of AOD onto L2; (iii) the same set but adding spring injection at 60°N and 60°S (green) adds the ability to significantly increase summer AOD at high latitudes; (iv) now adding back in equatorial injection (purple) provides some limited ability to achieve an equatorward-increasing projection of AOD onto L2, and finally (v) the set considered in the text (black) adds the ability to seasonally modulate the AOD over either northern- or southern-hemisphere mid-latitudes.

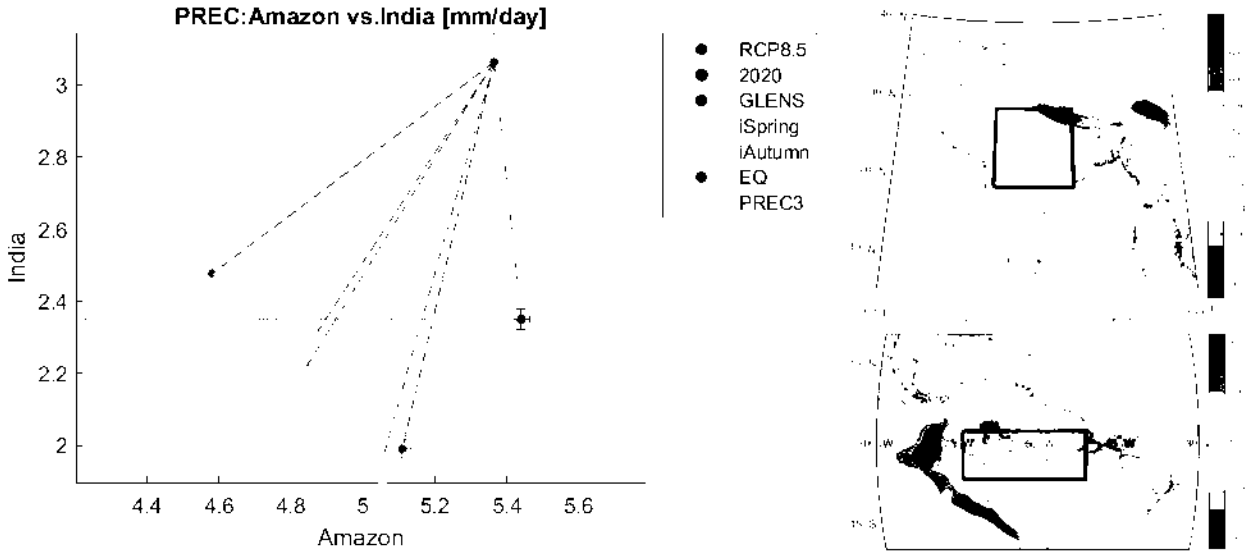

Figure 3: Left: Annual-mean precipitation over northern India (19-29°N, 74°-85° E) and Amazon (7°S-2°N, 51°-74°W) for 5 different independent simulations conducted in CESM1(WACCM), all of which maintained global mean temperature at baseline (2010-2030) levels; these regions were chosen because there was a clear decrease in precipitation in the GLENS simulations [42, 5]; right-hand panels. If the response is linear, then anywhere in the blue-shaded region (convex hull of the 5 simulations) can be achieved while maintaining global-mean temperature, and anywhere in the gray-shaded region can be achieved if higher temperatures are permitted (convex hull of the 5 simulations plus the RCP8.5 simulation). It would be premature to conclude that a trade-off between these variables exists without both a physical understanding of the mechanisms involved, and a more complete exploration of the design space, as there may be other options that achieve different outcomes. Nonetheless, this is illustrative of the questions that need to be addressed in modeling different SAI strategies.

tifying "unachievable climates" could have significant implications for developing the capacity for governance [24]; while it has certainly been postulated that different regions might have different preferences (e.g. [40]), the issue has never been settled when considering the entire design space rather than the over-simplified analogy of a single global "thermostat". Conversely, if it is possible to identify strategies that do allow multiple regions to each better satisfy regional objectives, that would also impact the needs of governance.

Pareto-optimal strategies are those in which no objective can be further improved without making some other objective worse; characterizing the set of Pareto-optimal strategies is thus a useful way of visualizing and quantifying trade-offs [33]. Initial work in exploring Pareto-optimal trade-offs in geoengineering was conducted in [25], using spatially- and seasonally-varying patterns of solar reduction in a relatively simple climate model. While this demonstrated a methodology and the idea that optimization could be used to explore trade-offs, the design space with stratospheric aerosols is constrained by stratospheric transport and aerosol lifetime, and thus the actual results obtained for solar reduction are not directly relevant.

2.4 Feedback

Feedback has been shown to be a valuable tool in past simulations to manage both uncertainty and nonlinearity. In each year of the simulation, the output from past years can be used to adjust the injection rates for the next year to meet specific objectives. Provided that the algorithm converges, this effectively "learns" the right injection rates to use for each degree of freedom (latitude/season of injection) in order to meet a particular set of objectives. This was first demonstrated for geoengineering for a single degree of freedom [28], extended to multiple degrees of freedom [23], and demonstrated for adjusting SO_2 injection rates rather than patterns of solar reduction [22]; the same process has also been used in other climate models [21, 4, 44]. A similar approach might be used if SAI were ever deployed in the real world [24].

Feedback allows us to construct and compare different simulations not on the basis of specified injection rates for different choices of latitudes/seasons (plug in a strategy and see what happens in the model), but on the basis of specified goals (tell the feedback algorithm what you want to happen and let it figure out what is needed to get there). In addition to the temperature-based metrics used in [28, 23, 22, 46, 50], we have also now demonstrated the ability to use feedback to manage goals such as global mean precipitation, ITCZ latitude, and September Arctic sea ice extent (Figure 4). The feedback algorithm in each case is based on physical understanding (in the simplest case, if it is too warm, increase injection, if it is too cool, decrease injection), allowing some confidence that the same algorithm will converge in other models (or possibly in a hypothetical real world deployment).

2.5 Gaps

While many of the building-blocks are in place to meet the Objectives in Section 1, there are a number of key gaps that need to be filled in. These are linked directly to the Statement of Work in Section 3.1.

1. Is the set of injection degrees of freedom identified in Section 2.2 robust, both across models, and for additional latitudes of aerosol injection? (Task 1 in the Statement of Work)

2. While a few different simulations have been conducted, there has never been a comprehensive evaluation of the overall space of achievable climate outcomes. (Tasks 4, 6)

3. Without this comprehensive evaluation, it is impossible to know whether some impact of SAI in some particular simulation is an inherent limitation or simply an accident of the limited set of strategies considered. (Task 7)

4. Developing the capability to explore many different strategies rather than just a few relies on approaches to do so in a computationally efficient manner, including (i) developing feedback algorithms for different climate objectives, and (ii) validating the separation between computing spatiotemporal patterns of AOD and the response to those patterns. (Tasks 3, 5)

5. Connection with policy needs – is there additional input that should be considered in defining potential goals (corresponding to the interests of different potential actors), and what are the broader implications of uncovering trade-offs? (Tasks 2 and 8)

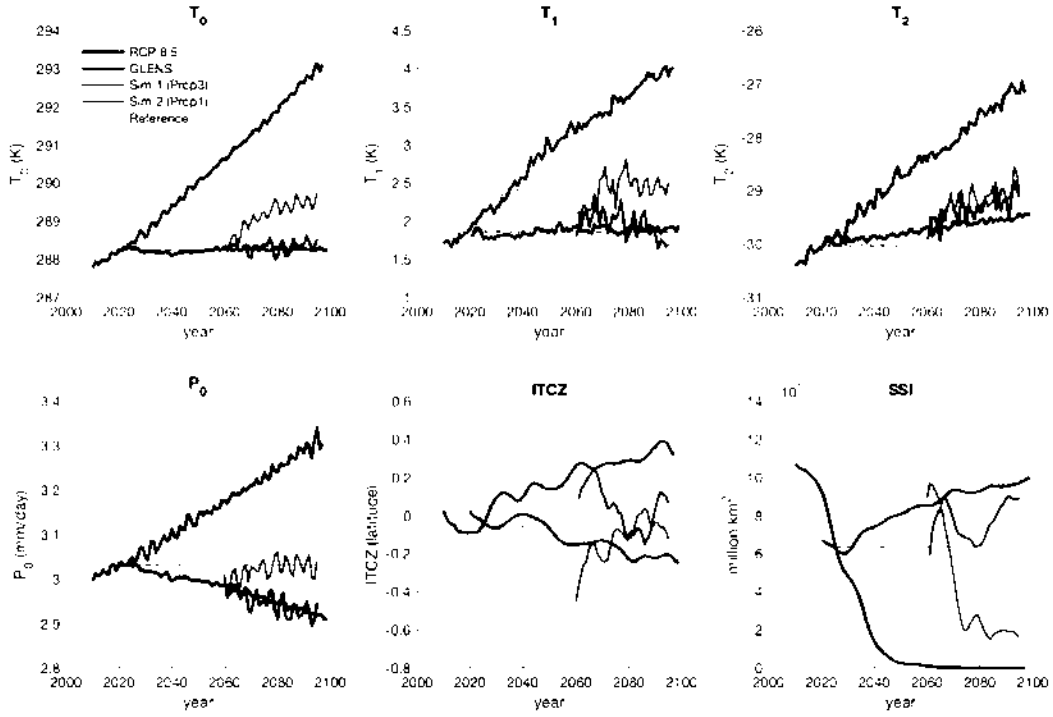

Figure 4: Illustration of the ability of feedback to manage different types of metrics and different sets. In addition to the reference RCP8.5 simulation (black), the GLENS simulations that use feedback to manage three temperature-based metrics are shown in blue [22, 46], along with two additional simulations that manage (a) global mean temperature, ITCZ, and September sea ice (red) and (b) global mean precipitation and ITCZ (purple). Note that the inability of GLENS to meet T2, and of the new simulation to meet september sea ice, are not a failure of the feedback algorithm but a limitation imposed by the combination of the set of degrees of freedom considered in these simulations and constraints imposed by stratospheric transport.

3 Technical Approach:

The background work described above enables an approach to quantifying the design space of SAI, specifically in determining the space of achievable climates. In this section, we describe our technical approach toward meeting this proposal's objectives (see also Figure 5 below).

3.1 Statement of Work

1. Use new model version CESM2(WACCM6), and repeat 5-year SO_2-injection simulations at multiple latitudes and seasons to evaluate the robustness of spatiotemporal AOD patterns. Compare with results from CESM1(WACCM), and with other models where output is available.
2. Engage policy/governance experts regarding span of climate goals to consider.

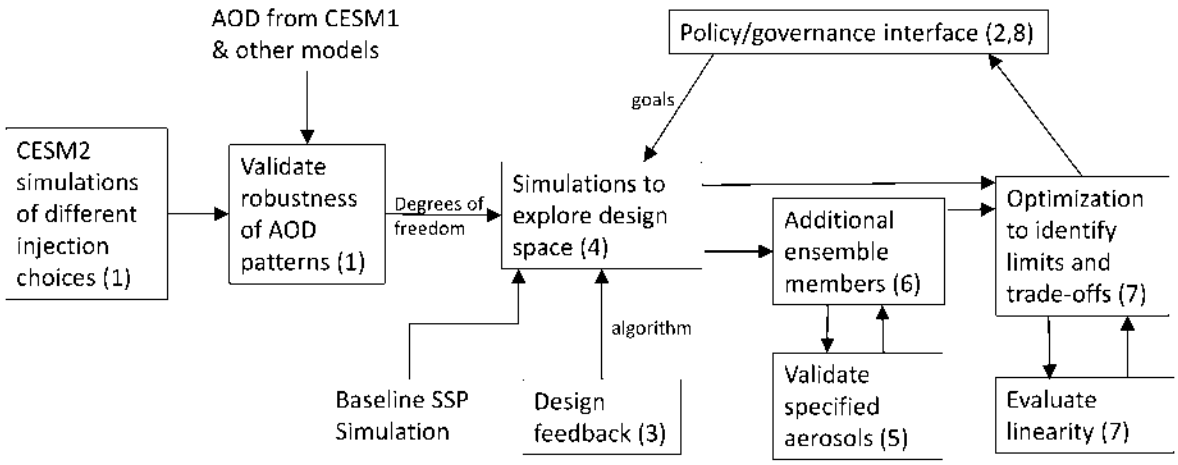

Figure 5: Flowchart illustrating relationship among the various tasks described in the SOW (numbers in brackets refer to the numbering in the SOW).

3. Design feedback laws needed to simultaneously adjust multiple degrees of freedom to meet heretofore novel goals in SAI, including objectives focused on temperature, hydrological cycle, or sea ice, both on global and regional scales (e.g., precipitation over India).
4. Generate independent simulations out to 2100, with each adjusting injection rates for different sets of latitudes/seasons to manage different combinations of climate goals.
5. Validate that simulations with specified aerosols in (low-top) CESM2(CAM6) result in similar tropospheric climate response to the full CESM2(WACCM6).
6. Generate additional ensemble members for each of the simulation options in step 5, using specified aerosols in CESM2(CAM6) and assess ensemble-averaged climate response across a broad set of climate objectives for each of the 21st century simulations.
7. Conduct optimization to evaluate different Pareto-Optimal solutions and identify fundamental trade-offs.
8. Engage policy/governance experts regarding governance implications of trade-offs.

Tasks 1-3 will be completed in year 1, 4-6 in year 2, and 7-8 in year 3, with results documented in publications along the way.

3.2 Climate Model

This research will rely on CESM2(WACCM6), the more recent version of the model used in the work described above, at the same ~1 degree resolution used previously. The newer version has already been used in one study on SAI [44], validating the ability to use the feedback algorithms developed previously in the new model version. The first step in our research will compare results in CESM2(WACCM6) with those previously obtained with CESM1(WACCM); we already know from [44] that there are indeed some differences in climate response between the model versions.

3.3 Simulations and Analysis

(a) Robustness of AOD patterns:
The first step is to understand the set of injection options and number of degrees of freedom in the newer model CESM2(WACCM6), and to evaluate these conclusions across models to understand model differences, both through comparison with simulations previously conducted in CESM1(WACCM) and through comparison with additional models. To do this, we will conduct a set of 5-year simulations in CESM2(WACCM6) to evaluate the spatiotemporal patterns of AOD due to different choices of latitude and season. Previous research has shown that 5 years is sufficient to reach steady-state AOD values [51]; see Figure 1. We do not propose to directly fund other modeling centers to deliver similar results with their models, however we will work with other modeling groups to obtain and compare output where possible. We have colleagues who have expressed interest in producing simulation results at several different latitudes from GISS Model E [15], ECHAM, and possibly GEOS-5; some comparisons can also be made with models participating in GeoMIP6 that conducted the G6 scenario [18].

(b) Baseline scenario:
The baseline case that we will use for subsequent geoengineering simulations is the SSP2-4.5 scenario; this has already been conducted with both CESM2(CAM6), and with the high-top version CESM2(WACCM6) so there is no need to repeat these simulations. The GLENS studies [46] used RCP8.5 as a baseline; while that provides a high signal-to-noise ratio for improved detectability, and re-scaling to project outcomes for a different emissions pathway is in principle possible [31], we prefer to sacrifice some signal-to-noise ratio in order to better emphasize that geoengineering should only be considered in addition to mitigation and not in place of it. In the PI's experience, conducting simulations where the background scenario involves no mitigation complicates essential conversations with policy experts and the broader public, limiting the impact of this research. Furthermore, evaluating differences in an extreme scenario can potentially over-emphasize small changes that may not be detectable in a more moderate scenario [31] and put undue attention on nonlinearities. To make a stronger tie to policy-relevance, we will start geoengineering simulations in 2030, a plausible estimate for when 1.5°C of climate warming will be achieved [13]; the 1.5°C target is already reached by 2020 in CESM2(WACCM6), which clearly isn't valid in the real world.

(c) Climate response to SAI strategies:
To evaluate the climate response to different injection choices with high enough signal-to-noise ratio to distinguish the SAI-response from natural variability, we need multi-decadal simulations, each with multiple ensemble members. There are three broad considerations that influence our design of these simulations.

i) We need to establish a *basis* that spans the space of achievable objectives. In the past, this was done by conducting single simulations at each latitude/season of interest and then forming combinations of those simulations to understand how chosen objectives could be met [25]. However, this mathematical approach cannot account for nonlinearities (like non-additivity between two different injections), and the results of the simulations themselves are not directly policy-relevant. Instead, we will design a series of simulations, each of which meets a different set of objectives as described below. These simulations implicitly form a basis and are more directly relevant for subsequent analysis of tradeoffs or downstream applications like impact analysis.

ii) Climate outcomes will be maintained using feedback as in prior simulations [22, 46, 44, 50]. This compensates for uncertainty and nonlinearity, and enables simulations that maintain particular

sets of objectives without a time-consuming trial-and-error approach for learning the necessary injection rates.

iii) The first simulation for each set of objectives will be conducted with the "high-top" model version CESM2(WACCM6) that includes a full representation of stratospheric dynamics, chemistry, and aerosol microphysics. To obtain additional ensemble members, the aerosol fields from this simulation will be applied in specified-aerosol configuration in CESM2(CAM6), which is a factor of 3 less computationally expensive. We will validate whether the two model versions yield similar climate outcomes (which we expect will be a valuable paper by itself!). We expect small differences due to climate sensitivity (5.3 with CAM6 vs 4.8 with WACCM, [7]) and climate-aerosol interactions. This step is novel and enables separating how injection choices affect AOD (requiring an accurate stratosphere that relatively fewer climate models capture, but not requiring fully dynamic ocean for example) from intercomparisons to evaluate how those patterns of AOD affect surface climate (requiring longer simulations, but not requiring stratospheric modeling capability that many models do not have).

(d) Climate objectives and SAI strategies:
Previous and ongoing studies have chosen impacts-relevant objectives like global-scale temperature [22, 46] or precipitation, P-E, and sea-ice extent (Figure 4). However, moving beyond purely proof-of-concept natural science/engineering studies requires a broader investigation of objectives. We will engage with policy and governance experts to better design more societally-relevant simulations. From a policy perspective, relevant scenarios for assessing the range of SAI options include not only "global" strategies that balance possibly competing goals, but also regionally-focused strategies. Additional objectives could include regional changes (e.g., precipitation over India), polar-only objectives (e.g. sea ice or permafrost area), and potentially single-hemisphere approaches (which will have negative impacts on ITCZ [12]; including options like this captures possible poor choices for deployment and thus increases the span of possible outcomes). Each simulation would manage multiple goals simultaneously using multiple different input degrees of freedom, as in other recent studies [22, 50].

Finding injection strategies to meet these objectives requires some physical understanding of the relationship between injection strategy and outcomes. For example, feedback will not be effective if the response is an order of magnitude different than we thought, or if we get the sign wrong. Prior studies have been successful by separating how injection rates affect patterns of AOD and how those AOD patterns affect climate objectives [29]. For example, using feedback to manage ITCZ latitude requires knowing that the ITCZ position depends primarily on the interhemispheric gradient of AOD (L1), which in turn depends on injection rates at different latitudes, but the magnitude of the relationship does not need to be known exactly.

Expanding on this general idea, an example objective could be maintaining Indian monsoon precipitation under climate change. This requires three observations:

1. Indian monsoon precipitation is strongly influenced by summer temperature contrast between the Tibetan plateau and the Indian ocean [52, 39].
2. Ocean temperature does not react strongly to seasonal variations in AOD, but the Tibetan plateau temperature does [50].
3. Changing the season of injection at 30°N results in the mid-latitude AOD varying with season [50], see also Figure 2).

This information is sufficient to design a feedback algorithm that can adjust injection rates in an effort to maintain precipitation rates over India, provided that objective is achievable (aerosol lifetime and stratospheric circulation will limit how much seasonal variation in AOD is possible) and compatible with other objectives. In another example, Arctic sea ice will respond to high-latitude summer AOD (in addition to heat transport from lower latitudes; [45]): all else being equal, then increased spring injection at 60°N will increase sea ice. This will also shift the ITCZ southward, which could be counter-balanced by a corresponding injection in the southern hemisphere, similarly to the solar-reduction study by Kravitz et al [23].

(e) Pareto-optimality:
The simulations will be analyzed both individually, evaluating the climate response for each simulation, and collectively as an overall set that describes the achievable space of climate responses in order to identify underlying trade-offs. The latter can be characterized in terms of Pareto-Optimal surfaces – for any given set of objectives, what set of strategies are optimal for some relative weighting between them, and which strategies are never optimal (that is, some other strategy yields better outcomes for at least one metric, and no worse outcome for any). As an example, in Figure 3, depending on the relative weighting on precipitation over India vs the Amazon, the "best" choice (for these two metrics) is some linear combination of the equatorial, the new simulation labeled "PREC", or GLENS, and neither the seasonal injection simulations (labeled iSPRING or iAUTUMN) is ever better; for different choices of metrics the result will be different.

Given some set of N climate objectives, the outcome of the i^{th} simulation can be described as a vector a_i of length N. With M different strategies simulated, the space of achievable outcomes can be described by $z - Au$, where the $N \times M$ matrix A is composed of the columns a_i, the elements of the vector $u \in \mathbb{R}^M$ describe how much of each strategy to use, and the vector z describes the predicted outcome of a combination of strategies. For any objective function involving z, the optimal choice of u can be estimated [25]. With $N \gg M$, it will not be possible to simultaneously achieve all climate objectives with any combination of the simulated strategies; we seek to understand what outcomes are or are not achievable.

An important assumption in this process is that predicted outcomes can be obtained from linear combinations of the specified forcing simulations. While imperfect, this is a reasonable approximation (e.g. [25, 29, 31]). Nonetheless, it is useful to evaluate whether there are particular objectives for which the linearity approximation is poorer than for others; we thus include in our computational requirements a final evaluation simulation. This involves choosing a particular optimization criterion, finding the predicted optimal vector u, which can then be related into a particular set of injection rates at each latitude and each season, simulating this case, and comparing the simulated outcomes with the predicted ones.

The overall summary of proposed simulations is given in Table 1, along with the computational requirements (which are roughly commensurate with our previous allocation on Cheyenne); if more limited resources were available then additional prioritization will be made (e.g., reducing the length of simulations to evaluate AOD, or conducting these without dynamic ocean).

3.4 Policy integration

While it is straightforward to come up with a list of relevant climate goals involving temperature, global and regional precipitation changes, sea ice, and so forth, one of the first steps in this research will be to engage policy and governance experts, including those internationally (e.g., through the

Purpose	Model	# of years	# of sims	Simulation-years	Core-hours
AOD, different latitudes & seasons	CESM2(WACCM6)	5	24	120	1.2M
Performance-evaluation	CESM2(WACCM6)	70/30*	9	310	3.1M
Performance with specified-aerosols	CESM2(CAM6)	70/30*	18	620	2.1M
Linearity assessment	CESM2(WACCM6)	30	1	30	0.3M
Total				460 + 620	6.7M

Table 1: Simulations required and estimated computation time. To reduce total computational requirements, simulations marked with * will involve a single simulation 2030-2100, with alternate performance objectives branched from this run in 2070 and only simulating the final 30 years, allowing 10 years to re-converge for different objectives, and 20 years for analysis. This approach has already been demonstrated [50]. CESM2(CAM6) uses 3431 core-hours/year (https://csegweb.cgd.ucar.edu/timing/cgi-bin/timings.cgi). CESM2(WACCM6) uses ~8000 core-hours/year with only middle-atmosphere chemistry, but no dynamic ocean, based on PI experience and NCAR WACCM liaison; we estimate 10,000 with dynamic ocean, and we budget above to use the full ocean through the project, although it is not necessary for the first set of simulations.

DECIMALS program and C2G), to ensure that we have captured many of the most critical concerns regarding physical impacts of SAI. We have included in our budget travel allocation to participate in two SRMGI workshops that will enable direct conversations regarding these issues with scientists and policy-makers in the developing world.

In addition, to strengthen the pathway to impact, we will hold a focused workshop near the end of the proposed research that will bring both physical scientists and policy/governance experts together (including from SRMGI, C2G, and academics) to discuss the implications of identified trade-offs and limitations, how these might shape governance concerns, and explore steps for further research to support the development of policy and governance.

3.5 Team and Management:

Douglas MacMartin will be the overall project PI, responsible for overall project direction and supervision of the graduate student and any undergraduate researchers working on this project. He has extensive experience in geoengineering research, including design of feedback algorithms and optimization. Ben Kravitz, Indiana University, will serve as co-PI, contributing expertise throughout the project but in particular on coding of specified-aerosol simulations and coordinating simulations with other models. Assistance from Jadwiga (Yaga) Richter and others at NCAR is available if needed in setting up simulations with WACCM.

Broader Impacts

While geoengineering should never be considered as a substitute for mitigation, it might be the only pathway to limit some climate change impacts. This poses a crucial need to understand geoengineering risks, especially potential tradeoffs in geoengineering, which are directly related to the policy-relevant questions of a design-space (what climates can geoengineering achieve?) and geopolitics/ethics (will there be winners and losers?). Moreover, despite the outcomes of geoengineering depending upon design, most climate model simulations of SAI have employed ad hoc strategies, and even those that have considered deliberate design (including significant work by the PI and collaborators) have still made some arbitrary choices out of computational necessity with an aim of demonstrating potential rather than rigorously assessing the design space. GLENS [46], for example, is being used internationally for impacts research (e.g., [38]), yet it represents only a single strategy among many possibilities, conducted with a single model. The research herein will both provide a more comprehensive set of simulations covering different options that meet different sets of climate objectives, and will assess the extent to which different objectives can or cannot be simultaneously met – that is, what are the fundamental limits or trade-offs. By engaging governance communities both early in the research (to discuss specific climate objectives to consider in simulations), and through a workshop towards the end of the project that will disseminate the results, we will enable a reflexive process whereby the identified trade-offs will influence governance concerns, and define further research needs. The PI has long-standing connections with the geoengineering governance community; indeed, the proposed research is in part born out of those conversations and the need to provide better information for policy-makers.

Furthermore, the simulations conducted herein will be made available to the wider international community, including developing world researchers funded through DECIMALS, enabling a more holistic perspective on impact assessment rather than assessing one particular deployment strategy. The PI and Co-I are advisors to the DECIMALS program, providing a pathway toward more broad use of these simulations. Furthermore, we budgeted travel support for the PI to attend SRMGI workshops, allowing a first-hand discussion with a broader cross-section of participants in developing-world countries (scientists and policy-makers) regarding what climate objectives are of particular importance.

In addition to supporting a graduate student that will conduct the bulk of the research, this project will also provide an opportunity for undergraduate research involvement. Undergraduate engineering students at Cornell can fulfill design requirements for their degree through additional for-credit design-related activity connected with coursework. The project PI teaches the undergraduate/graduate feedback design class, in which undergraduates have been successfully involved in this research area. Specifically, potential senior design projects associated with this research include (i) constructing low-order dynamic models from system identification simulations, (ii) design of feedback algorithms based on dynamic models, and (iii) optimization of climate impacts, given simulated climate response functions.

Finally, this research integrates an engineering perspective into climate science research. One of the outputs, therefore, is not simply the research knowledge itself, but the ideas and engineering tools, that have the potential to impact not only how the scientific community thinks about geoengineering, but could potentially impact climate science more broadly. Training a truly interdisciplinary graduate student, integrated into a network of expert collaborators, is thus a valuable output of this work in itself.

Results from prior NSF Support

a) NSF award CBET-1818759, $299,529, April 1, 2018 – March 31, 2021: "EAGER: Introducing a design element into stratospheric aerosol geoengineering" (PI Douglas MacMartin).

Intellectual Merit: Solar geoengineering is not just a scientific endeavor, but also an engineering one. Much of the research conducted under this award has been described in the background above as it is an enabler for the research proposed herein. Key results include (i) demonstrating for the first time that not only does the latitude of aerosol injection affect the climate response, but so does the season of injection, including the potential to alter critical outcomes such as Indian monsoonal precipitation, (ii) demonstrating the ability to design feedback algorithms to manage metrics other than temperature-based ones, including precipitation, ITCZ, or sea ice (see Figure 4 above), and (iii) preliminary assessment of the "size" of the SAI design space, including latitudes, seasons, and in particular including single-season injection at high-latitude that greatly enhances efficiency relative to annually-constant high-latitude injection, and thus opens up a new range of as-yet-unexplored possible SAI strategies.

Broader Impacts: It is plausible that temporary and limited geoengineering deployment could be used to reduce climate risks, but making such an assessment requires understanding projected impacts and particularly the undesired side-effects. This research has taken a major step forwards towards that objective, illustrating the potential to reduce side-effects through seasonal injection strategies. Furthermore, the multidisciplinary perspective gained by applying engineering optimization, dynamic systems, and feedback design to climate science provides an opportunity to broaden both communities with the potential to spark additional insights and research.

Publications to date: References [26, 20, 51, 50], with two additional papers in preparation; one on managing different objectives (Figure 4), and one looking at the number of relevant degrees of freedom (roughly Section 2.2).

Research products and availability: Initial climate model output is available through the PI's website at Cornell; further climate model simulations are still being analyzed, and will then be archived either at NCAR or Cornell, with links provided in papers and through the PI's website.

b) NSF Award CBET-1931641, $299,994, 7/1/2019 6/30/2021: "EAGER: Marine Sky Brightening: Prospects and Consequences" (PI: Ben Kravitz).

Intellectual Merit: The aim of the project is to use models on a variety of scales to understand the effectiveness, feasibility, and efficiency of Marine Sky Brightening, which focuses on geoengineering via direct scattering of sea salt aerosols in the marine boundary layer. This idea will, for the first time, be systematically compared to Marine Cloud Brightening, a long studied geoengineering idea. The team has begun preliminary simulations using CESM to understand the sensitivity of the global climate to various strengths of solar reduction (a proxy for aerosol cooling) over the Gulf of Mexico and has identified and begun setting up regional and radiative transfer models to look at different scales of impact.

Broader Impacts: Marine Sky Brightening is applicable to regions where there are not clouds that can be reliably brightened. Does it work? Is it effective? What are the side effects and trade-offs? Understanding these questions will allow decision makers to better evaluate geoengineering options in the future.

References

[1] V. Aquila, C. I. Garfinkel, P. A. Newman, L. D. Oman, and D. W. Waugh. Modifications of the quasi-biennial oscillation by a geoengineering perturbation of the stratospheric aerosol layer. *Geophys. Res. Lett.*, 41(5), 2014. doi:10.1002/2013GL058818.

[2] G. Bala, P. B. Duffy, and K. E. Taylor. Impact of geoengineering schemes on the global hydrological cycle. *PNAS*, 105(22):7664 7669, 2008.

[3] G. A. Ban-Weiss and K. Caldeira. Geoengineering as an optimization problem. *Environ. Res. Lett.*, 5:034009, 2010. doi:10.1088/1748-9326/5/3/034009.

[4] L. Cao and J. Jiang. Simulated effect of carbon cycle feedback on climate response to solar geoengineering. *Geophy. Res. Lett.*, 44(24):12,484–12,491, 2017. doi: 10.1002/2017GL076546.

[5] W. Cheng, D. G. MacMartin, K. Dagon, B. Kravitz, S. Tilmes, J. H. Richter, M. J. Mills, and I. R. Simpson. Soil moisture and other hydrological changes in a stratospheric aerosol geoengineering large ensemble. *J. Geophys Res. A*, 2019.

[6] Z. Dai, D. Weisenstein, and D. W. Keith. Tailoring meridional and seasonal radiative forcing by sulfate aerosol solar geoengineering. *Geophys. Res. Lett.*, 2018. DOI: 10.1002/2017GL076472.

[7] G. Danabasoglu et al. The Community Earth System Model Version 2 (CESM2). *J. Adv. Modeling Earth Systems*, 12, 2019. doi:10.1029/2019MS001916.

[8] J. M. English, O. B. Toon, and M. J. Mills. Microphysical simulations of large volcanic eruptions: Pinatubo and Toba. *J. Geophys. Res. Atmos.*, 118:1880 1895, 2013. doi:10.1002/jgrd.50196.

[9] C. B. Field and K. J. Mach. Rightsizing carbon dioxide removal. *Science*, 356(6339):706 707, 2017. doi: 10.1126/science.aam9726.

[10] S. Fuss, J. G. Canadell, G. P. Peters, M. Tavoni, R. M. Andrew, P. Ciais, R. B. Jackson, C. D. Jones, F. Kraxner, N. Nakicenovic, C. Le Quéré, M. R. Raupach, A. Sharifi, P. Smith, and Y. Yamagata. Betting on negative emissions. *Nature Climate Change*, 4(10):850–853, 2014.

[11] A. Gettelman et al. The Whole Atmosphere Community Climate Model Version 6 (WACCM6). *J. Geophys. Res. A*, 124(23):12380 12403, 2019. doi: 10.1029/2019JD030943.

[12] J. M. Haywood, A. Jones, N. Bellouin, and D. Stephenson. Asymmetric forcing from stratospheric aerosols impacts Sahelian rainfall. *Nature Climate Change*, pages 660 665, 2013. doi:10.1038/nclimate1857.

[13] IPCC. *Global Warming of 1.5°C, an IPCC special report on the impacts of global warming of 1.5°C above pre-industrial levels and related global greenhouse gas emission pathways, in the context of strengthening the global response to the threat of climate change, sustainable development, and efforts to eradicate poverty.* IPCC, 2018.

[14] P. J. Irvine and D. W. Keith. Halving warming with stratospheric aerosol geoengineering moderates policy-relevant climate hazards. *Env. Res. Lett.*, 15(044011), 2020. doi: 10.1088/1748-9326/ab76dc.

[15] M. Kelley et al. GISS-E2.1: Configurations and climatology. *submitted, J. Adv. Model. Earth Systems*, 2020.

[16] A. Kleidon, B. Kravitz, and M. Renner. The hydrological sensitivity to global warming and solar geoengineering derived from thermodynamic constraints. *Geophys. Res. Lett.*, 42:138–144, 2015. doi:10.1002/2014GL062589.

[17] B. Kravitz et al. An energetic perspective on hydrological cycle changes in the Geoengineering Model Intercomparison Project (GeoMIP). *J. Geophys. Res.*, 118:13087 13102, 2013. doi:10.1002/2013JD020502.

[18] B. Kravitz et al. The Geoengineering Model Intercomparison Project Phase 6 (GeoMIP6): Simulation design and preliminary results. *Geoscientific Model Development*, 8(10):3379–3392, 2015. doi: 10.5194/gmd-8-3379-2015.

[19] B. Kravitz et al. Comparing surface and stratospheric impacts of geoengineering with different SO_2 injection strategies. *J. Geophys. Res. A*, 124, 2019.

[20] B. Kravitz and D. G. MacMartin. Uncertainty and the basis for confidence in solar geoengineering research. *Nature Reviews Earth and Environment*, 1:64–75, 2020. Doi: 10.1038/s43017-019-0004-7.

[21] B. Kravitz, D. G. MacMartin, D. T. Leedal, P. J. Rasch, and A. J. Jarvis. Explicit feedback and the management of uncertainty in meeting climate objectives with solar geoengineering. *Env. Res. Lett.*, 9(4), 2014.

[22] B. Kravitz, D. G. MacMartin, M. J. Mills, J. H. Richter, S. Tilmes, J.-F. Lamarque, J. J. Tribbia, and F. Vitt. First simulations of designing stratospheric sulfate aerosol geoengineering to meet multiple simultaneous climate objectives. *J. Geophys. Res. A*, 122:12,616 12,634, 2017. doi:10.1002/2017JD026874.

[23] B. Kravitz, D. G. MacMartin, H. Wang, and P. J. Rasch. Geoengineering as a design problem. *Earth Systems Dynamics*, 7:469 497, 2016. doi:10.5194/esd-7-469-2016.

[24] D. G. MacMartin, P. J. Irvine, B. Kravitz, and J. Horton. Technical characteristics of solar geoengineering deployment and implications for governance. *Climate Policy*, 19(10), 2019.

[25] D. G. MacMartin, D. W. Keith, B. Kravitz, and K. Caldeira. Management of trade-offs in geoengineering through optimal choice of non-uniform radiative forcing. *Nature Climate Change*, 3:365 368, 2013. doi:10.1038/nclimate1722.

[26] D. G. MacMartin and B. Kravitz. The engineering of climate engineering. *Annual Reviews of Control, Robotics, and Autonomous Systems*, 2:445–467, 2019. doi:10.1146/annurev-control-053018-023725.

[27] D. G. MacMartin and B. Kravitz. Mission-driven research for stratospheric aerosol geoengineering. *Proc. National Academy of Sciences*, 116(4):1089 1094, 2019.

[28] D. G. MacMartin, B. Kravitz, D. W. Keith, and A. J. Jarvis. Dynamics of the coupled human-climate system resulting from closed-loop control of solar geoengineering. *Clim. Dyn.*, 43(1–2):243–258, 2014.

[29] D. G. MacMartin, B. Kravitz, S. Tilmes, J. H. Richter, M. J. Mills, J.-F. Lamarque, J. J. Tribbia, and F. Vitt. The climate response to stratospheric aerosol geoengineering can be tailored using multiple injection locations. *J. Geophys. Res. A*, 122:12,574 12,590, 2017. doi:10.1002/2017JD026868.

[30] D. G. MacMartin, K. L. Ricke, and D. W. Keith. Solar geoengineering as part of an overall strategy for meeting the 1.5°C Paris target. *Phil. Trans. Royal Soc. A*, 2018. doi:10.1098/rsta.2016.0454.

[31] D. G. MacMartin, W. Wang, B. Kravitz, S. Tilmes, J. Richter, and M. J. Mills. Timescale for detecting the climate response to stratospheric aerosol geoengineering. *J. Geophys. Res. A*, 124(3), 2019.

[32] M. Mills, J. H. Richter, S. Tilmes, B. Kravitz, D. G. MacMartin, A. A. Glanville, J. J. Tribbia, J.-F. Lamarque, F. Vitt, A. Schmidt, A. Gettelman, C. Hannay, J. T. Bacmeister, and D. E. Kinnison. Radiative and chemical response to interactive stratospheric aerosols in fully coupled CESM1(WACCM). *J. Geophys. Res. A.*, 122:13,061–13,078, 2017. doi:10.1002/2017JD027006.

[33] J. Moreno-Cruz, K. Ricke, and D. W. Keith. A simple model to account for regional inequalities in the effectiveness of solar radiation management. *Climatic Change*, 110(3-4):649 668, 2012. DOI:10.1007/s10584-011-0103-z.

[34] National Academy of Sciences. *Climate Intervention: Reflecting Sunlight to Cool Earth.* The National Academies Press, 500 Fifth St. NW, Washington DC 20001, 2015.

[35] National Academy of Sciences. *Developing a Research Agenda for Carbon Dioxide Removal and Reliable Sequestration.* The National Academies Press, 500 Fifth St. NW, Washington DC 20001, 2019.

[36] U. Niemeier and C. Timmreck. What is the limit of climate engineering by stratospheric injection of SO_2? *Atmos. Chem. Phys.*, 15:9129–9141, 2015.

[37] J. R. Pierce, D. K. Weisenstein, P. Heckendorn, T. Peter, and D. W. Keith. Efficient formation of stratospheric aerosol for climate engineering by emission of condensible vapor from aircraft. *Geophys. Res. Lett.*, 37, 2010. L18805. doi:10.1029/2010GL043975.

[38] I. Pinto, C. Jack, C. Lennard, S. Tilmes, and R. C. Oloulami. Africa's climate response to solar radiation management with stratospheric aerosol. *Geophys. Res. Lett.*, 47(2), 2020. doi: 10.1029/2019GL086047.

[39] B. Rajagopalan and P. Molnar. Signatures of tibetan plateau heating on indian summer monsoon rainfall variability. *J. Geophys. Res. A*, 118(3):1170–1178, 2013. doi:10.1002/jgrd.50124.

[40] K. L. Ricke, M. Granger Morgan, and M. R. Allen. Regional climate response to solar-radiation management. *Nature Geoscience*, 3:537–541, 2010.

[41] J. Rogelj, M. den Elzen, N. Höhne, T. Fransen, H. Fekete, H. Winkler, R. Schaeffer, F. Sha, K. Riaha, and M. Meinshausen. Paris Agreement climate proposals need a boost to keep warming well below 2°C. *Nature*, 534:631 639, 2016. doi:10.1038/nature18307.

[42] I. Simpson et al. The regional hydroclimate response to stratospheric sulfate geoengineering and the role of stratospheric heating. *J. Geophys. Res. A*, 124, 2019. doi:10.1029/2019GL085758.

[43] S. Tilmes et al. The hydrological impact of geoengineering in the Geoengineering Model Intercomparison Project (GeoMIP). *J. Geophys. Res.*, 118(19):11036–11058, 2013. doi:10.1002/jgrd.50868.

[44] S. Tilmes et al. Reaching 1.5°C and 2.0°C global surface temperature targets using stratospheric aerosol geoengineering in CMIP6. *submitted, Earth Sys. Dyn.*, 2020.

[45] S. Tilmes, A. Jahn, J. E. Kay, M. Holland, and J.-F. Lamarque. Can regional climate engineering save the summer Arctic sea ice? *Geophys. Res. Lett.*, 41:880 885, 2014. doi:10.1002/2013GL058731.

[46] S. Tilmes, J. H. Richter, B. Kravitz, D. G. MacMartin, M. J. Mills, I. Simpson, A. S. Glanville, J. T. Fasullo, A. S. Phillips, J.-F. Lamarque, J. Tribbia, J. Edwards, S. Mickelson, and S. Gosh. CESM1(WACCM) stratospheric aerosol geoengineering large ensemble (GLENS) project. *Bull. Am. Met. Soc.*, 2018. doi:10.1175/BAMS-D-17-0267.1.

[47] S. Tilmes, J. H. Richter, M. J. Mills, B. Kravitz, D. G. MacMartin, F. Vitt, J. J. Tribbia, and J.-F. Lamarque. Sensitivity of aerosol distribution and climate response to stratospheric SO_2 injection locations. *J. Geophys. Res. A.*, 122:12,591 12,615, 2017. doi:10.1002/2017JD026888.

[48] S. Tilmes, J. H. Richter, M. M. Mills, B. Kravitz, D. G. MacMartin, R. R. Garcia, D. E. Kinnison, J.-F. Lamarque, J. Tribbia, and F. Vitt. Effects of different stratospheric so_2 injection altitude on stratospheric chemistry and dynamics. *J. Geophys. Res. A*, 2018. doi:10.1002/2017JD028146.

[49] D. G. Victor, K. Akimoto, Y. Kaya, M. Yamaguchi, D. Cullenward, and C. Hepburn. Prove Paris was more than paper promises. *Nature*, 548, 2017. doi:10.1038/548025a.

[50] D. Visioni, D. G. MacMartin, B. Kravitz, J. H. Richter, S. Tilmes, and M. J. Mills. Seasonally modulated stratospheric aerosol geoengineering alters climate outcomes. *to appear, Geophys. Res. Lett.*, 2020.

[51] D. Visioni, D. G. MacMartin, B. Kravitz, S. Tilmes, M. J. Mills, J. H. Richter, and M. P. Boudreau. Seasonally injection strategies for stratospheric aerosol geoengineering. *Geophys. Res. Lett.*, 46, 2019. doi:10.1029/2019GL083680.

[52] M. Yanai and G.-X. Wu. *The Asian Monsoon*, chapter Effects of the Tibetan Plateau, pages 513–549. Springer, 2006.

Revised 05/01/2020 **NSF BIOGRAPHICAL SKETCH** **OMB-3145-0058**

NAME: Douglas MacMartin

POSITION TITLE & INSTITUTION: Senior Research Associate, Cornell University

A. PROFESSIONAL PREPARATION
(see PAPPG Chapter II.C.2.f.(i)(a))

INSTITUTION	LOCATION	MAJOR/AREA OF STUDY	DEGREE (if applicable)	YEAR (YYYY)
University of Toronto	Toronto, Canada	Engineering Science	B. A. Sc.	1987
Massachusetts Institute of Technology	Cambridge, MA	Aeronautics and Astronautics	S.M.	1990
Massachusetts Institute of Technology	Cambridge, MA	Aeronautics and Astronautics	Ph.D.	1992
Massachusetts Institute of Technology	Cambridge, MA	Aeronautics and Astronautics	Postdoctoral associate	1992-1993

B. APPOINTMENTS
(see PAPPG Chapter II.C.2.f.(i)(b))

From - To	Position Title, Organization and Location
2015-present	Senior Research Associate and Senior Lecturer, Sibley School of Mechanical & Aerospace Engineering, and Faculty Fellow, Atkinson Center for Sustainability, Cornell University
2015-present	Visiting Associate, Computing and Mathematical Sciences, California Institute of Tech.
2008-2015	Research Professor of Computing and Mathematical Sciences, California Institute Tech.
2008-2014	Visiting investigator, Carnegie Institution for Science (Dept. Global Ecology).
2010	Guest researcher, Lund University, Sweden, Department of Astronomy
2006	Visiting Scientist, University of New South Wales and University of Adelaide
2002-2008	Senior Research Fellow, Department of Control & Dynamical Systems, Caltech
2000-2002	Visiting Associate, Department of Control & Dynamical Systems, Caltech
1994-2000	Flow Control Program Manager (99-00), Active Control Theme Leader (96-99), and Senior Research Engineer (94-96), United Technologies Research Center
1993-1994	Assistant Research Officer, Institute for Aerospace Research, National Research Council of Canada
1992-1993	Postdoctoral Fellow, Department of Aeronautics and Astronautics, MIT
1987-1992	Research Assistant, Department of Aeronautics and Astronautics, MIT

C. PRODUCTS

(see PAPPG Chapter II.C.2.f.(i)(c))

Products Most Closely Related to the Proposed Project

1. Visioni, D., D.G. MacMartin, B. Kravitz, J.H. Richter, S. Tilmes, and M.J. Mills, "Seasonally modulated stratospheric aerosol geoengineering alters the climate outcomes", to appear, Geophys. Res. Lett.
2. MacMartin, D.G., and B. Kravitz, "The engineering of climate engineering", Annual Reviews of Control, Robotics, and Autonomous Systems, 2(1), 2019. doi:annurev-control-053018-023725
3. MacMartin, D.G., B. Kravitz, S. Tilmes, J.H. Richter, M.J. Mills, J.-F. Lamarque, J.J. Tribbia, and F. Vitt, "The climate response to stratospheric aerosol geoengineering can be tailored using multiple injection locations" J. Geophys. Res. A. 122, 12,574–12,590, 2017. doi: 10.1002/2017JD026868
4. Kravitz, B., D.G. MacMartin, M. J. Mills, J. H. Richter, S. Tilmes, J.-F. Lamarque, J. J. Tribbia and F. Vitt, "First simulations of designing stratospheric sulfate aerosol geoengineering to meet multiple simultaneous climate objectives", J. Geophys. Res. A. 122, 12,616–12,634, 2017, doi:10.1002/2017JD026874
5. Kravitz, B., D. G. MacMartin, H. Wang, and P. J. Rasch, "Geoengineering as a design problem", Earth System Dynamics, 7, 469-497, 2016. doi:10.5194/esd-7-469-2016

Other Significant Products, Whether or Not Related to the Proposed Project

1. Kravitz, B., and D. G. MacMartin, "Uncertainty and the basis for confidence in solar geoengineering research", Nature Reviews Earth & Environment, 1, 64-75 (2020). Doi: 10.1038/s43017-019-0004-7
2. MacMartin, D.G., P. Irvine, B. Kravitz, and J. Horton, "Technical characteristics of solar geoengineering deployment and implications for governance", Climate Policy, 19(10), 2019. Doi 10.1080/14693062.2019.1668347
3. MacMartin, D.G. and B. Kravitz, "Mission-driven research for stratospheric aerosol geoengineering", Proc. National Academy of Sciences, 2019. https://doi.org/10.1073/pnas.1811022116
4. MacMartin, D. G., K. L. Ricke, and D. W. Keith, "Solar Geoengineering as part of an overall strategy for meeting the 1.5°C Paris target", Phil. Trans. Royal Soc. A., 2017. doi:10.1098/rsta.2016.0454
5. MacMartin, et al, Nature Climate Change, doi: 10.1038/nclimate1722

D. SYNERGISTIC ACTIVITIES

(see PAPPG Chapter II.C.2.f.(i)(d))

• Member of the Committee on Developing a Research Agenda and Research Governance Approaches for Climate Intervention Strategies that Reflect Sunlight to Cool Earth, US National Academies of Sciences Engineering and Medicine.
• Testified in US Congress, subcommittee on Environment and Subcommittee on Energy, Hearing on Geoengineering: Innovation, Research, and Technology, 11/8/2017.
• Advisor for DECIMALS projects supporting developing-world impacts analysis of geoengineering
• Co-chair, 2017 Gordon Research Conference on Climate Engineering, and chair for 2022 conference (formerly the 2020 conference postponed due to Covid-19).

NSF BIOGRAPHICAL SKETCH

NAME: Kravitz, Ben

POSITION TITLE & INSTITUTION: Assistant Professor, Indiana University

(a) PROFESSIONAL PREPARATION

INSTITUTION	LOCATION	MAJOR / AREA OF STUDY	DEGREE (if applicable)	YEAR YYYY
Northwestern University	Evanston, IL	Mathematics	BA	2004
Purdue University	West Lafayette, Indiana	Mathematics	MS	2007
Rutgers University	New Brunswick, NJ	Atmospheric Science	MS	2009
Rutgers University	New Brunswick, NJ	Atmospheric Science	PHD	2011
Carnegie Institution for Science	Stanford, CA		Postdoctoral Fellow	2011 - 2012
Pacific Northwest National Laboratory	Richland, WA		Postdoctoral Fellow	2012 - 2015

(b) APPOINTMENTS

2019 - present Assistant Professor, Indiana University, Bloomington, IN
2016 - 2018 Scientist III, Pacific Northwest National Laboratory, Richland, WA
2015 - 2015 Scientist II, Pacific Northwest National Laboratory, Richland, WA
2012 - 2015 Postdoctoral Research Associate, Pacific Northwest National Laboratory, Richland, WA
2011 - 2012 Postdoctoral Research Associate, Carnegie Institution for Science, Stanford, CA

(c) PRODUCTS

Products Most Closely Related to the Proposed Project

1. Kravitz B, MacMartin D, Mills M, Richter J, Tilmes S, Lamarque J, Tribbia J, Vitt F. First Simulations of Designing Stratospheric Sulfate Aerosol Geoengineering to Meet Multiple Simultaneous Climate Objectives. Journal of Geophysical Research: Atmospheres. 2017 December 07; 122(23):-. Available from: https://onlinelibrary.wiley.com/doi/abs/10.1002/2017JD026874 DOI: 10.1002/2017JD026874
2. Kravitz B, Robock A. Climate effects of high-latitude volcanic eruptions: Role of the time of year. Journal of Geophysical Research. 2011 January 07; 116(D1):-. Available from: http://doi.wiley.com/10.1029/2010JD014448 DOI: 10.1029/2010JD014448
3. Visioni D, MacMartin D, Kravitz B, Tilmes S, Mills M, Richter J, Boudreau M. Seasonal Injection Strategies for Stratospheric Aerosol Geoengineering. Geophysical Research Letters. 2019 July 08; 46(13):7790-7799. Available from: https://onlinelibrary.wiley.com/doi/abs/10.1029/2019GL083680 DOI: 10.1029/2019GL083680
4. Kravitz B, MacMartin D, Leedal D, Rasch P, Jarvis A. Explicit feedback and the management of

uncertainty in meeting climate objectives with solar geoengineering. Environmental Research Letters. 2014 April 01; 9(4):044006-. Available from: https://iopscience.iop.org/article/10.1088/1748-9326/9/4/044006 DOI: 10.1088/1748-9326/9/4/044006

5. Kravitz B, MacMartin D, Wang H, Rasch P. Geoengineering as a design problem. Earth System Dynamics. 2016 May 24; 7(2):469-497. Available from: https://www.earth-syst-dynam.net/7/469/2016/ DOI: 10.5194/esd-7-469-2016

Other Significant Products, Whether or Not Related to the Proposed Project

1. Marvel K, Kravitz B, Caldeira K. Geophysical limits to global wind power. Nature Climate Change. 2012; 3(2):118-121. Available from: http://www.nature.com/articles/nclimate1683 DOI: 10.1038/nclimate1683
2. MacMartin D, Keith D, Kravitz B, Caldeira K. Management of trade-offs in geoengineering through optimal choice of non-uniform radiative forcing. Nature Climate Change. 2012 October 21; 3(4):365-368. Available from: http://www.nature.com/articles/nclimate1722 DOI: 10.1038/nclimate1722
3. Yoon J, Wang S, Gillies R, Kravitz B, Hipps L, Rasch P. Increasing water cycle extremes in California and in relation to ENSO cycle under global warming. Nature Communications. 2015 October 21; 6(1):-. Available from: http://www.nature.com/articles/ncomms9657 DOI: 10.1038/ncomms9657
4. Seneviratne S, Phipps S, Pitman A, Hirsch A, Davin E, Donat M, Hirschi M, Lenton A, Wilhelm M, Kravitz B. Land radiative management as contributor to regional-scale climate adaptation and mitigation. Nature Geoscience. 2018; 11(2):88-96. Available from: http://www.nature.com/articles/s41561-017-0057-5 DOI: 10.1038/s41561-017-0057-5
5. Fasullo J, Tilmes S, Richter J, Kravitz B, MacMartin D, Mills M, Simpson I. Persistent polar ocean warming in a strategically geoengineered climate. Nature Geoscience. 2018 October 29; 11(12):910-914. Available from: http://www.nature.com/articles/s41561-018-0249-7 DOI: 10.1038/s41561-018-0249-7

(d) SYNERGISTIC ACTIVITIES

1. Contributing Author, Intergovernmental Panel on Climate Change (IPCC) Sixth Assessment Report, Working Group I, Chapter 4: Future global climate: scenario-based projections and near-term information.

2. Editor, Earth System Dynamics.

3. Director, Geoengineering Model Intercomparison Project (GeoMIP), http://climate.envsci.rutgers.edu/GeoMIP/.

4. Committee Member, Fall Program Committee for Global Environmental Change, American Geophysical Union Fall Meeting, 2015-2020.

5. International Steering Committee Member, Climate Engineering Conference 2020.

SUMMARY PROPOSAL BUDGET

YEAR 1

FOR NSF USE ONLY	
PROPOSAL NO.	DURATION (months) Proposed / Granted
AWARD NO.	

ORGANIZATION
Cornell University
PRINCIPAL INVESTIGATOR / PROJECT DIRECTOR
Douglas MacMartin

A. SENIOR PERSONNEL: PI/PD, Co-PI's, Faculty and Other Senior Associates (List each separately with title, A.7. show number in brackets)	NSF Funded Person-months CAL	ACAD	SUMR	Funds Requested By proposer	Funds granted by NSF (if different)
1. **Douglas G MacMartin - PI**				(b)(4): (b)(6)	
2.					
3.					
4.					
5.					
6. (**0**) OTHERS (LIST INDIVIDUALLY ON BUDGET JUSTIFICATION PAGE					
7. (**1**) TOTAL SENIOR PERSONNEL (1 - 6)					
B. OTHER PERSONNEL (SHOW NUMBERS IN BRACKETS)					
1. (**0**) POST DOCTORAL SCHOLARS					
2. (**0**) OTHER PROFESSIONALS (TECHNICIAN, PROGRAMMER, ETC.)					
3. (**1**) GRADUATE STUDENTS					
4. (**0**) UNDERGRADUATE STUDENTS					
5. (**0**) SECRETARIAL - CLERICAL (IF CHARGED DIRECTLY)					
6. (**0**) OTHER					
TOTAL SALARIES AND WAGES (A + B)					
C. FRINGE BENEFITS (IF CHARGED AS DIRECT COSTS)					
TOTAL SALARIES, WAGES AND FRINGE BENEFITS (A + B + C)					
D. EQUIPMENT (LIST ITEM AND DOLLAR AMOUNT FOR EACH ITEM EXCEEDING $5,000.)					
TOTAL EQUIPMENT				(b)(4)	
E. TRAVEL 1. DOMESTIC (INCL. U.S. POSSESSIONS)					
2. INTERNATIONAL					
F. PARTICIPANT SUPPORT COSTS					
1. STIPENDS $ **0**					
2. TRAVEL **0**					
3. SUBSISTENCE **0**					
4. OTHER **0**					
TOTAL NUMBER OF PARTICIPANTS (**0**) TOTAL PARTICIPANT COSTS				**0**	
G. OTHER DIRECT COSTS					
1. MATERIALS AND SUPPLIES				(b)(4): (b)(6)	
2. PUBLICATION COSTS/DOCUMENTATION/DISSEMINATION					
3. CONSULTANT SERVICES					
4. COMPUTER SERVICES					
5. SUBAWARDS					
6. OTHER					
TOTAL OTHER DIRECT COSTS					
H. TOTAL DIRECT COSTS (A THROUGH G)					
I. INDIRECT COSTS (F&A)(SPECIFY RATE AND BASE) **Facilities and administrative** (b)(4)					
TOTAL INDIRECT COSTS (F&A)				(b)(4)	
J. TOTAL DIRECT AND INDIRECT COSTS (H + I)				**128,654**	
K. FEE				**0**	
L. AMOUNT OF THIS REQUEST (J) OR (J MINUS K)				**128,654**	
M. COST SHARING PROPOSED LEVEL $ **0** AGREED LEVEL IF DIFFERENT $					

PI/PD NAME	FOR NSF USE ONLY		
Douglas MacMartin	INDIRECT COST RATE VERIFICATION		
ORG. REP. NAME*	Date Checked	Date Of Rate Sheet	Initials - ORG
Tammy Custer			

1 *ELECTRONIC SIGNATURES REQUIRED FOR REVISED BUDGET

SUMMARY PROPOSAL BUDGET YEAR 2

FOR NSF USE ONLY	
PROPOSAL NO.	DURATION (months) Proposed / Granted
AWARD NO.	

ORGANIZATION
Cornell University
PRINCIPAL INVESTIGATOR / PROJECT DIRECTOR
Douglas MacMartin

A. SENIOR PERSONNEL: PI/PD, Co-PI's, Faculty and Other Senior Associates (List each separately with title, A.7. show number in brackets)	NSF Funded Person-months CAL	ACAD	SUMR	Funds Requested By proposer	Funds granted by NSF (if different)
1. **Douglas G MacMartin - PI**	(b)(4): (b)(6)				
2.					
3.					
4.					
5.					
6. (**0**) OTHERS (LIST INDIVIDUALLY ON BUDGET JUSTIFICATION PAGE)					
7. (**1**) TOTAL SENIOR PERSONNEL (1 - 6)					
B. OTHER PERSONNEL (SHOW NUMBERS IN BRACKETS)					
1. (**0**) POST DOCTORAL SCHOLARS					
2. (**0**) OTHER PROFESSIONALS (TECHNICIAN, PROGRAMMER, ETC.)					
3. (**1**) GRADUATE STUDENTS					
4. (**0**) UNDERGRADUATE STUDENTS					
5. (**0**) SECRETARIAL - CLERICAL (IF CHARGED DIRECTLY)					
6. (**0**) OTHER					
TOTAL SALARIES AND WAGES (A + B)					
C. FRINGE BENEFITS (IF CHARGED AS DIRECT COSTS)					
TOTAL SALARIES, WAGES AND FRINGE BENEFITS (A + B + C)					
D. EQUIPMENT (LIST ITEM AND DOLLAR AMOUNT FOR EACH ITEM EXCEEDING $5,000.)					
TOTAL EQUIPMENT				(b)(4)	
E. TRAVEL 1. DOMESTIC (INCL. U.S. POSSESSIONS)					
2. INTERNATIONAL					
F. PARTICIPANT SUPPORT COSTS					
1. STIPENDS $ **0**					
2. TRAVEL **0**					
3. SUBSISTENCE **0**					
4. OTHER **0**					
TOTAL NUMBER OF PARTICIPANTS (**0**) TOTAL PARTICIPANT COSTS				**0**	
G. OTHER DIRECT COSTS					
1. MATERIALS AND SUPPLIES				(b)(4): (b)(6)	
2. PUBLICATION COSTS/DOCUMENTATION/DISSEMINATION					
3. CONSULTANT SERVICES					
4. COMPUTER SERVICES					
5. SUBAWARDS					
6. OTHER					
TOTAL OTHER DIRECT COSTS					
H. TOTAL DIRECT COSTS (A THROUGH G)					
I. INDIRECT COSTS (F&A)(SPECIFY RATE AND BASE)					
Facilities and administrative (b)(4)					
TOTAL INDIRECT COSTS (F&A)				(b)(4)	
J. TOTAL DIRECT AND INDIRECT COSTS (H + I)				**121,927**	
K. FEE				**0**	
L. AMOUNT OF THIS REQUEST (J) OR (J MINUS K)				**121,927**	

M. COST SHARING PROPOSED LEVEL $ **0** AGREED LEVEL IF DIFFERENT $

PI/PD NAME
Douglas MacMartin
ORG. REP. NAME*
Tammy Custer

FOR NSF USE ONLY		
INDIRECT COST RATE VERIFICATION		
Date Checked	Date Of Rate Sheet	Initials - ORG

SUMMARY PROPOSAL BUDGET

YEAR 3

FOR NSF USE ONLY	
PROPOSAL NO.	DURATION (months) Proposed / Granted
AWARD NO.	

ORGANIZATION
Cornell University
PRINCIPAL INVESTIGATOR / PROJECT DIRECTOR
Douglas MacMartin

A. SENIOR PERSONNEL: PI/PD, Co-PI's, Faculty and Other Senior Associates (List each separately with title, A.7. show number in brackets)	NSF Funded Person-months CAL	ACAD	SUMR	Funds Requested By proposer	Funds granted by NSF (if different)
1. **Douglas G MacMartin - PI**	(b)(4): (b)(6)				
2.					
3.					
4.					
5.					
6. (**0**) OTHERS (LIST INDIVIDUALLY ON BUDGET JUSTIFICATION PAGE					
7. (**1**) TOTAL SENIOR PERSONNEL (1 - 6)					
B. OTHER PERSONNEL (SHOW NUMBERS IN BRACKETS)					
1. (**0**) POST DOCTORAL SCHOLARS					
2. (**0**) OTHER PROFESSIONALS (TECHNICIAN, PROGRAMMER, ETC.)					
3. (**1**) GRADUATE STUDENTS					
4. (**0**) UNDERGRADUATE STUDENTS					
5. (**0**) SECRETARIAL - CLERICAL (IF CHARGED DIRECTLY)					
6. (**0**) OTHER					
TOTAL SALARIES AND WAGES (A + B)					
C. FRINGE BENEFITS (IF CHARGED AS DIRECT COSTS)					
TOTAL SALARIES, WAGES AND FRINGE BENEFITS (A + B + C)					
D. EQUIPMENT (LIST ITEM AND DOLLAR AMOUNT FOR EACH ITEM EXCEEDING $5,000.)					
TOTAL EQUIPMENT				(b)(4)	
E. TRAVEL 1. DOMESTIC (INCL. U.S. POSSESSIONS)					
2. INTERNATIONAL					
F. PARTICIPANT SUPPORT COSTS					
1. STIPENDS $ **0**					
2. TRAVEL **0**					
3. SUBSISTENCE **0**					
4. OTHER **0**					
TOTAL NUMBER OF PARTICIPANTS (**0**) TOTAL PARTICIPANT COSTS				**0**	
G. OTHER DIRECT COSTS					
1. MATERIALS AND SUPPLIES				(b)(4): (b)(6)	
2. PUBLICATION COSTS/DOCUMENTATION/DISSEMINATION					
3. CONSULTANT SERVICES					
4. COMPUTER SERVICES					
5. SUBAWARDS					
6. OTHER					
TOTAL OTHER DIRECT COSTS					
H. TOTAL DIRECT COSTS (A THROUGH G)					
I. INDIRECT COSTS (F&A)(SPECIFY RATE AND BASE) **Facilities and administrative** (b)(4)					
TOTAL INDIRECT COSTS (F&A)				(b)(4)	
J. TOTAL DIRECT AND INDIRECT COSTS (H + I)				**147,562**	
K. FEE				**0**	
L. AMOUNT OF THIS REQUEST (J) OR (J MINUS K)				**147,562**	

M. COST SHARING PROPOSED LEVEL $ **0** AGREED LEVEL IF DIFFERENT $

PI/PD NAME
Douglas MacMartin
ORG. REP. NAME*
Tammy Custer

FOR NSF USE ONLY		
INDIRECT COST RATE VERIFICATION		
Date Checked	Date Of Rate Sheet	Initials - ORG

 *ELECTRONIC SIGNATURES REQUIRED FOR REVISED BUDGET

SUMMARY PROPOSAL BUDGET

FOR NSF USE ONLY	
PROPOSAL NO.	DURATION (months) Proposed / Granted
AWARD NO.	

ORGANIZATION
Cornell University
PRINCIPAL INVESTIGATOR / PROJECT DIRECTOR
Douglas MacMartin

A. SENIOR PERSONNEL: PI/PD, Co-PI's, Faculty and Other Senior Associates (List each separately with title, A.7. show number in brackets)	NSF Funded Person-months CAL	ACAD	SUMR	Funds Requested By proposer	Funds granted by NSF (if different)
1. **Douglas G MacMartin - PI**	(b)(4): (b)(6)				
2.					
3.					
4.					
5.					
6. ( ) OTHERS (LIST INDIVIDUALLY ON BUDGET JUSTIFICATION PAGE)					
7. (**1**) TOTAL SENIOR PERSONNEL (1 - 6)					
B. OTHER PERSONNEL (SHOW NUMBERS IN BRACKETS)					
1. (**0**) POST DOCTORAL SCHOLARS					
2. (**0**) OTHER PROFESSIONALS (TECHNICIAN, PROGRAMMER, ETC.)					
3. (**3**) GRADUATE STUDENTS					
4. (**0**) UNDERGRADUATE STUDENTS					
5. (**0**) SECRETARIAL - CLERICAL (IF CHARGED DIRECTLY)					
6. (**0**) OTHER					
TOTAL SALARIES AND WAGES (A + B)					
C. FRINGE BENEFITS (IF CHARGED AS DIRECT COSTS)					
TOTAL SALARIES, WAGES AND FRINGE BENEFITS (A + B + C)					
D. EQUIPMENT (LIST ITEM AND DOLLAR AMOUNT FOR EACH ITEM EXCEEDING $5,000.)					
TOTAL EQUIPMENT				(b)(4)	
E. TRAVEL 1. DOMESTIC (INCL. U.S. POSSESSIONS)					
2. INTERNATIONAL					
F. PARTICIPANT SUPPORT COSTS					
1. STIPENDS $ **0**					
2. TRAVEL **0**					
3. SUBSISTENCE **0**					
4. OTHER **0**					
TOTAL NUMBER OF PARTICIPANTS (**0**) TOTAL PARTICIPANT COSTS				**0**	
G. OTHER DIRECT COSTS					
1. MATERIALS AND SUPPLIES				(b)(4): (b)(6)	
2. PUBLICATION COSTS/DOCUMENTATION/DISSEMINATION					
3. CONSULTANT SERVICES					
4. COMPUTER SERVICES					
5. SUBAWARDS					
6. OTHER					
TOTAL OTHER DIRECT COSTS					
H. TOTAL DIRECT COSTS (A THROUGH G)					
I. INDIRECT COSTS (F&A)(SPECIFY RATE AND BASE)					
TOTAL INDIRECT COSTS (F&A)				(b)(4)	
J. TOTAL DIRECT AND INDIRECT COSTS (H + I)				**398,143**	
K. FEE				**0**	
L. AMOUNT OF THIS REQUEST (J) OR (J MINUS K)				**398,143**	
M. COST SHARING PROPOSED LEVEL $ **0** AGREED LEVEL IF DIFFERENT $					

PI/PD NAME	FOR NSF USE ONLY		
Douglas MacMartin	INDIRECT COST RATE VERIFICATION		
ORG. REP. NAME*	Date Checked	Date Of Rate Sheet	Initials - ORG
Tammy Custer			

C *ELECTRONIC SIGNATURES REQUIRED FOR REVISED BUDGET

Cornell University Budget Justification

Cornell utilizes the calendar year for compliance with the NSF's limitation on senior personnel salary requests.

Salaries and Wages

Principal Investigator (Douglas MacMartin): This proposal requests salary support for (b)(4): (b)(6) of academic-year effort each period to oversee the coordination and scientific direction of the proposed work. PI will guide the graduate research assistant in the planning and execution of climate model simulations, in the analysis of model output, and in the preparation of manuscripts and conference presentations for dissemination of the work. The PI will also interface with governance and policy experts regarding climate goals (including travel to SRMGI meetings), and in planning a final workshop with these experts.

Graduate Students: This proposal requests salary support for (b)(4) of effort for 1 Graduate Research Assistant in each budget year. The salary support includes the stipend each period, inclusive of a (b)(4) increase at the beginning of each academic year (August 16th). The GRA will primarily responsible for conducting and analyzing simulations and documenting results, and conducting all research work for this project as outlined in the project description.

GRA Stipend Support	Period 1	Period 2	Period 3	Total
GRA AY Stipend	(b)(4)			
GRA Summer Stipend				
Total GRA Stipend				

All Cornell University non-student salaries use a base rate of current FY20 salary rates and include a budgeted increase in July of each budget period under Cornell University policy.

Consistent with federal cost principles, Cornell University estimates personnel time on a percentage of total effort. Cornell University does not track work hours for FLSA (Fair Labor Standard Act) exempt staff and is unable to provide billing or time records based on hours. Following OMB 2 CFR Part 200 §430(i), Cornell allocates a level of effort utilizing a Plan Confirmation System. The percentages of personnel effort are into months of personnel effort in this budget proposal.

Fringe Benefits

Employee Benefit rates budgeted within this proposal are (b)(4) for all non-student compensation through June 30, 2020, and (b)(4) effective July 1, 2020, for Cornell's endowed colleges.

Fringe benefit rates comply with rates approved by Cornell's Cognizant Agency: Department of Health and Human Services. For more information on Cornell University employee benefit rates, see https://www.dfa.cornell.edu/capitalassets/cost/employee.

Travel

Domestic: This proposal requests funding for domestic travel to enable the project participants to attend conferences and PI meetings to promote transfer of the knowledge gained, by presenting their research results. Cost estimates rely on current airfare and GSA per diem rates for lodging and meals and incidental expenses (M&IE). Examples of possible travel used for budgeting purposes include attending the AGU fall meeting, and travel by the graduate student to the National Center for Atmospheric Research (NCAR) to work with collaborators.

International: This proposal requests funding for international travel to enable the project PI to attend two SRMGI meetings in the developing world (specific locations TBD) to better obtain firsthand knowledge on the potential climate objectives and plausible future scenarios in support of Task 2 of the Statement of Work. The PI has attended a past SRMGI meeting in Jamaica and costs have been estimated using that as an example.

Travel Purpose	Travel Destination	Travel Origin	# of PPL	Registration	Airfare/ Mileage	# of Nights	Per Diem (Lodging)	# of Days	Per Diem (M&IE)	Estimated Trip Cost	# of Trips	Total Cost
AGU Fall Meeting		(b)(4): (b)(6)										
NCAR Conference	TBD											
SRMGI Meeting (International)	TBD											

Other Direct Costs

Publication Costs

This proposal requests funding for publication costs to promote technology transfer by presenting research results at the planned conferences, the submission of manuscripts for publication in peer-reviewed journals (printing, page charges, and postage), and costs associated with the creation of posters.

Subcontracts

This proposal requests funds for a subcontract to Indiana University in the amount of (b)(4) Indiana University PI Ben Kravitz will provide scientific expertise and participate in all stages of research. He will also be responsible for setting up and conducting simulations for Tasks 1, 5, and 6, as well as contributing to analyses of output. Kravitz has experience running and evaluating output from the CESM and GISS ModelE climate models, which are central to the completion of these tasks. Kravitz was also the first to implement a solar geoengineering feedback algorithm in either of these models.

Workshop

This proposal requests funds to support a small workshop at Cornell University to bring governance and policy experts together with the project team and other climate scientists to discuss the implications of the research results regarding underlying trade-offs and possible future scenarios, along with future research needs; this workshop will provide a direct linkage to broader impacts of the work. Costs have been estimated to support travel costs of 8 policy and governance experts along with local meals.

Other

Graduate Tuition and Mandatory Fees

This proposal requests support for 12 months of effort for 1 Graduate Research Assistant in each budget year to conduct research work for this project as outlined above. The support includes tuition and mandatory health insurance fees each period. Health insurance fees include a (b)(4) annual increase, effective August 1st of each year, and no projected increases for tuition.

GRA Other Direct Costs	Period 1	Period 2	Period 3	Total
GRA AY Tuition	(b)(4)			
GRA Health Insurance Fee				
Total GRA ODCs				

Indirect Costs

Facilities and Administrative Costs (F&A) rates are (b)(4) for endowed college research as approved by Cornell's Cognizant Agency: Department of Health and Human Services. For more information on Cornell University's indirect cost rates, see http://www.dfa.cornell.edu/sites/default/files/dhhsrateagreement.pdf.

Modified Total Direct Cost (MTDC) exclusions include GRA tuition remission, GRA health insurance fees, and the portion of each subaward in excess of (b)(4)

Endowed F&A: Total Direct Costs (b)(4) Exclusion of (b)(4) = MTDC Cost Base (b)(4) **F&A.**

SUMMARY PROPOSAL BUDGET

YEAR 1

FOR NSF USE ONLY	
PROPOSAL NO.	DURATION (months) Proposed / Granted
AWARD NO.	

ORGANIZATION
Indiana University
PRINCIPAL INVESTIGATOR / PROJECT DIRECTOR
Benjamin Kravitz

A. SENIOR PERSONNEL: PI/PD, Co-PI's, Faculty and Other Senior Associates (List each separately with title, A.7. show number in brackets)	NSF Funded Person-months CAL	ACAD	SUMR	Funds Requested By proposer	Funds granted by NSF (if different)
1. **Benjamin Kravitz - CO-PI**	(b)(4): (b)(6)				
2.					
3.					
4.					
5.					
6. (**0**) OTHERS (LIST INDIVIDUALLY ON BUDGET JUSTIFICATION PAGE)					
7. (**1**) TOTAL SENIOR PERSONNEL (1 - 6)					
B. OTHER PERSONNEL (SHOW NUMBERS IN BRACKETS)					
1. (**0**) POST DOCTORAL SCHOLARS					
2. (**0**) OTHER PROFESSIONALS (TECHNICIAN, PROGRAMMER, ETC.)					
3. (**0**) GRADUATE STUDENTS					
4. (**0**) UNDERGRADUATE STUDENTS					
5. (**0**) SECRETARIAL - CLERICAL (IF CHARGED DIRECTLY)					
6. (**0**) OTHER					
TOTAL SALARIES AND WAGES (A + B)					
C. FRINGE BENEFITS (IF CHARGED AS DIRECT COSTS)					
TOTAL SALARIES, WAGES AND FRINGE BENEFITS (A + B + C)					
D. EQUIPMENT (LIST ITEM AND DOLLAR AMOUNT FOR EACH ITEM EXCEEDING $5,000.)					
TOTAL EQUIPMENT				**0**	
E. TRAVEL 1. DOMESTIC (INCL. U.S. POSSESSIONS)				**0**	
2. INTERNATIONAL				**0**	
F. PARTICIPANT SUPPORT COSTS					
1. STIPENDS $ **0**					
2. TRAVEL **0**					
3. SUBSISTENCE **0**					
4. OTHER **0**					
TOTAL NUMBER OF PARTICIPANTS (**0**) TOTAL PARTICIPANT COSTS				**0**	
G. OTHER DIRECT COSTS					
1. MATERIALS AND SUPPLIES				**0**	
2. PUBLICATION COSTS/DOCUMENTATION/DISSEMINATION				**0**	
3. CONSULTANT SERVICES				**0**	
4. COMPUTER SERVICES				**0**	
5. SUBAWARDS				**0**	
6. OTHER				**0**	
TOTAL OTHER DIRECT COSTS				**0**	
H. TOTAL DIRECT COSTS (A THROUGH G)				(b)(4): (b)(6)	
I. INDIRECT COSTS (F&A)(SPECIFY RATE AND BASE) **Facilities and administrative** (b)(4)					
TOTAL INDIRECT COSTS (F&A)				(b)(4)	
J. TOTAL DIRECT AND INDIRECT COSTS (H + I)				**9,199**	
K. FEE				**0**	
L. AMOUNT OF THIS REQUEST (J) OR (J MINUS K)				**9,199**	

M. COST SHARING PROPOSED LEVEL $ **0** AGREED LEVEL IF DIFFERENT $

PI/PD NAME
Benjamin Kravitz
ORG. REP. NAME*
Tammy Custer

FOR NSF USE ONLY		
INDIRECT COST RATE VERIFICATION		
Date Checked	Date Of Rate Sheet	Initials - ORG

1 *ELECTRONIC SIGNATURES REQUIRED FOR REVISED BUDGET

SUMMARY PROPOSAL BUDGET YEAR 2

FOR NSF USE ONLY	
PROPOSAL NO.	DURATION (months) Proposed / Granted
AWARD NO.	

ORGANIZATION
Indiana University
PRINCIPAL INVESTIGATOR / PROJECT DIRECTOR
Benjamin Kravitz

A. SENIOR PERSONNEL: PI/PD, Co-PI's, Faculty and Other Senior Associates (List each separately with title, A.7. show number in brackets)	NSF Funded Person-months CAL	ACAD	SUMR	Funds Requested By proposer	Funds granted by NSF (if different)
1. **Benjamin Kravitz - CO-PI**	(b)(4): (b)(6)				
2.					
3.					
4.					
5.					
6. (**0**) OTHERS (LIST INDIVIDUALLY ON BUDGET JUSTIFICATION PAGE)					
7. (**1**) TOTAL SENIOR PERSONNEL (1 - 6)					
B. OTHER PERSONNEL (SHOW NUMBERS IN BRACKETS)					
1. (**0**) POST DOCTORAL SCHOLARS					
2. (**0**) OTHER PROFESSIONALS (TECHNICIAN, PROGRAMMER, ETC.)					
3. (**0**) GRADUATE STUDENTS					
4. (**0**) UNDERGRADUATE STUDENTS					
5. (**0**) SECRETARIAL - CLERICAL (IF CHARGED DIRECTLY)					
6. (**0**) OTHER					
TOTAL SALARIES AND WAGES (A + B)					
C. FRINGE BENEFITS (IF CHARGED AS DIRECT COSTS)					
TOTAL SALARIES, WAGES AND FRINGE BENEFITS (A + B + C)					
D. EQUIPMENT (LIST ITEM AND DOLLAR AMOUNT FOR EACH ITEM EXCEEDING $5,000.)					
TOTAL EQUIPMENT				**0**	
E. TRAVEL 1. DOMESTIC (INCL. U.S. POSSESSIONS)				**0**	
2. INTERNATIONAL				**0**	
F. PARTICIPANT SUPPORT COSTS					
1. STIPENDS $ **0**					
2. TRAVEL **0**					
3. SUBSISTENCE **0**					
4. OTHER **0**					
TOTAL NUMBER OF PARTICIPANTS (**0**) TOTAL PARTICIPANT COSTS				**0**	
G. OTHER DIRECT COSTS					
1. MATERIALS AND SUPPLIES				**0**	
2. PUBLICATION COSTS/DOCUMENTATION/DISSEMINATION				**0**	
3. CONSULTANT SERVICES				**0**	
4. COMPUTER SERVICES				**0**	
5. SUBAWARDS				**0**	
6. OTHER				**0**	
TOTAL OTHER DIRECT COSTS				**0**	
H. TOTAL DIRECT COSTS (A THROUGH G)				(b)(4): (b)(6)	
I. INDIRECT COSTS (F&A)(SPECIFY RATE AND BASE) **Facilities and administrative** (b)(4)					
TOTAL INDIRECT COSTS (F&A)				**3,497**	
J. TOTAL DIRECT AND INDIRECT COSTS (H + I)				**9,475**	
K. FEE				**0**	
L. AMOUNT OF THIS REQUEST (J) OR (J MINUS K)				**9,475**	

M. COST SHARING PROPOSED LEVEL $ **0** AGREED LEVEL IF DIFFERENT $

PI/PD NAME
Benjamin Kravitz
ORG. REP. NAME*
Tammy Custer

FOR NSF USE ONLY		
INDIRECT COST RATE VERIFICATION		
Date Checked	Date Of Rate Sheet	Initials - ORG

 *ELECTRONIC SIGNATURES REQUIRED FOR REVISED BUDGET

SUMMARY PROPOSAL BUDGET YEAR 3

FOR NSF USE ONLY	
PROPOSAL NO.	DURATION (months) Proposed / Granted
AWARD NO.	

ORGANIZATION
Indiana University
PRINCIPAL INVESTIGATOR / PROJECT DIRECTOR
Benjamin Kravitz

A. SENIOR PERSONNEL: PI/PD, Co-PI's, Faculty and Other Senior Associates (List each separately with title, A.7. show number in brackets)	NSF Funded Person-months CAL	ACAD	SUMR	Funds Requested By proposer	Funds granted by NSF (if different)
1. **Benjamin Kravitz - CO-PI**	(b)(4): (b)(6)				
2.					
3.					
4.					
5.					
6. (**0**) OTHERS (LIST INDIVIDUALLY ON BUDGET JUSTIFICATION PAGE)					
7. (**1**) TOTAL SENIOR PERSONNEL (1 - 6)					
B. OTHER PERSONNEL (SHOW NUMBERS IN BRACKETS)					
1. (**0**) POST DOCTORAL SCHOLARS					
2. (**0**) OTHER PROFESSIONALS (TECHNICIAN, PROGRAMMER, ETC.)					
3. (**0**) GRADUATE STUDENTS					
4. (**0**) UNDERGRADUATE STUDENTS					
5. (**0**) SECRETARIAL - CLERICAL (IF CHARGED DIRECTLY)					
6. (**0**) OTHER					
TOTAL SALARIES AND WAGES (A + B)					
C. FRINGE BENEFITS (IF CHARGED AS DIRECT COSTS)					
TOTAL SALARIES, WAGES AND FRINGE BENEFITS (A + B + C)					
D. EQUIPMENT (LIST ITEM AND DOLLAR AMOUNT FOR EACH ITEM EXCEEDING $5,000.)					
TOTAL EQUIPMENT				**0**	
E. TRAVEL 1. DOMESTIC (INCL. U.S. POSSESSIONS)				**0**	
2. INTERNATIONAL				**0**	
F. PARTICIPANT SUPPORT COSTS					
1. STIPENDS $ **0**					
2. TRAVEL **0**					
3. SUBSISTENCE **0**					
4. OTHER **0**					
TOTAL NUMBER OF PARTICIPANTS (**0**) TOTAL PARTICIPANT COSTS				**0**	
G. OTHER DIRECT COSTS					
1. MATERIALS AND SUPPLIES				**0**	
2. PUBLICATION COSTS/DOCUMENTATION/DISSEMINATION				**0**	
3. CONSULTANT SERVICES				**0**	
4. COMPUTER SERVICES				**0**	
5. SUBAWARDS				**0**	
6. OTHER				**0**	
TOTAL OTHER DIRECT COSTS				**0**	
H. TOTAL DIRECT COSTS (A THROUGH G)				(b)(4)	
I. INDIRECT COSTS (F&A)(SPECIFY RATE AND BASE) **Facilities and administrative** (b)(4)					
TOTAL INDIRECT COSTS (F&A)				**3,602**	
J. TOTAL DIRECT AND INDIRECT COSTS (H + I)				**9,759**	
K. FEE				**0**	
L. AMOUNT OF THIS REQUEST (J) OR (J MINUS K)				**9,759**	

M. COST SHARING PROPOSED LEVEL $ **0** AGREED LEVEL IF DIFFERENT $

PI/PD NAME
Benjamin Kravitz
ORG. REP. NAME*
Tammy Custer

FOR NSF USE ONLY		
INDIRECT COST RATE VERIFICATION		
Date Checked	Date Of Rate Sheet	Initials - ORG

 *ELECTRONIC SIGNATURES REQUIRED FOR REVISED BUDGET

SUMMARY PROPOSAL BUDGET

FOR NSF USE ONLY	
PROPOSAL NO.	DURATION (months) Proposed / Granted
AWARD NO.	

ORGANIZATION
Indiana University
PRINCIPAL INVESTIGATOR / PROJECT DIRECTOR
Benjamin Kravitz

A. SENIOR PERSONNEL: PI/PD, Co-PI's, Faculty and Other Senior Associates (List each separately with title, A.7. show number in brackets)	NSF Funded Person-months CAL	ACAD	SUMR	Funds Requested By proposer	Funds granted by NSF (if different)
1. **Benjamin Kravitz - CO-PI**	(b)(4); (b)(6)				
2.					
3.					
4.					
5.					
6. ( ) OTHERS (LIST INDIVIDUALLY ON BUDGET JUSTIFICATION PAGE)					
7. (**1**) TOTAL SENIOR PERSONNEL (1 - 6)					
B. OTHER PERSONNEL (SHOW NUMBERS IN BRACKETS)					
1. (**0**) POST DOCTORAL SCHOLARS					
2. (**0**) OTHER PROFESSIONALS (TECHNICIAN, PROGRAMMER, ETC.)					
3. (**0**) GRADUATE STUDENTS					
4. (**0**) UNDERGRADUATE STUDENTS					
5. (**0**) SECRETARIAL - CLERICAL (IF CHARGED DIRECTLY)					
6. (**0**) OTHER					
TOTAL SALARIES AND WAGES (A + B)					
C. FRINGE BENEFITS (IF CHARGED AS DIRECT COSTS)					
TOTAL SALARIES, WAGES AND FRINGE BENEFITS (A + B + C)					
D. EQUIPMENT (LIST ITEM AND DOLLAR AMOUNT FOR EACH ITEM EXCEEDING $5,000.)					
TOTAL EQUIPMENT				**0**	
E. TRAVEL 1. DOMESTIC (INCL. U.S. POSSESSIONS)				**0**	
2. INTERNATIONAL				**0**	
F. PARTICIPANT SUPPORT COSTS					
1. STIPENDS $ **0**					
2. TRAVEL **0**					
3. SUBSISTENCE **0**					
4. OTHER **0**					
TOTAL NUMBER OF PARTICIPANTS (**0**) TOTAL PARTICIPANT COSTS				**0**	
G. OTHER DIRECT COSTS					
1. MATERIALS AND SUPPLIES				**0**	
2. PUBLICATION COSTS/DOCUMENTATION/DISSEMINATION				**0**	
3. CONSULTANT SERVICES				**0**	
4. COMPUTER SERVICES				**0**	
5. SUBAWARDS				**0**	
6. OTHER				**0**	
TOTAL OTHER DIRECT COSTS				**0**	
H. TOTAL DIRECT COSTS (A THROUGH G)				(b)(4)	
I. INDIRECT COSTS (F&A)(SPECIFY RATE AND BASE)					
TOTAL INDIRECT COSTS (F&A)				**10,494**	
J. TOTAL DIRECT AND INDIRECT COSTS (H + I)				**28,433**	
K. FEE				**0**	
L. AMOUNT OF THIS REQUEST (J) OR (J MINUS K)				**28,433**	

M. COST SHARING PROPOSED LEVEL $ **0** AGREED LEVEL IF DIFFERENT $

PI/PD NAME
Benjamin Kravitz
ORG. REP. NAME*
Tammy Custer

FOR NSF USE ONLY		
INDIRECT COST RATE VERIFICATION		
Date Checked	Date Of Rate Sheet	Initials - ORG

* ELECTRONIC SIGNATURES REQUIRED FOR REVISED BUDGET

Budget Justification
What are the fundamental limits / trade-offs of stratospheric aerosol geoengineering?
Indiana University (PI: Ben Kravitz)

Salary

The PI's summer salary is calculated at (b)(4): (b)(6) of his actual salary at Indiana University. PI academic year salary in year 1 is based on anticipated 2020-21 salary, with (b)(4): (b)(6) increases in years 2 and 3. Total salary requested is (b)(4): (b)(6)

For NSF: Indiana University defines the term "year" as the university fiscal year (July-June) for purposes of the NSF limitation on salary compensation for senior personnel.

Fringe Benefits

Fringe benefit rates are set by the University and approved by the Board of Trustees. The summer fringe benefit rate is 39.11%, with 5% increases in years 2 and 3. Total fringe requested is S5,044 over three years.

Travel

None budgeted

Materials and Supplies

None budgeted

Other Direct Costs

None budgeted

Indirect Costs

Indirect cost is calculated at a rate of (b)(4) of the modified total direct cost, which excludes fee remissions, equipment over S5,000, and subcontract amounts in excess of the first $25,000. This rate has been approved by the Department of Health and Human Services on May 22, 2019.

The amount of indirect cost requested is (b)(4) in the first year, with increases per the salary and fringe changes outlined above, for a total of (b)(4)

NSF CURRENT AND PENDING SUPPORT

PI/co-PI/Senior Personnel: Kravitz, Ben

PROJECT/PROPOSAL CURRENT SUPPORT

1. Project/Proposal Title: Dynamical Downscaling for Indiana in the 21st Century

   Proposal/Award Number (if available):

   Source of Support: Indiana University PfEC Grand Challenge Initiative

   Primary Place of Performance: Indiana University

   Project/Proposal Support Start Date (if available): 2019/10

   Project/Proposal Support End Date (if available): 2021/09

   Total Award Amount (including Indirect Costs): $94,433

   Person-Month(s) (or Partial Person-Months) Per Year Committed to the Project:

Year	Person-months per year committed
2019	(b)(4): (b)(6)
2020	
2021	

2. Project/Proposal Title: Marine Sky Brightening: Prospects and Consequences

   Proposal/Award Number (if available): UPNL0001

   Source of Support: National Center for Atmospheric Research

   Primary Place of Performance: Indiana University

   Project/Proposal Support Start Date (if available): 2019/10

   Project/Proposal Support End Date (if available): 2021/09

   Total Award Amount (including Indirect Costs): $0

   Person-Month(s) (or Partial Person-Months) Per Year Committed to the Project:

Year	Person-months per year committed
2020	(b)(4): (b)(6)

3. Project/Proposal Title: EAGER: Marine Sky Brightening: Prospects and Consequences

Proposal/Award Number (if available): CBET-1931641

Source of Support: National Science Foundation

Primary Place of Performance: Indiana University

Project/Proposal Support Start Date (if available): 2019/07

Project/Proposal Support End Date (if available): 2021/06

Total Award Amount (including Indirect Costs): $299,994

Person-Month(s) (or Partial Person-Months) Per Year Committed to the Project:

Year	Person-months per year committed		
2020		(b)(4): (b)(6)	
2021			

PROJECT/PROPOSAL PENDING SUPPORT

(b)(4): (b)(6)

(b)(4): (b)(6)

Current and Pending Support
(See GPG Section II.D.8 for guidance on information to include on this form.)

The following information should be provided for each investigator and other senior personnel. Failure to provide this information may delay consideration of this proposal.

Investigator: **MacMartin, Douglas Graham**	Other agencies (including NSF) to which this proposal has been/will be submitted.

Support: X Current Pending Submission Planned in Near Future *Transfer of Support

Project/Proposal Title: **INTRODUCING A DESIGN ELEMENT INTO STRATOSPHERIC AEROSOL GEOENGINEERING**

Source of Support: **National Science Foundation**

Total Award Amount: **$299,529.00** Total Award Period Covered: **01-Apr-2018 to 31-Mar-2021**

Location of Project: **Cornell University**

Person-Months Per Year Committed to the Project: (b)(4): (b)(6)

(b)(4): (b)(6)

Facilities, Equipment and Other Resources

Sufficient office space is available at Cornell for project personnel. This project does not require any equipment beyond computer simulation time. Computational resources (on Cheyenne) at NCAR for running climate model simulations will be requested after the proposal is awarded. This project will require a large allocation request, but care has been taken in prioritizing simulations to ensure that the total resources required are reasonable; if the allocation provided is smaller than requested then additional reprioritization will be necessary (e.g. reducing the number of ensemble members of simulations). The computational requirements will be spread roughly evenly across the 3-year duration of the project.

This project will also benefit from unfunded collaboration with Jadwiga (Yaga) Richter at the National Center for Atmospheric Research (NCAR), an expert in stratospheric dynamics. In addition to expertise that may be valuable in understanding aspects associated with stratospheric circulation and changes, NCAR will provide support with running the Whole Atmosphere Community Climate Model version of the Community Earth System Model, CESM2(WACCM6), and assist with the interpretation of the findings. Anticipating that portions of the graduate student's work may be best performed at NCAR, a graduate student may be hosted for focused research visits at NCAR as needed. These tasks fall under the NCAR mission "to support, enhance and extend the capabilities of the university community and the broader scientific community", and can be performed without additional funding from this NSF project. The proposed work is also of interest to NCAR and it is advancing the capabilities of the Community Earth System Model.

Data Management Plan

Types of data

The research in this proposal will result in climate model simulation output that will be valuable for the broader research community, including those in the developing world. Some analysis code may be generated throughout the course of the research.

Data and metadata standards

Simulation output will be in the form of netcdf files. An index into the available simulation output will be created in an open file format.

Policies for access and sharing

Any broadly useful analysis code will be freely available and posted on the PI's website, http://climate-engineering.mae.cornell.edu/, along with the index into available simulation output. Full 3D climate model simulation output will be multiple terabytes, and will be archived at NCAR and on external hard drives and available to other researchers on request (if there is sufficient interest, these could be made public on the Earth System Grid). Summary data (e.g., 2D surface climate fields, aerosol fields) sufficient for most impact research by other groups, and for other researchers to compare using their own climate models, will be made available on the PI's website.

Policies and provisions for re-use, re-distribution

Data will be made available as soon as possible; at least when publications associated with the research have been submitted.

Plans for archiving and preservation of access

As climate models improve and ideas for designing geoengineering mature, we do not foresee that the direct simulation output itself will need to be archived for more than 5 years. Computer modeling code will be archived indefinitely on the PI's website.

Withheld pursuant to exemption

(b)(4) ; (b)(6)

of the Freedom of Information and Privacy Act

Project Report Printer Friendly Version 2024-2565 [illegible] "UNCLASSIFIED" 7/16/2025 Click here to print

Preview of Award 2038246 - Annual Project Report

Cover

Federal Agency and Organization Element to Which Report is Submitted:	**4900**
Federal Award or Other Identifying Number Assigned by Agency:	**2038246**
Project Title:	**Fundamental limits and trade-offs of stratospheric aerosol geoengineering**
PD/PI Name:	**Douglas G MacMartin, Principal Investigator** **Benjamin Kravitz, Co-Principal Investigator**
Recipient Organization:	**Cornell University**
Project/Grant Period:	**01/01/2021 - 12/31/2024**
Reporting Period:	**01/01/2023 - 12/31/2023**
Submitting Official (if other than PD\PI):	**Douglas G MacMartin** **Principal Investigator**
Submission Date:	**01/05/2024**
Signature of Submitting Official (signature shall be submitted in accordance with agency specific instructions)	**Douglas G MacMartin**

Accomplishments

*** What are the major goals of the project?**

Geoengineering (in particular we focus on stratospheric aerosol injection) would cool the climate, reducing some impacts from climate change, but it would not simply reverse changes due to increased atmospheric greenhouse gas concentrations, leading to residual changes. These changes, however, depend on how it is done – particularly what latitudes or seasons that aerosols are added to the stratosphere. The main goal of the project is to understand what geoengineering can and cannot do. This will help us understand which decisions matter, which uncertainties need to be resolved or managed, fundamental limits to how well it can compensate for climate change, and where any trade-offs might be. All of these are essential for informing future decisions about whether and how to deploy geoengineering.

*** What was accomplished under these goals and objectives (you must provide information for at least one of the 4 categories below)?** 2024-256F 00000000869 "UNCLASSIFIED" 7/16/2025

Major Activities:

There are a number of significant activities from this project, the first 3 listed below were completed in previous years and reported, but included here for completeness and context; the last 3 below have been conducted since the last annual report.

(i) We have integrated previously conducted geoengineering simulations that use different combinations of locations (latitudes) and times of year (season) to achieve different sets of climate objectives with simulations at many different latitudes and seasons to estimate the total number of independent "design" degrees of freedom available; (ii) building on that, we have designed and conducted a set of simulations that collectively span a complete range of independent strategies; these include four different hemispherically-symmetric strategies including one more polar-focused, as well as an Arctic-focused strategy, and a default multi-objective strategy considered in previous model version, as well as an updated and longer set of fixed-injection-rate cases, (iii) we have also designed and completed simulations that consider a range of different plausible future deployment scenarios, involving in particular different amounts of cooling, but also different start dates and inconsistencies in deployment; this both helps assess nonlinearities and transients as well as being valuable on its own for informing dependence of impacts on scenario, (iv) we have conducted some preliminary optimization for different climate metrics to assess both how much the strategy depends on the metric chosen as well as how much "better" one might be able to achieve than with current strategies, (v) the simulations conducted have been used already to look at some impact analyses (such as risks from Antarctic ice melt), and finally (vi) we have collaborated with other climate modeling centers to conduct similar analyses, resulting in several papers with U. Exeter; simulations conducted as part of this project have motivated the design of both scenarios and strategies for the next set of Geoengineering Model Intercomparison Project (GeoMIP) simulations.

Specific Objectives:

Significant Results:

The first 3 significant results described here are largely unchanged from the previous report; we add a fourth below. (1) For global cooling of up to 1.5°C, there are approximately 6-8 independent degrees of freedom for SAI that would lead to detectably different climate outcomes. These include injection at 30N, 15N, equator, 15S, 30S, as well as spring injection at 60N and 60S. This also means that as many as 6-8 independent climate objectives might be simultaneously managed; previous studies have considered at most 3, suggesting both that there is considerable scope for exploring distinct strategies, and that this scope is "small" enough that this exploration is feasible. (2) Different strategies involving different combinations of these latitudes yield different outcomes not only in surface temperature and precipitation, but on Arctic sea ice, hurricane indices, ITCZ, Antarctic sea ice risks (this particular analysis is new relative to the previous annual report), etc. (3) Arctic-focused and polar-focused strategies are plausible, with injection at lower altitude but high latitude; these preferentially cool at higher latitude with less tropical cooling, yielding greater efficiency for some impacts but different trade-offs relative to other strategies. (This last one is also particularly noteworthy because it would be easier to deploy at lower altitude, and many risks people care about are at high latitude) (4) A hemispherically-symmetric strategy that injects equal amounts at roughly 30N and 30S (15N and 15S might do as well) is simpler to implement in other models and is not too sub-optimal relative to more complicated strategies for many metrics (in particular, it roughly maintains equator-to-pole temperature gradients without formally needing to control for them)

Key

Key outcomes or Other achievements:

Results from this project have led to collaboration with U. Exeter to conduct a subset of similar simulations in the UKESM model, and are serving as the basis for designing the next round of GeoMIP simulations. Preliminary analyses are also being conducted with policy experts on different scenarios using these simulations.

Two PhD theses were supported or partially supported by this award; Yan Zhang and Walker Lee.

*** What opportunities for training and professional development has the project provided?**

The project has directly supported the research of two graduate students in engineering; work related to this project has also involved two postdoctoral research associates with a background in climate science (one of whom is now faculty at Cornell in Atmospheric Science, the other a researcher at NOAA). This provides a learning experience for both; the graduate students benefit from the expertise of the postdocs, and the postdocs gain an appreciation for engineering design principles, as well as some experience in mentoring graduate students. The graduate students have learned how to run CESM(WACCM), analyze the output, write papers, and prepare the results for presentations at conferences. Both students have graduated; Walker Lee is currently at NCAR working on design and feedback for Marine Cloud Brightening

*** Have the results been disseminated to communities of interest? If so, please provide details.**

The first paper from this award (partly supported by a previous NSF award) was published early in 2022 in Earth Systems Dynamics; a paper on scenarios was published in PNAS in 2022; a paper on Arctic-focused approach published in Earth's Future in 2023, a paper comparing multiple strategies published in Atm. Chem. Phys. and another under review. Results using simulations that were generated as part of this research have been published in several papers, and there are a further two papers (one published, one in review) with the UKESM climate model. All work is being presented at conferences (e.g., at AGU fall meeting in 2021 and 2022, and Gordon Research Conference in 2022; some results have been used in a presentation at Arctic Circle meeting; results will be highlighted in two talks at the 2024 GRC in February). Work on scenarios and strategies was discussed in a meeting held at NCAR focusing on scenario design; this research was also discussed at an IAI-sponsored international meeting in Jamaica. Research results are also disseminated to the research community through geoengineering email lists. Most important of all, simulations have been made available and are being used by other researchers exploring impacts including those in the developing world.

*** What do you plan to do during the next reporting period to accomplish the goals?**

A final paper is being drafted that will explore the potential for optimization to identify new strategies, assess fundamental limits and trade-offs, and evaluate how different the strategy and outcome is depending on what metrics are being optimized; a draft of this paper appears as a chapter in Yan Zhang's PhD thesis. The implications of all of this work will be strengthened through a small workshop being planned to engage more governance and policy community. We will continue to be engaged in a larger and essential discussion on scenario design for geoengineering.

Products

Books

Book Chapters

2024-256F 00000000869 "UNCLASSIFIED" 7/16/2025

Inventions

Journals or Juried Conference Papers

View all journal publications currently available in the for this award.

The results in the NSF Public Access Repository will include a comprehensive listing of all journal publications recorded to date that are associated with this award.

Visioni, D. and Bednarz, E. M. and MacMartin, D. G. and Kravitz, B. and Goddard, P. B.. (2023). The Choice of Baseline Period Influences the Assessments of the Outcomes of Stratospheric Aerosol Injection. *Earth's Future*. 11 (8) . Status = Added in NSF-PAR Federal Government's License = Acknowledged. (Completed by MacMartin, null on 01/04/2024)

Goddard, P. B. and Kravitz, B. and MacMartin, D. G. and Visioni, D. and Bednarz, E. M. and Lee, W. R.. (2023). Stratospheric Aerosol Injection Can Reduce Risks to Antarctic Ice Loss Depending on Injection Location and Amount. *Journal of Geophysical Research: Atmospheres*. 128 (22) . Status = Added in NSF-PAR Federal Government's License = Acknowledged. (Completed by MacMartin, null on 01/04/2024)

Bednarz, Ewa M. and Butler, Amy H. and Visioni, Daniele and Zhang, Yan and Kravitz, Ben and MacMartin, Douglas G.. (2023). Injection strategy â€“ a driver of atmospheric circulation and ozone response to stratospheric aerosol geoengineering. *Atmospheric Chemistry and Physics*. 23 (21) . Status = Added in NSF-PAR Federal Government's License = Acknowledged. (Completed by MacMartin, Douglas on 01/04/2024)

Henry, Matthew and Haywood, Jim and Jones, Andy and Dalvi, Mohit and Wells, Alice and Visioni, Daniele and Bednarz, Ewa M. and MacMartin, Douglas G. and Lee, Walker and Tye, Mari R.. (2023). Comparison of UKESM1 and CESM2 simulations using the same multi-target stratospheric aerosol injection strategy. *Atmospheric Chemistry and Physics*. 23 (20) . Status = Added in NSF-PAR Federal Government's License = Acknowledged. (Completed by MacMartin, null on 01/04/2024)

Lee, Walker Raymond and MacMartin, Douglas G. and Visioni, Daniele and Kravitz, Ben and Chen, Yating and Moore, John C. and Leguy, Gunter and Lawrence, David M. and Bailey, David A.. (2023). Highâ€ Latitude Stratospheric Aerosol Injection to Preserve the Arctic. *Earth's Future*. 11 (1) . Status = Added in NSF-PAR Federal Government's License = Acknowledged. (Completed by MacMartin, Douglas on 01/04/2024)

Bednarz, Ewa M. and Visioni, Daniele and Butler, Amy H. and Kravitz, Ben and MacMartin, Douglas G. and Tilmes, Simone. (2023). Potential Nonâ€ Linearities in the High Latitude Circulation and Ozone Response to Stratospheric Aerosol Injection. *Geophysical Research Letters*. 50 (22) . Status = Added in NSF-PAR Federal Government's License = Acknowledged. (Completed by MacMartin, null on 01/04/2024)

Visioni, Daniele and MacMartin, Douglas G. and Kravitz, Ben and Lee, Walker and Simpson, Isla R. and Richter, Jadwiga H.. (2020). Reduced Poleward Transport Due to Stratospheric Heating Under Stratospheric Aerosols Geoengineering. *Geophysical Research Letters*. 47 (17) . Status = Added in NSF-PAR Federal Government's License = Acknowledged. (Completed by Kravitz, null on 10/21/2021)

MacMartin, D. G. and Visioni, D. and Kravitz, B. and Richter, J.H. and Felgenhauer, T. and Lee, W. R. and Morrow, D. R. and Parson, E. A. and Sugiyama, M.. (2022). Scenarios for modeling solar radiation modification. *Proceedings of the National Academy of Sciences*. 119 (33) . Status = Added in NSF-PAR Federal Government's License = Acknowledged. (Completed by MacMartin, Douglas on 12/08/2022)

Zhang, Yan and MacMartin, Douglas G. and Visioni, Daniele and Kravitz, Ben. (2022). How large is the design space for stratospheric aerosol geoengineering?. *Earth System Dynamics*. 13 (1) 201 to 217. Status = Added in NSF-PAR Federal Government's License = Acknowledged. (Completed by MacMartin, Douglas on 12/08/2022)

Bednarz, Ewa M. and Visioni, Daniele and Banerjee, Antara and Braesicke, Peter and Kravitz, Ben and MacMartin, Douglas G.. (2022). The Overlooked Role of the Stratosphere Under a Solar Constant Reduction. *Geophysical Research Letters*. 49 (12) . Status = Added in NSF-PAR Federal Government's License = Acknowledged. (Completed by MacMartin, Douglas on 12/08/2022)

Visioni, Daniele and MacMartin, Douglas G. and Kravitz, Ben and Richter, Jadwiga H. and Tilmes, Simone and Mills, Michael J.. (2020). Seasonally Modulated Stratospheric Aerosol Geoengineering Alters the Climate Outcomes. *Geophysical Research Letters*. 47 (12) . Status = Added in NSF-PAR Federal Government's License = Acknowledged. (Completed by Kravitz, null on 10/21/2021)

Licenses

Other Conference Presentations / Papers

Other Products

Other Publications

Patent Applications

Technologies or Techniques

Thesis/Dissertations

Yan Zhang. *DESIGN SPACE EXPLORATION FOR STRATOSPHERIC AEROSOL INJECTION.* (2023). Cornell University. Acknowledgement of Federal Support = No

Walker Lee. *Exploring, Mapping, and Expanding the Design Space of Climate Intervention via Stratospheric Aerosol Injection.* (2023). Cornell University. Acknowledgement of Federal Support = No

Websites or Other Internet Sites

Participants/Organizations

What individuals have worked on the project?

Name	Most Senior Project Role	Nearest Person Month Worked
(b)(6)	PD/PI	(b)(4): (b)(6)
	Co PD/PI	
	Faculty	
	Graduate Student (research assistant)	
	Graduate Student (research assistant)	

Full details of individuals who have worked on the project:

Douglas G MacMartin
Email: dgm224@cornell.edu
Most Senior Project Role: PD/PI
Nearest Person Month Worked: (b)(6)
Contribution to the Project: Overall project management, supervising postdocs and students, editing papers
Funding Support: Related funding from Atkinson Center for a Sustainable Future (supporting further analysis of simulations developed under NSF funding)
Change in active other support: Yes
International Collaboration: Yes, United Kingdom
International Travel: No

Benjamin Kravitz
Email: bkravitz@iu.edu
Most Senior Project Role: Co PD/PI
Nearest Person Month Worked: (b)(6)
Contribution to the Project: Support on project direction, coding of feedback algorithms; support on paper writing
Funding Support: None directly supporting this effort
Change in active other support: Yes
International Collaboration: No
International Travel: No

Daniele Visioni
Email: dv224@cornell.edu 2024-256F 00000000869 "UNCLASSIFIED" 7/16/2025
Most Senior Project Role: Faculty
Nearest Person Month Worked: (b)(4):
Contribution to the Project: Assisted graduate students in running climate models, assisted graduate students in writing papers, but was only supported by NSF funding early in the project
Funding Support: Cornell Atkinson Center for a Sustainable Future
International Collaboration: No
International Travel: No

(b)(6)

Most Senior Project Role: Graduate Student (research assistant)
Nearest Person Month Worked: (b)(4):
Contribution to the Project: Developing simulations of Arctic injection in particular (and Arctic+Antarctic), analyzing, and writing papers
Funding Support: Also supported by Cornell Atkinson Center for a Sustainable Future for related research on Arctic impacts and processes
International Collaboration: Yes, United Kingdom
International Travel: No

(b)(6)

Most Senior Project Role: Graduate Student (research assistant)
Nearest Person Month Worked: (b)(4): (b)(6)
Contribution to the Project: Designing simulations, conducting simulations, analyzing simulations, writing papers
Funding Support: Summer salary came from Cornell Atkinson Center for Sustainable Futures
International Collaboration: No
International Travel: No

What other organizations have been involved as partners?

Nothing to report.

Were other collaborators or contacts involved? If so, please provide details.

Matthew Henry, Alice Wells, Jim Haywood, and Andy Jones at U. Exeter in UK, have been conducting similar simulations in the UKESM climate model. Ewa Bednarz and Amy Butler at NOAA have been conducting analysis using our simulations and have helped graduate students with interpretations and analysis. Paul Goddard at Indiana University used NSF-funded simulations to look at impacts on Antarctic. None of these were funded by NSF (but Cornell PI and Cornell grad students supported by NSF were involved in the collaboration, and IU PI for work by P. Goddard)

Impacts

What is the impact on the development of the principal discipline(s) of the project?

We are demonstrating the importance of strategy (and the scenario as well) for influencing outcomes from SAI – that it cannot meaningfully be considered as “one thing” and that one cannot simply pick some ad hoc choice for injection strategy; this then provides guidance for how geoengineering can/should be simulated. It is becoming well recognized now that outcomes depend on strategy, and that there are multiple plausible approaches for a hypothetical future deployment of SAI with different sets of outcomes. This recognition is critical for research not only into outcomes, but also uncertainty. Other modeling groups have now started looking at design aspects, duplicating strategies we developed in UKESM for example; strategies developed herein will serve as the basis for new GeoMIP simulations. In

addition to understanding strategies that optimize for different metrics, it is also important to evaluate how much penalty there is for considering simpler strategies that would be easier to simulate in a large multi-model intercomparison. The design-based approach is also being planned for research into marine cloud brightening.

What is the impact on other disciplines?

We have created a dataset of geoengineering simulations that can and are being used by numerous other disciplines (for example, to assess various impacts). Understanding the extent to which there are inherent trade-offs between different objectives, or to what extent there are broadly "best" ways of deploying that would simultaneously satisfy many actors, is essential for informing the development of governance in this area. Understanding the range of different plausible strategies is similarly essential, e.g., the potential for an "Arctic-focused" strategy that could be deployed without requiring development of new aircraft, or more "polar-focused" strategies that could target Antarctic impacts more effectively.

What is the impact on the development of human resources?

Graduate students trained in engineering are being cross-trained in climate science; similarly postdocs (not supported by this award but part of our research group) trained in climate science are exposed to engineering design ideas; this thus builds interdisciplinary expertise.

What was the impact on teaching and educational experiences?

None yet; but results will be incorporated into courses on geoengineering.

What is the impact on physical resources that form infrastructure?

Nothing to report.

What is the impact on institutional resources that form infrastructure?

Nothing to report.

What is the impact on information resources that form infrastructure?

Nothing to report.

What is the impact on technology transfer?

Nothing to report.

What is the impact on society beyond science and technology?

This project is ultimately aimed at providing decision support for geoengineering. The limits and tradeoffs in geoengineering are essential pieces of information for deciding if, when, where, and how geoengineering might be done in the future. The results from our project could directly inform that decision process, as well as the development of international governance capacity to support that decision process, and the methods we are demonstrating will enable other researchers to pursue similar lines of investigation.

What percentage of the award's budget was spent in a foreign country?

Nothing to report.

Changes/Problems

Changes in approach and reason for change

Nothing to report.

Actual or Anticipated problems or delays and actions or plans to resolve them

One year extension was granted to finalize final paper (graduate student graduated and is working, so progress somewhat slower) and to plan and hold small workshop.

Changes that have a significant impact on expenditures

Nothing to report.

Significant changes in use or care of human subjects

Nothing to report.

Significant changes in use or care of vertebrate animals

Nothing to report.

Significant changes in use or care of biohazards

Nothing to report.

Change in primary performance site location

Nothing to report.

Project Report Printer Friendly Version 2024-2655 [illegible] "UNCLASSIFIED" 7/16/2025 Click here to print

Preview of Award 2038246 - Annual Project Report

Cover

Federal Agency and Organization Element to Which Report is Submitted:	**4900**
Federal Award or Other Identifying Number Assigned by Agency:	**2038246**
Project Title:	**Fundamental limits and trade-offs of stratospheric aerosol geoengineering**
PD/PI Name:	**Douglas G MacMartin, Principal Investigator** **Benjamin Kravitz, Co-Principal Investigator**
Recipient Organization:	**Cornell University**
Project/Grant Period:	**01/01/2021 - 12/31/2023**
Reporting Period:	**01/01/2022 - 12/31/2022**
Submitting Official (if other than PD\PI):	**Douglas G MacMartin** **Principal Investigator**
Submission Date:	**12/15/2022**
Signature of Submitting Official (signature shall be submitted in accordance with agency specific instructions)	**Douglas G MacMartin**

Accomplishments

*** What are the major goals of the project?**

Geoengineering (in particular we focus on stratospheric aerosol injection) would cool the climate, reducing some impacts from climate change, but it would not simply reverse changes due to increased atmospheric greenhouse gas concentrations, leading to residual changes. These changes, however, depend on how it is done – particularly what latitudes or seasons that aerosols are added to the stratosphere. The main goal of the project is to understand what geoengineering can and cannot do. This will help us understand which decisions matter, which uncertainties need to be resolved or managed, fundamental limits to how well it can compensate for climate change, and where any trade-offs might be. All of these are essential for informing future decisions about whether and how to deploy geoengineering.

*** What was accomplished under these goals and objectives (you must provide information for at least one of the 4 categories below)?** 2024-256F 00000000868 "UNCLASSIFIED" 7/16/2025

Major Activities:

(i) We have integrated previously conducted geoengineering simulations that use different combinations of locations (latitudes) and times of year (season) to achieve different sets of climate objectives with simulations at many different latitudes and seasons to estimate the total number of independent "design" degrees of freedom available; (ii) building on that, we have designed and conducted a set of simulations that collectively span a complete range of independent strategies; these include four different hemispherically-symmetric strategies including one more polar-focused, as well as an Arctic-focused strategy, and a default multi-objective strategy considered in previous model version, as well as an updated and longer set of fixed-injection-rate cases and (iii) we have also designed and completed simulations that consider a range of different plausible future deployment scenarios, involving in particular different amounts of cooling, but also different start dates and inconsistencies in deployment; this both helps assess nonlinearities and transients as well as being valuable on its own for informing dependence of impacts on scenario.

Specific Objectives:

Significant Results:

(1) For global cooling of up to 1.5°C, there are approximately 6-8 independent degrees of freedom for SAI that would lead to detectably different climate outcomes. These include injection at 30N, 15N, equator, 15S, 30S, as well as spring injection at 60N and 60S. This also means that as many as 6-8 independent climate objectives might be simultaneously managed; previous studies have considered at most 3, suggesting both that there is considerable scope for exploring distinct strategies, and that this scope is "small" enough that this exploration is feasible. (2) Different strategies involving different combinations of these latitudes yield different outcomes not only in surface temperature and precipitation, but on Arctic sea ice, hurricane indices, ITCZ, etc. (3) Arctic-focused and polar-focused strategies are plausible, with injection at lower altitude but high latitude; these preferentially cool at higher latitude with less tropical cooling, yielding greater efficiency for some impacts but different trade-offs relative to other strategies. (This last one is also particularly noteworthy because it would be easier to deploy at lower altitude, and many risks people care about are at high latitude)

Key outcomes or Other achievements:

*** What opportunities for training and professional development has the project provided?**

The project has directly supported the research of two graduate students in engineering; work related to this project has also involved two postdoctoral research associates with a background in climate science. This provides a learning experience for both; the graduate students benefit from the expertise of the postdocs, and the postdocs gain an appreciation for engineering design principles, as well as some experience in mentoring graduate students. The graduate students have learned how to run CESM(WACCM), analyze the output, write papers, and prepare the results for presentations at conferences.

*** Have the results been disseminated to communities of interest? If so, please provide details.**

The first paper from this award (partly supported by a previous NSF award) was published early in 2022 in Earth Systems Dynamics; a paper on scenarios was published in PNAS in 2022; a paper on Arctic-focused approach is currently under review and a paper comparing multiple strategies is nearing submission. All work is being presented at conferences (e.g., at AGU fall meeting in 2021 and 2022, and Gordon Research Conference in 2022; some results have been used in a presentation at Arctic Circle meeting). Work on scenarios and strategies was discussed in a meeting held at NCAR focusing on scenario design; this research was also discussed at an IAI-sponsored international meeting in Jamaica. Research results are also disseminated to the research community through geoengineering email lists. Most important of all, simulations have been made available and are being used by other researchers exploring impacts including those in the developing world.

*** What do you plan to do during the next reporting period to accomplish the goals?**

We will continue to analyze the simulations that span a range of different possible strategies (corresponding to different choices for injection latitude, season, and the goals) , and in particular will explore the potential for optimization to identify new strategies, assess fundamental limits and trade-offs, and evaluate how different the strategy and outcome is depending on what metrics are being optimized, and will document all results in scientific papers. We will continue to be engaged in a larger and essential discussion on scenario design for geoengineering.

Supporting Files

Filename	Description	Uploaded By	Uploaded On
Revised_Manuscript.pdf	Ã¢Â€Â¢ Lee, W.R., D.G. MacMartin, D. Visioni, B. Kravitz, Y. Chen, J.C. Moore, G. Leguy, D.M. Lawrence and D.A. Bailey, Ã¢Â€ÂœHigh-latitude stratospheric aerosol injection to preserve the ArcticÃ¢Â€Â , submitted, EarthÃ¢Â€Â™s Future	Douglas Macmartin	12/07/2022

Products

Books

Book Chapters

Inventions

Journals or Juried Conference Papers

View all journal publications currently available in the for this award.

The results in the NSF Public Access Repository will include a comprehensive listing of all journal publications recorded to date that are associated with this award.

Visioni, Daniele and MacMartin, Douglas G. and Kravitz, Ben and Lee, Walker and Simpson, Isla R. and Richter, Jadwiga H.. (2020). Reduced Poleward Transport Due to Stratospheric Heating Under Stratospheric Aerosols Geoengineering. *Geophysical Research Letters*. 47 (17) . Status = Added in NSF-PAR Federal Government's License = Acknowledged. (Completed by Kravitz, null on 10/21/2021)

MacMartin, D. G. and Visioni, D. and Kravitz, B. and Richter, J.H. and Felgenhauer, T. and Lee, W. R. and Morrow, D. R. and Parson, E. A. and Sugiyama, M.. (2022). Scenarios for modeling solar radiation modification. *Proceedings of the National Academy of Sciences*. 119 (33) . Status = Added in NSF-PAR Federal Government's License = Acknowledged. (Completed by MacMartin, Douglas on 12/08/2022)

Zhang, Yan and MacMartin, Douglas G. and Visioni, Daniele and Kravitz, Ben. (2022). How large is the design space for stratospheric aerosol geoengineering?. *Earth System Dynamics*. 13 (1) 201 to 217. Status = Added in NSF-PAR Federal Government's License = Acknowledged. (Completed by MacMartin, Douglas on 12/08/2022)

Bednarz, Ewa M. and Visioni, Daniele and Banerjee, Antara and Braesicke, Peter and Kravitz, Ben and MacMartin, Douglas G.. (2022). The Overlooked Role of the Stratosphere Under a Solar Constant Reduction. *Geophysical Research Letters*. 49 (12) . Status = Added in NSF-PAR Federal Government's License = Acknowledged. (Completed by MacMartin, Douglas on 12/08/2022)

Visioni, Daniele and MacMartin, Douglas G. and Kravitz, Ben and Richter, Jadwiga H. and Tilmes, Simone and Mills, Michael J.. (2020). Seasonally Modulated Stratospheric Aerosol Geoengineering Alters the Climate Outcomes. *Geophysical Research Letters*. 47 (12) . Status = Added in NSF-PAR Federal Government's License = Acknowledged. (Completed by Kravitz, null on 10/21/2021)

Zhang, Y., D. G. MacMartin, D. Visioni, and B. Kravitz, â€œHow large is the design space for stratospheric aerosol geoengineering?â€ , Earth System Dynamics, 13, 201â€“217, 2022. https://doi.org/10.5194/esd-13-201-2022. Status = PUBLISHED.

Licenses

Other Conference Presentations / Papers

Other Products

Other Publications

Patent Applications

2024-256F 00000000868 "UNCLASSIFIED" 7/16/2025

Technologies or Techniques

Thesis/Dissertations

Websites or Other Internet Sites

Participants/Organizations

What individuals have worked on the project?

Name	Most Senior Project Role	Nearest Person Month Worked
	PD/PI	(b)(4): (b)(6)
	Co PD/PI	
	Postdoctoral (scholar, fellow or other postdoctoral position)	
(b)(6)	Graduate Student (research assistant)	
	Graduate Student (research assistant)	

Full details of individuals who have worked on the project:

Douglas G MacMartin
Email: dgm224@cornell.edu
Most Senior Project Role: PD/PI
Nearest Person Month Worked: (b)(4): (b)(6)
Contribution to the Project: Overall guidance and supervision of graduate students
Funding Support: None
Change in active other support: No
International Collaboration: No
International Travel: No

Benjamin Kravitz
Email: bkravitz@iu.edu
Most Senior Project Role: Co PD/PI
Nearest Person Month Worked: (b)(4): (b)(6)
Contribution to the Project: Participating in discussions of direction, supporting writing of papers
Funding Support: None
Change in active other support: No
International Collaboration: No
International Travel: No

Daniele Visioni
Email: dv224@cornell.edu
Most Senior Project Role: Postdoctoral (scholar, fellow or other postdoctoral position)
Nearest Person Month Worked: (b)(4): (b)(6)
Contribution to the Project: Assisted graduate students in running climate models, assisted graduate students in writing papers.

Funding Support: Cornell Atkinson Center for a Sustainable Future
International Collaboration: No
International Travel: No

Walker Lee
Email: wl644@cornell.edu
Most Senior Project Role: Graduate Student (research assistant)
Nearest Person Month Worked: (b)(4); (b)(6)
Contribution to the Project: Developing simulations of Arctic injection in particular (and Arctic+Antarctic), analyzing, and writing papers
Funding Support: Also supported by Cornell Atkinson Center for a Sustainable Future for related research on Arctic impacts and processes
International Collaboration: No
International Travel: No

Yan Zhang
Email: yz2545@cornell.edu
Most Senior Project Role: Graduate Student (research assistant)
Nearest Person Month Worked: (b)(4); (b)(6)
Contribution to the Project: Designing simulations, conducting simulations, analyzing simulations, writing papers
Funding Support: Summer salary came from Cornell Atkinson Center for Sustainable Futures
International Collaboration: No
International Travel: No

What other organizations have been involved as partners?

Nothing to report.

Were other collaborators or contacts involved? If so, please provide details.

Jadwiga (Yaga) Richter at NCAR

Impacts

What is the impact on the development of the principal discipline(s) of the project?

We are demonstrating the importance of strategy (and the scenario as well) for influencing outcomes from SAI – that it cannot meaningfully be considered as "one thing" and that one cannot simply pick some ad hoc choice for injection strategy; this then provides guidance for how geoengineering can/should be simulated. This is critical for research not only into outcomes, but also uncertainty. Other modeling groups have now started looking at design aspects, duplicating strategies we developed in UKESM for example. In addition to understanding strategies that optimize for different metrics, it is also important to evaluate how much penalty there is for considering simpler strategies that would be easier to simulate in a large multi-model intercomparison (e.g., future GeoMIP)

What is the impact on other disciplines?

We are creating a dataset of geoengineering simulations that can be used by numerous other disciplines (for example, to assess various impacts). Understanding the extent to which there are inherent trade-offs between different objectives, or to what extent there are broadly "best" ways of deploying that would simultaneously satisfy many actors, is essential for informing the development of governance in this area. Understanding the range of different plausible strategies is similarly essential, e.g., the potential for an "Arctic-focused" strategy that could be deployed without

requiring development of new aircraft, or more “polar-focused” strategies that could target Antarctic impacts more effectively.

What is the impact on the development of human resources?

Graduate students trained in engineering are being cross-trained in climate science; similarly postdocs (not supported by this award but part of our research group) trained in climate science are exposed to engineering design ideas; this thus builds interdisciplinary expertise.

What was the impact on teaching and educational experiences?

None yet; but results will be incorporated into courses on geoengineering.

What is the impact on physical resources that form infrastructure?

Nothing to report.

What is the impact on institutional resources that form infrastructure?

Nothing to report.

What is the impact on information resources that form infrastructure?

Nothing to report.

What is the impact on technology transfer?

Nothing to report.

What is the impact on society beyond science and technology?

This project is ultimately aimed at providing decision support for geoengineering. The limits and tradeoffs in geoengineering are essential pieces of information for deciding if, when, where, and how geoengineering might be done in the future. The results from our project could directly inform that decision process, as well as the development of international governance capacity to support that decision process, and the methods we are demonstrating will enable other researchers to pursue similar lines of investigation.

What percentage of the award's budget was spent in a foreign country?

Nothing to report.

Changes/Problems

Changes in approach and reason for change

Nothing to report.

Actual or Anticipated problems or delays and actions or plans to resolve them

Nothing to report.

Changes that have a significant impact on expenditures

Nothing to report.

Significant changes in use or care of human subjects

Nothing to report.

Significant changes in use or care of vertebrate animals

Nothing to report.

Significant changes in use or care of biohazards

Nothing to report.

Change in primary performance site location

Nothing to report.

Project Report Printer Friendly Version

Click here to print

Preview of Award 2038246 - Annual Project Report

Cover

Federal Agency and Organization Element to Which Report is Submitted:	**4900**
Federal Award or Other Identifying Number Assigned by Agency:	**2038246**
Project Title:	**Fundamental limits and trade-offs of stratospheric aerosol geoengineering**
PD/PI Name:	**Douglas G MacMartin, Principal Investigator** **Benjamin Kravitz, Co-Principal Investigator**
Recipient Organization:	**Cornell University**
Project/Grant Period:	**01/01/2021 - 12/31/2023**
Reporting Period:	**01/01/2021 - 12/31/2021**
Submitting Official (if other than PD\PI):	**Douglas G MacMartin** **Principal Investigator**
Submission Date:	**11/03/2021**
Signature of Submitting Official (signature shall be submitted in accordance with agency specific instructions)	**Douglas G MacMartin**

Accomplishments

*** What are the major goals of the project?**

Geoengineering (in particular we focus on stratospheric aerosol injection) would cool the climate, reducing some impacts from climate change, but it would not simply reverse changes due to increased atmospheric greenhouse gas concentrations, leading to residual changes. These changes, however, depend on how it is done – particularly what latitudes or seasons that aerosols are added to the stratosphere. The main goal of the project is to understand what geoengineering can and cannot do. This will help us understand which decisions matter, which uncertainties need to be resolved or managed, fundamental limits to how well it can compensate for climate change, and where any trade-offs might be. All of these are essential for informing future decisions about whether and how to deploy geoengineering.

*** What was accomplished under these goals and objectives (you must provide information for at least one of the 4 categories below)?**

Major Activities:

i) We have integrated previously conducted geoengineering simulations that use different combinations of locations (latitudes) and times of year (season) to achieve different sets of climate objectives with simulations at many different latitudes and seasons to make an estimate for the total independent degrees of freedom available; (ii) building on that, we have begun a set of simulations that collectively will span a complete range of independent strategies, and (iii) we have also completed simulations that consider different amounts of cooling, corresponding to different plausible future deployment scenarios.

Specific Objectives:

Significant Results:

For global cooling of up to 1.5°C, there are approximately 6-8 independent degrees of freedom for SAI that would lead to detectably different climate outcomes. These include injection at 30N, 15N, equator, 15S, 30S, as well as spring injection at 60N and 60S. This also means that as many as 6-8 independent climate objectives might be simultaneously managed; previous studies have considered at most 3, suggesting both that there is considerable scope for exploring distinct strategies, and that this scope is "small" enough that this exploration is feasible.

Key outcomes or Other achievements:

*** What opportunities for training and professional development has the project provided?**

The project has directly supported the research of two graduate students in engineering; work related to this project has also involved two postdoctoral research associates with a background in climate science. This provides a learning experience for both; the graduate students benefit from the expertise of the postdocs, and the postdocs gain an appreciation for engineering design principles, as well as some experience in mentoring graduate students. The graduate students have learned how to run CESM(WACCM), analyze the output, write papers, and prepare the results for presentations at conferences.

*** Have the results been disseminated to communities of interest? If so, please provide details.**

The first paper from this award (partly supported by a previous NSF award) has been submitted for publication to a peer-reviewed journal; all work is also being presented at conferences (e.g., at AGU fall meeting; some results have been used in a presentation at Arctic Circle meeting). Research results are also disseminated to the research community through geoengineering email lists.

*** What do you plan to do during the next reporting period to accomplish the goals?**

We will continue to conduct simulations spanning a range of different possible strategies (corresponding to different choices for injection latitude, season, and the goals), analyze the output to evaluate differences and understand impacts of different strategies, and explore the potential for optimization to identify new strategies, and will document results in scientific papers. We are also producing guidelines on scenario design for geoengineering.

Supporting Files

Filename	Description	Uploaded By	Uploaded On
How_large_is_the_design_space_for_stratospheric_aerosol_geoengineering_updated.pdf	Zhang, Y., D. G. MacMartin, D. Visioni, and B. Kravitz, How large is the design space for stratospheric aerosol geoengineering?, submitted, Earth System Dynamics.	Douglas Macmartin	10/21/2021

2024-256F 00000000867 "UNCLASSIFIED" 7/16/2025

Products

Books

Book Chapters

Inventions

Journals or Juried Conference Papers

View all journal publications currently available in the for this award.

The results in the NSF Public Access Repository will include a comprehensive listing of all journal publications recorded to date that are associated with this award.

Zhang, Y., D. G. MacMartin, D. Visioni, and B. Kravitz, â€œHow large is the design space for stratospheric aerosol geoengineering? â€ , Earth System Dynamics Discussion, https://doi.org/10.5194/esd-2021-70. Status = SUBMITTED.

Licenses

Other Conference Presentations / Papers

Other Products

Databases
Data from Zhang et al 2021 (submitted), "How large is the design space for stratospheric aerosol geoengineering"; data available at https://ecommons.cornell.edu/handle/1813/104261

Other Publications

Patent Applications

Technologies or Techniques

Thesis/Dissertations

Websites or Other Internet Sites

Participants/Organizations

What individuals have worked on the project?

Name	Most Senior Project Role	Nearest Person Month Worked
	PD/PI	(b)(4): (b)(6)
	Co PD/PI	
(b)(6)	Graduate Student (research assistant)	
	Graduate Student (research assistant)	
	Postdoctoral (scholar, fellow or other postdoctoral position)	

Full details of individuals who have worked on the project:

Douglas G MacMartin
Email: dgm224@cornell.edu
Most Senior Project Role: PD/PI
Nearest Person Month Worked: (b)(4): (b)(6)
Contribution to the Project: Overall project direction, supervising graduate students
Funding Support: No other support
Change in active other support: Yes
International Collaboration: No
International Travel: No

Benjamin Kravitz
Email: bkravitz@iu.edu
Most Senior Project Role: Co PD/PI
Nearest Person Month Worked: (b)(4): (b)(6)
Contribution to the Project: Simulations, analysis, contributing to writing
Funding Support: None
Change in active other support: Yes
International Collaboration: Yes, United Kingdom
International Travel: No

(b)(6)
Most Senior Project Role: Graduate Student (research assistant)
Nearest Person Month Worked: (b)(4): (b)(6)
Contribution to the Project: Wrote paper that assesses the size of the design space for SAI; working on new simulations and will ultimately conduct optimization
Funding Support: Only NSF
International Collaboration: No
International Travel: No

(b)(6)
Most Senior Project Role: Graduate Student (research assistant)
Nearest Person Month Worked: (b)(4): (b)(6)
Contribution to the Project: Developing simulations of Arctic injection in particular (and Arctic+Antarctic)
Funding Support: Also supported by Cornell Atkinson Center for a Sustainable Future (2 months) for related research on Arctic impacts and processes
International Collaboration: No
International Travel: No

Daniele Visioni
Email: dv224@cornell.edu
Most Senior Project Role: Postdoctoral (scholar, fellow or other postdoctoral position)
Nearest Person Month Worked: (b)(4): (b)(6)
Contribution to the Project: Assisted graduate students in running climate models, assisted graduate students in writing papers.
Funding Support: Cornell Atkinson Center for a Sustainable Future
International Collaboration: No
International Travel: No

What other organizations have been involved as partners?

Nothing to report.

Were other collaborators or contacts involved? If so, please provide details.

Jadwiga (Yaga) Richter at NCAR

Impacts

What is the impact on the development of the principal discipline(s) of the project?

We are demonstrating the importance of strategy (and to some extent the scenario as well) for influencing outcomes from SAI – that it cannot meaningfully be considered as "one thing" and that one cannot simply pick some ad hoc choice for injection strategy; this then provides guidance for how geoengineering can/should be simulated. This is critical for research not only into outcomes, but also uncertainty.

What is the impact on other disciplines?

We are creating a dataset of geoengineering simulations that can be used by numerous other disciplines (for example, impacts and ecosystems). Understanding the extent to which there are inherent trade-offs between different objectives, or to what extent there are broadly "best" ways of deploying that would simultaneously satisfy many actors, is essential for informing the development of governance in this area. Understanding the range of different plausible strategies is similarly essential, e.g., the potential for an "Arctic-focused" strategy that could be deployed without requiring development of new aircraft.

What is the impact on the development of human resources?

Graduate students trained in engineering are being cross-trained in climate science; similarly postdocs (not supported by this award but part of our research group) trained in climate science are exposed to engineering design ideas; this thus builds interdisciplinary expertise.

What was the impact on teaching and educational experiences?

None yet; results may be incorporated into courses on geoengineering.

What is the impact on physical resources that form infrastructure?

Nothing to report.

What is the impact on institutional resources that form infrastructure?

Nothing to report.

What is the impact on information resources that form infrastructure?

Nothing to report.

What is the impact on technology transfer?

Nothing to report.

What is the impact on society beyond science and technology?

This project is ultimately aimed at providing decision support for geoengineering. The limits and tradeoffs in geoengineering are essential pieces of information for deciding where and how geoengineering might be done in the future. The results from our project

could directly inform that decision process, as well as the development of international governance capacity to support that decision process, and the methods we are demonstrating will enable other researchers to pursue similar lines of investigation.

What percentage of the award's budget was spent in a foreign country?

Nothing to report.

Changes/Problems

Changes in approach and reason for change

Nothing to report.

Actual or Anticipated problems or delays and actions or plans to resolve them

Nothing to report.

Changes that have a significant impact on expenditures

Nothing to report.

Significant changes in use or care of human subjects

Nothing to report.

Significant changes in use or care of vertebrate animals

Nothing to report.

Significant changes in use or care of biohazards

Nothing to report.

Change in primary performance site location

Nothing to report.